The Dissertation Committee for Mara Rachel London Certifies that this is the approved version of the following dissertation

MODELING AUTOHYDROGENOTROPHIC TREATMENT OF PERCHLORATE-CONTAMINATED WATER IN THE PRESENCE OF NITRATE

Committee:

Lynn E. Katz, Supervisor

Gerald E. Speitel Jr., Co-Supervisor

James A. Holcombe

Mary Jo Kirisits

Howard M. Liljestrand

MODELING AUTOHYDROGENOTROPHIC TREATMENT OF PERCHLORATE-CONTAMINATED WATER IN THE PRESENCE OF NITRATE

by

Mara Rachel London, B.S.; M.S.

Dissertation

Presented to the Faculty of the Graduate School of

The University of Texas at Austin

in Partial Fulfillment

of the Requirements

for the Degree of

Doctor of Philosophy

The University of Texas at Austin

August 2009

Dedication

For my family

Acknowledgements

I would like to thank my advisors Lynn E. Katz and Gerald E. Speitel, Jr. for their guidance throughout my time at The University of Texas at Austin. I appreciate their efforts to make me successful and for helping me to overcome challenges. I would also like to thank my committee members, James A. Holcombe, Mary Jo Kirisits, and Howard M. Liljestrand for all of their advice, comments, and suggestions. Other great professors in the department also enriched my interest and knowledge of environmental engineering issues; special thanks to Desmond F. Lawler and Kerry A. Kinney for their mentorship and wisdom.

Several individuals were instrumental in helping to train and mentor me in the laboratory. I sincerely thank David Wahman, Greg Pope, Keith Lai, Chia-chen Chen, and Charles Perego for their assistance and patience. I am also grateful for the assistance of my two undergraduate students, Emily Underriner and Andrea Mena, who were a pleasure to mentor and always brought a smile with them into the lab. I am especially thankful to Ellison Carter for all the hours she spent monitoring my experiments when I was out of town and Rebecca Christian for her administrative assistance and friendly chats.

MODELING AUTOHYDROGENOTROPHIC TREATMENT OF PERCHLORATE-CONTAMINATED WATER IN THE PRESENCE OF NITRATE

Publication No._____

Mara Rachel London, Ph.D.

The University of Texas at Austin, 2009

Supervisors: Lynn E. Katz and Gerald E. Speitel, Jr.

Perchlorate contamination is widespread. Perchlorate, a water contaminant, disrupts iodide uptake to the thyroid, inhibiting growth and mental development. Recent studies have demonstrated autohydrogenotrophic perchlorate reduction to chloride. Hydrogen gas can be produced in-situ via the corrosion of zero-valent iron (ZVI), thereby avoiding problems related to the low aqueous solubility of hydrogen gas. The presence of nitrate has been shown inhibit autohydrogenotrophic perchlorate reduction. However, no studies have modeled the effects of nitrate on autohydrogenotrophic perchlorate biokinetics or developed a model to function as a design tool to predict long-term performance of ZVI/biotic perchlorate treatment systems in the presence of nitrate.

Batch experiments demonstrated the presence of nitrate significantly inhibited perchlorate degradation by an autohydrogenotrophic microbial consortium. However, the

consortium was capable of significant perchlorate reduction while the bulk of the nitrate was still present. A modified competitive inhibition model successfully predicted autohydrogenotrophic perchlorate degradation in the presence of nitrate. The model describes perchlorate degradation as a function of the biomass, perchlorate, hydrogen, and nitrate concentrations, as well as the single-component perchlorate, hydrogen, and nitrate half-saturation coefficients and perchlorate maximum substrate utilization rate. To obtain the single-component parameters, a series of batch experiments were performed under perchlorate-, nitrate-, and hydrogen-limiting conditions. The single-component biokinetic parameters and model predictions indicate the consortium could treat perchlorate-contaminated water with concentrations in the low hundreds of µg/L and in states with perchlorate treatment goals in the low µg/L range.

The consortium biokinetic parameters and modified competitive inhibition model were used in the development of an AQUASIM based biofilm model. The model also integrated physical parameters, ZVI hydrogen production, and abiotic nitrate reduction. The model was calibrated using the long-term performance results of a laboratory-scale ZVI/biotic column. Both laboratory and modeling results showed when the column becomes hydrogen-limited, the presence of nitrate decreases perchlorate removal efficiency. Full-scale simulations demonstrated the model could prove useful as a predictive design tool. Simulations suggest that a permeable reactive barrier that includes 10% ZVI and additional media capable of pH buffering could remove typical contaminated ground water concentrations of perchlorate in the presence of typical oxygen and nitrate concentrations.

Table of Contents

List of Tables

List of Figures

Chapter 1: Introduction

1.1. PROBLEM STATEMENT

Concern regarding the presence of perchlorate in drinking water has increased dramatically over the past decade and at least 35 states have known perchlorate contamination (USEPA, 2005a). Perchlorate, ClO_4^-, prevents uptake of iodide ions from the bloodstream to the thyroid; this results in reduced hormone production by the thyroid gland and consequently inhibits growth, mental development, and metabolism. According to the studies to date, perchlorate can be harmful to human health at the µg/L (part per billion [ppb]) level (NRC, 2005). Typically, perchlorate is ingested as an ion dissolved in water; therefore, the presence of perchlorate in drinking water is a major public health concern.

Perchlorate tends to persist in the aqueous environment under typical ground and surface water conditions because it sorbs weakly to most soil minerals, is highly soluble, and nonreactive (Urbansky, 1998; 2002). Perchlorate contamination is frequently attributed to its use as a propellant in the defense and aerospace industries and in products such as fireworks and road flares (Gullick et al., 2001). Additionally, it has been hypothesized that naturally-occurring perchlorate in the environment is a result of atmospheric deposition. (Dasgupta et al., 2005; Rajagopalan et al., 2006; Rao et al., 2007). Furthermore, perchlorate has also been found in the drinking water disinfectant sodium hypochlorite (Greiner et al., 2008), as well as produce, milk (both dairy and breast) (USFDA, 2004; Kirk et al., 2005), and powdered infant formula (Schier et al., 2009).

Contaminated ground water perchlorate concentrations are typically in the low hundreds of µg/L (Gullick et al., 2001; Urbansky, 1998) and most drinking water source concentrations are less than 20 µg/L (Hatzinger, 2005; Wang et al., 2002). Federal regulation of perchlorate is still under consideration by the EPA; in the interim the EPA issued a health advisory level for perchlorate in drinking water of 15 µg/L, based on the reference dose recommended by the National Academy of Science (USEPA, 2008). However, some states, such as California and Massachusetts, have set their own maximum contaminant levels for perchlorate in drinking water at 6 µg/L and 2 µg/L respectively (CDEP, 2008; MDEP, 2009).

Biodegradation of perchlorate is an appealing remediation technology because of its ability to completely degrade perchlorate to innocuous products (chloride ions, water, and cell mass), thereby eliminating the need for disposal or residual treatment. Microorganisms capable of degrading perchlorate are ubiquitous in the environment (Coates and Achenbach, 2004) and autohydrogenotrophic microbial reduction of perchlorate to chloride has proven effective in the treatment of perchlorate-contaminated ground and drinking water (Giblin et al., 2000; Logan and LaPoint, 2002; Nerenberg et al., 2002; Sanchez, 2003; Yu et al., 2007). However, to fully take advantage of these treatment systems for perchlorate-contaminated water, nitrate co-contamination must be taken into account.

Nitrate co-contamination is of considerable concern because it has been shown to slow or inhibit biological perchlorate reduction in autohydrogenotrophic treatment systems (Van Ginkel et al., 2008; Nerenberg et al., 2002; Yu et al., 2006). Nitrate is often a co-contaminant with perchlorate, is usually present at concentrations several orders of magnitude greater than that of perchlorate (Gu et al., 2002a; Kimbrough and Parekh, 2007; van Ginkel et al., 2008) and can also be degraded autotrophically using

hydrogen gas as the electron donor (e.g., Kurt et al., 1987; Liessens et al., 1992). Thus, the presence of nitrate in perchlorate-contaminated water may reduce the effectiveness of autohydrogenotrophic perchlorate treatment process.

1.2. OBJECTIVES AND APPROACH

In-situ generation of hydrogen gas via the corrosion of zero-valent iron (ZVI) is advantageous over systems requiring an external hydrogen gas feed because of the considerable hydrogen partial pressures required as a result of the low aqueous solubility of hydrogen. ZVI/biotic treatment systems have been shown to be effective in the treatment of perchlorate- and/or nitrate-contaminated water in both batch and column studies (Gandhi et al., 2002; Ginner et al., 2004; Sanchez, 2003; Son et al., 2006; Till et al., 1998; Yu et al., 2006; 2007).

The overall objective of this research was to develop models to describe autohydrogenotrophic treatment of perchlorate-contaminated water in the presence of nitrate. The specific research objectives include:

1. Extend previous perchlorate reduction kinetics work for an autohydrogenotrophic microbial consortium, accounting for potential inhibitory/competitive effects of nitrate co-contamination by determination of kinetic parameters and appropriate kinetic models

2. Quantify hydrogen production rates and assess the long-term viability of a ZVI/biotic treatment system for perchlorate reduction with and without the presence of nitrate

3. Create a steady-state mathematical biofilm model of the ZVI/biotic treatment process for perchlorate-contaminated water in the presence of nitrate based on experimental observations

In order to meet the above objectives, five main research tasks are outlined below:

Task 1 involved batch kinetic experiments for an autohydrogenotrophic microbial consortium under hydrogen-limiting, perchlorate-limiting, nitrate-limiting, and perchlorate-in-the-presence-of-nitrate conditions. Results afforded key kinetic parameters and expressions for use in simulating biodegradation in the treatment system that account for either hydrogen and perchlorate as the rate-limiting substrate, as well as the inhibitory effect of nitrate co-contamination.

Task 2 examined batch hydrogen production rates and passivation in the absence of microorganisms, at constant pH, and under a variety of water chemistry conditions. Prior to running a column study, the results obtained in Task 2 were used to confirm that the iron filings have the potential to provide the necessary hydrogen concentrations needed for biodegradation of perchlorate if the environmental conditions are favorable.

Task 3 was carried out to verify that abiotic-only reduction of perchlorate by ZVI does not occur at an appreciable rate. If abiotic-only reduction is negligible (as expected), then it is not an operational process of importance that needs to be considered when predicting long-term performance of a treatment system.

Task 4 demonstrated long-term perchlorate biodegradation performance of the ZVI/biotic treatment system, using a laboratory-scale, continuous-flow column in the presence of varying levels of nitrate. In addition to perchlorate and nitrate observations, hydrogen concentrations were monitored and the hydrogen production rate in the column

calculated. A surface analysis on the iron filings in the column was also performed to determine if the composition of the solids at the inlet and outlet differed after over two years of operation and if there were any indications of passivation.

Task 5 developed a steady-state mathematical model of the process using physical parameters and data obtained in Tasks 1 through 4. Initially, a batch version of the model was tested using data from batch ZVI/biotic perchlorate degradation experiments. The model was verified against experimental results obtained during Task 4 and applied to ZVI/biotic perchlorate treatment systems of another research group discussed in the literature (Yu et al., 2007). Finally, the model was used to simulate full-scale, in-situ ZVI/biotic treatment scenarios with and without the presence of nitrate. Full-scale simulations were used to show treatment process feasibility and the potential of the model as a predictive design tool.

1.3. DISSERTATION STRUCTURE

Background information and a literature review can be found in Chapter 2. The following three chapters are devoted to experimental results and discussion and are written in manuscript format for journal papers (to be submitted). Chapter 3 focuses on perchlorate degradation kinetics of an autohydrogenotrophic microbial consortium in the presence of nitrate. Chapter 4 focuses on laboratory experimental results leading to the development of a steady-state mathematical model of the ZVI/biotic treatment process for perchlorate-contaminated water, while Chapter 5 expands upon the laboratory experimental results and model presented in Chapter 4 by incorporating nitrate co-contamination. Finally, Chapter 6 provides conclusions and recommendations for future research. A bibliography and appendices with more detailed information than what is provided in Chapters 3 through 5 follows.

5

Chapter 2: Literature Review

2.1. THE PERCHLORATE PROBLEM

Known health problems associated with ingestion of perchlorate have led to concerns regarding its presence in drinking water supplies. Perchlorate, ClO_4^-, may prevent the uptake of iodide ions from the bloodstream to the thyroid via competition, thus reducing the hormone production in the thyroid gland and potentially inhibiting growth, mental development, and metabolism. According to the studies to date, perchlorate can be harmful to human health at the µg/L level (NRC, 2005). Production of perchlorate in the United States began in the 1890s and increased dramatically during the 1940s due to demand from the aerospace and military industries. The physical and chemical properties of perchlorate make it exceedingly mobile and stable in aqueous environments, and under typical ground and surface water conditions, perchlorate is likely to persist for long periods of time. Although the presence of perchlorate in drinking water is a public health concern, currently no federal drinking water standard exists for perchlorate. The development of a drinking water standard will be based in part on the availability and cost of suitable treatment technologies.

2.2. HEALTH EFFECTS

The need to regulate perchlorate stems from its ability to inhibit functionality of the thyroid gland in humans. The high aqueous solubility of perchlorate, poor ligand strength, and low volatility make it likely to be found as an anion in aqueous environments. The major pathway of human perchlorate exposure is oral ingestion because of rapid uptake from the gastrointestinal tract.

The thyroid gland produces two hormones, thyrozine (T_4) and triiodothyronine (T_3). Synthesis and secretion of T_3 and T_4 are usually maintained within narrow limits by an efficient regulatory mechanism. T_3 is the biologically active thyroid hormone in most body tissue, while T_4 is primarily a precursor hormone with little or no inherent biological activity. T_4 is converted to T_3, and T_3 is required for normal development of the central nervous system and skeletal system in infants and fetuses. Both hormones are critical determinants of metabolic activity and affect the function of virtually every organ system in both children and adults. Iodide is a component of both T_3 and T_4, and uptake of iodide into the thyroid gland is a critical step in synthesis of the hormones. Perchlorate may interfere with thyroid function by preventing the uptake of iodide ions from the bloodstream to the thyroid via competition (NRC, 2005).

2.3. SOURCES AND OCCURRENCES OF PERCHLORATE CONTAMINATION

Both naturally-occurring and anthropogenic sources of perchlorate have been found in the environment. Perchlorate contamination is present not only in water, but perchlorate has become bioconcentrated in agricultural products as well. Ammonium perchlorate is used as the primary ingredient in solid propellant for rockets, missiles, and fireworks. Salts of perchlorate are also used in air bag inflators, nuclear reactors, electroplating, road flares, electronic tubes, rubber manufacture, tanning and finishing leather, as an additive in lubricating oils, as a mordant for fabrics and dyes, and in the production of paints and enamels (Siddiqui et al., 1998).

Recently, the presence of perchlorate in the drinking water disinfectant sodium hypochlorite has become a concern because of the potential for wide spread perchlorate distribution in drinking water. Perchlorate in sodium hypochlorite is believed to form naturally from chlorate or be present as a result of contamination from ingredients or the

manufacturing process. NSF International tested drinking water treatment chemicals from the United States and Canada and found the presence of perchlorate in 91% of the sodium hypochlorite samples at a concentration range of 0.03 – 29 µg/L, and a correlation between the age of the sodium hypochlorite and increasing perchlorate levels was detected (Greiner et al., 2008).

Perchlorate contamination began to come into the spotlight in the early 1990s at the Aerojet General Corporation Superfund Site in Rancho Cordova, California where perchlorate was detected in a drinking water supply at mg/L levels. The presence of perchlorate at the site led to a request for the first evaluation of toxicity in the United States. Since the discovery of perchlorate contamination at the Aerojet facility and the development of an ion chromatography analytical method for detecting perchlorate at low concentrations ($\sim$ 4 µg/L) in 1997, drinking water wells have been monitored rigorously at suspected perchlorate contamination sites.

Some perchlorate contamination is the result of the demilitarization of weaponry (e.g., missiles) or discharge from rocket fuel manufacturing plants. Legal discharges of unregulated waste effluents containing ammonium perchlorate decades ago seem to be a major source of perchlorate contamination in the United States (Urbansky, 1998). However, naturally occurring perchlorate has been found in Chilean saltpeter deposits that have been mined for use as sodium nitrate fertilizer (Ericksen, 1983). Changes in the refining process in the year 2000 lowered the perchlorate concentrations to environmentally non-significant levels in fertilizer derived from the Chilean deposits. Considerable reservoirs of naturally occurring perchlorate have been found in various unsaturated zones, both semi-arid and arid, in the southwestern United States. These deposits co-occur with meteoric chloride that is believed to have been deposited approximately one thousand years ago or earlier. Climate change or re-charge from

irrigation water could cause the perchlorate in the unsaturated zone to affect the underlying groundwater (Dasgupta et al., 2005; Rajagopalan et al., 2006; Rao et al., 2007).

Over 11 million people in the United States have perchlorate in their public drinking water supplies at a concentration of 4 µg/L (the minimum reporting level [MRL]) or higher (NRC, 2005). As of 2005, over 35 states and Puerto Rico have confirmed perchlorate releases (USEPA, 2005a) and it has been reported that 152 public water systems have detected perchlorate (USEPA, 2005c). The highest concentrations of perchlorate in non-drinking water sources found in the United States are as follows: groundwater – 3,700 mg/L, surface water – 120 mg/L, and soil 2,000 mg/kg (USEPA, 2005b). However, perchlorate-contaminated ground water concentrations are typically in the low hundreds of µg/L (Urbansky, 1998; Gullick et al., 2001) and most drinking water source concentrations are less than 20 µg/L (Hatzinger, 2005; Wang et al., 2002).

Discharges into Lake Mead in Nevada from the Kerr-McGee manufacturing facility (perchlorate production 1945 – 1998) and the American Pacific Corporation (perchlorate production 1958 – 1988) contaminated both surface and ground water, including the Lower Colorado River. Contamination in the Lower Colorado River impacts 15 – 20 million people throughout Arizona, Southern California, Southern Nevada, Tribal Nations, and Mexico (USEPA, 2005b).

As for perchlorate contamination in agricultural products, a United States Food and Drug Administration (USFDA) study found perchlorate contamination in lettuce (1 – 52 parts-per-billion), in one bottled water source (0.56 µg/L), and dairy milk (0 – 11.3 µg/L) (USFDA, 2004). Kirk et al. (2005) also found perchlorate in dairy milk from 11 states at a mean concentration of 2 µg/L (max 11 µg/L), as well as in human breast milk from 18 states at a mean concentration of 10.5 µg/L (max 92 µg/L). Infants that do not

breastfeed may still be at risk for perchlorate exposure, as perchlorate-contamination has been observed in powdered infant formula reconstituted in perchlorate-free water (Schier et al., 2009). Perchlorate concentrations ranging from 0.08 to 5.05 µg/L were found in the five commercially available bovine and soy-based powdered infant formulas tested.

2.3.1. Perchlorate regulation

Although perchlorate contamination has been found to be widespread and possibly cause adverse health effects, currently there is no federal drinking water standard. In 1998, perchlorate was placed on the United States Environmental Protection Agency (EPA) Contaminant Candidate List 1, which designates unregulated contaminants in drinking water that may pose a threat to public health.   In 1999 perchlorate was made part of the EPA Unregulated Contaminant Monitoring Rule 1, which required that all large public water systems and a representative sample of small public water systems monitor for perchlorate starting in January of 2001. Perchlorate was then carried over and put on the EPA Contaminant Candidate List 2 (February 2005) and made part of their Unregulated Contaminant Monitoring Rule 2.

The EPA released the first formal perchlorate draft risk assessment in December of 1998 and sponsored a peer review of the document in 1999. The EPA released a revised draft risk assessment in 2002 that incorporated the 1999 peer review comments, as well as new data. A new peer review process commenced shortly thereafter. In February 2005, the EPA established an official reference dose (RfD) for perchlorate in the Integrated Risk Information System (IRIS) of 0.0007 mg/kg body weight/day based upon the recommended reference dose in a January 2005 National Academy of Science report on perchlorate. An RfD is a scientific estimate of the daily exposure level to

perchlorate that is expected to not cause unfavorable health effects in humans. This RfD for perchlorate equates to a drinking water equivalent level (DWEL) of 24.5 µg/L.

The DWEL is not necessarily the concentration at which perchlorate should be regulated because of the risk of additional exposure from agricultural products. Perchlorate intake in the general population was examined in a USFDA Total Diet Study that looked at 14 age/sex population subgroups. Consumption of perchlorate ranged from 0.08 – 0.39 µg/kg body weight/day (Murray et al., 2008). Although, the upper bound is less than the RfD, infants and children (sensitive populations) demonstrated the highest estimated intakes of perchlorate on a body weight basis. If perchlorate were to be regulated in drinking water a concentration of 24.5 µg/L, Ginsberg et al. (2007) estimates there would be a seven fold increase in breast milk perchlorate concentrations. Modeling results predict this would lead to 90% of nursing infants' exposure to exceed the RfD. A drinking water concentration of less than 6 µg/L would be necessary to keep the median nursing infants' exposure below the RfD and a drinking water concentration of less than 1.3 µg/L would be required to keep 90th percentile of nursing infants' exposure below the RfD. Thus, regulation of perchlorate based on the RfD is complex and will require careful analyses, especially for sensitive populations.

In October 2008, the EPA announced a *preliminary* regulatory decision for perchlorate, concluding that for public water systems, perchlorate is not a public health concern and therefore would not be regulated under the Safe Drinking Water Act (USEPA, 2008). In the meantime the EPA set an interim perchlorate health advisory level at 15 µg/L (USEPA, 2008). A great deal of critical comments were received after the decision was announced, including negative commentary from the EPA's own science advisory board (Renner, 2009). Therefore, in January 2009, after reviewing public and peer review comments on the preliminary regulatory decision for perchlorate, the EPA

decided to seek further input from the National Academy of Sciences prior to making a final regulatory decision.

Although no federal perchlorate drinking water standard exists yet, states such as California and Massachusetts, have set their own maximum contaminant levels for perchlorate in drinking water at 6 µg/L and 2 µg/L, respectively (CDPH, 2008; MDEP, 2009).

2.3.2. Physical and chemical properties

In order to successfully design remediation schemes and treatment technologies, it is important to understand the physical and chemical properties that make perchlorate likely to persist for long periods under typical ground and surface water conditions. The following sections describe properties of perchlorate such as, high activation energy, high aqueous solubility, and low likelihood of forming complexes, which all combine to make perchlorate exceedingly mobile and stable in aqueous environments.

2.3.2.1 Solubility and precipitation

Perchlorate salts are highly soluble, even in organic solvents, which suggests that the perchlorate ion will dominate perchlorate speciation in most solutions. The aqueous solubility of perchlorate salts decreases in the following progression: $Na > Li > NH_4 > K > Rb > Cs$ (Greenwood and Earnshaw, 1997).

2.3.2.2 Thermodynamics and chemical reduction

Perchlorate reduction is thermodynamically favorable under most conditions. The standard potentials for the stepwise reduction of perchlorate are given in Table 2.1

Table 2.1 Perchlorate standard potentials

Reaction	Standard Potential (V) Dean et al., 1999/Charlot, 1971
$ClO_4^- + 2H^+ + 2e^- = ClO_3^- + H_2O$	1.201 / 1.19
$ClO_3^- + 2H^+ + e^- = ClO_2 + H_2O$	1.175 / 1.15
$ClO_2 + H^+ + e^- = HClO_2$	1.188 / 1.27
$HClO_2 + 2H^+ + 2e^- = HClO + H_2O$	1.64 / 1.64
$2HClO + 2H^+ + 2e^- = Cl_2 + 2H_2O$	n/a / 1.63
$Cl_2 + 2e^- = 2Cl^-$	1.396 / 1.36
$ClO_4^- + 8H^+ + 8e^- = 4H_2O + Cl^-$	1.388 / 1.54

Though favorable from a thermodynamic standpoint, at ambient temperatures and in the absence of a catalyst, perchlorate has low reactivity as an oxidant due to a kinetic activation barrier. Common reducing agents (e.g., S_2O_3, SO_3^{2-}) do not reduce perchlorate (Urbansky, 1998).

2.3.2.3 Reactivity and stability

The perchlorate molecule consists of a chlorine atom in the center of a tetrahedral grouping of four oxygen atoms. The negative charge is dispersed evenly over all four of the oxygen atoms. This dispersion of charge is one reason perchlorate does not bind to positively charged metallic centers and why perchlorate complexes are rare in dilute aqueous solutions.

The chlorine atom in a perchlorate molecule is in the +VII oxidation state. The most stable compounds of chlorine are those in which chlorine is in either its highest (VII) or lowest (-I) oxidation state. Perchlorate is stable both in solution and as a solid at

room temperature. However, when heated, perchlorate tends to decompose by loss of an oxygen atom and become a vigorous oxidant (Greenwood and Earnshaw, 1997).

The stability of perchlorate stems from the tendency of the perchlorate ion to resist, at room temperature and in the absence of a catalyst, the initial loss of one oxygen atom to form the naturally unstable chlorate (ClO_3^-) ion. The stability of perchlorate and its high degree of ionization can be seen in the dissociation constant of aqueous perchloric acid solutions. The dissociation constant for $HClO_4^- \leftrightarrow H^+ + ClO_4^-$ is 10^{14}, which is the highest dissociation constant among common inorganic acids.

Urbansky and Brown (2003) studied 38 samples consisting of agriculturally significant soils, minerals, and roadside dust for perchlorate adsorbability. Greater than 90% perchlorate recovery was obtained in all samples, with many samples having perchlorate recovery greater than 99%. In fact, Urbansky and Brown (2003) were unable to conclusively determine that reduction in perchlorate concentrations were due to sorption rather than biodegradation since non-sterile samples were used.

2.4. BIOLOGICAL TREATMENT OF PERCHLORATE-CONTAMINATED WATER

Over the past twelve years, multiple technologies for the treatment of perchlorate-contaminated water have been developed and tested. The costs associated with national compliance to a stringent maximum contaminant level (MCL) for perchlorate of 4 µg/L, are estimated to be between 76 and 140 million dollars per year at a 3% discount rate (Russell et al., 2009).

Treatment of perchlorate-contaminated water usually focuses on three different types of techniques: anion exchange resins, membranes, and biological reduction. Perchlorate cannot be removed effectively from water using conventional activated carbon filtration because perchlorate ions are very soluble and kinetically inert in dilute

aqueous solutions (Gu et al., 2002a).   Choice of a viable treatment technology or combination of technologies will likely depend on a variety of factors including location, cost, extent of contamination, and background water chemistry.

Many of the current applications focus solely on ex-situ technologies and are plagued with the problem of waste brines or waste effluent streams. Currently, none of the aforementioned treatment schemes have as of yet been recognized as the most favorable treatment technology.   Therefore, current applications typically are chosen based upon practicality and economic considerations. Biodegradation of perchlorate is an appealing remediation technology because of the ability to completely degrade perchlorate to innocuous products (chloride ions, water, and cell mass), thereby eliminating the need for disposal or residual treatment of concentrated waste streams or brines. Microorganisms are able to overcome the high activation energy associated with perchlorate reduction, and perchlorate-reducing microorganisms are ubiquitous in the environment (Coates and Achenbach, 2004), making biological treatment an attractive option for remediation.

Both hetero- and autotrophic microbial reduction of perchlorate to chloride has proven effective in the treatment of perchlorate-contaminated groundwater (Hatzinger, 2005; Xu et al., 2003). Autotrophic systems using hydrogen gas (Giblin et al., 2000; Logan and LaPoint, 2002; Nerenberg et al., 2002; Sanchez, 2003; Son et al., 2006; Yu et al., 2007) are particularly well-suited for perchlorate treatment because of the decreased potential for additional cost, clogging, and contamination issues associated with use of an organic substrate (Giblin et al., 2000; Miller and Logan, 2000).

However, the low aqueous solubility of hydrogen has limited the application of autohydrogenotrophic degradation systems. In-situ generation of hydrogen gas from ZVI corrosion circumvents many of the limitations associated with external gas feeds

including explosion and mass transfer concerns. Corrosion of steel wool and micro-scale ZVI filings have been shown to be capable of producing bioavailable hydrogen gas for perchlorate biodegradation and ZVI/biotic treatment systems demonstrated to be effective on perchlorate-contaminated water in both batch and column studies (Sanchez, 2003; Son et al., 2006; Yu et al., 2006; 2007). However, to effectively design autohydrogenotrophic ZVI/biotic perchlorate treatment systems, kinetic models that are able to account for nitrate co-contamination and a tool that can predict long-term system performance are necessary.

The following sections discuss the basics of microbial perchlorate reduction, as well as reactors engineered to treat perchlorate-contaminated water, focusing on autohydrogenotrophic reduction and in particular on hydrogen production via the corrosion of ZVI.

2.4.1. Microorganisms capable of perchlorate reduction

More than 50 anaerobic perchlorate-reducing bacteria are now in pure culture. These environmental isolates have been found in a large range of environments and are metabolically diverse (Bruce et al., 1999; Coates et al., 1999; Rikken et al., 1996; Waller et al., 2004). Table 2.2 lists autohydrogenotrophic perchlorate-reducing isolates.

Table 2.2 Autohydrogenotrophic perchlorate-reducing isolates

Organism	Source
Dechloromonas sp. HZ	Huang and Zhang, 2002b
Dechloromonas sp. JDS5	Shrout et al., 2005a
Dechloromonas sp. JDS6	Shrout et al., 2005a
Dechloromonas sp. PC1	Nerenberg et al., 2006

2.4.2. Enzymes of perchlorate reduction

Similarities between the denitrification and perchlorate reduction pathways led to early hypotheses that perchlorate reduction was catalyzed by nitrate reductase. However, not all perchlorate-reducing strains are able to reduce nitrate and not all denitrifiers are able to reduce perchlorate (Bruce et al., 1999; Coates and Achenbach, 2004; Xu et al., 2004). In addition, nitrate and perchlorate reductases appear to be located in different parts of the cell. Perchlorate reductase appears to be in the periplasmic fraction, while nitrate reductase appears to be in the membrane fraction (Steinberg et al., 2005).

Currently, two enzymes have been described as necessary for the reduction of perchlorate, (per)chlorate reductase and chlorite dismutase. (Per)chlorate reductase sequentially reduces perchlorate to chlorate to chlorite. The single enzyme, (per)chlorate reductase, is used for both perchlorate and chlorate reduction (Steinberg et al., 2005), although not all chlorate-reducing microorganisms are capable of reducing perchlorate (Kengen et al., 1999). A dismutation of chlorite to chloride and oxygen is mediated by

the enzyme chlorite dismutase (van Ginkel et al., 1996). The oxygen produced is consumed during cell respiration and does not accumulate in solution. O'Connor and Coates (2002) found that chlorite dismutase is highly conserved and present on the outer membrane among known perchlorate-reducing bacteria and was only expressed when the perchlorate-reducing bacteria were grown anaerobically in the presence of perchlorate or chlorate. Equation 2.1 shows the overall reaction for perchlorate biodegradation when hydrogen is the electron donor. A total of 8 electrons are transferred.

$$ClO_4^- + 4\ H_2 \rightarrow 4\ H_2O + Cl^- \hspace{2cm} \text{Equation 2.1}$$
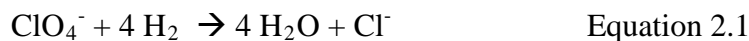
2.4.3. Inhibition/competition from other electron acceptors

Some perchlorate-reducing bacteria can use alternative electron acceptors such as chlorate, oxygen, and nitrate, and some strains preferentially use one acceptor over another (Chaudhuri et al., 2002; Dudley et al., 2008; Huang and Zhang, 2002b; Nerenberg et al., 2006; Xu et al., 2003).

Thermodynamics indicate that microbial reduction of perchlorate to chloride should be more energetically favorable than aerobic respiration. However, chlorite is toxic to microorganisms and must be dismutated to chloride and O_2 in a non-energy yielding reaction (chlorite dismutase enzyme). Therefore, from a free energy perspective oxygen is most likely the preferred electron acceptor (Coates et al., 2000; Rikken et al., 1996).

Nitrate is often a co-contaminant of perchlorate. It is also likely to be present at concentrations several orders of magnitude greater than that of perchlorate. Nitrate is present not only as a natural constituent of ground water, but due to the extensive

application of fertilizers and its presence in industrial waste and animal feeds (Gu et al., 2002a; Kimbrough and Parekh, 2007; Van Ginkel et al., 2008). Nitrate co-contamination is of considerable concern because it has been shown to slow or inhibit biological perchlorate reduction in autotrophic systems (Logan and LaPoint, 2002; Nerenberg et al., 2002; Van Ginkel et al., 2008; Yu et al., 2006; Yu et al., 2007). Although research suggests separate pathways are responsible for perchlorate and nitrate reduction, the potential for shared enzymes in the reduction pathway of perchlorate and nitrate for some perchlorate-reducing bacteria exists (Chaudhuri et al., 2002; Kengen et al., 1999; Rikken et al., 1996; Xu et al., 2004).

2.4.4. Kinetics of autohydrogenotrophic perchlorate biodegradation

To quantify the impact of nitrate on perchlorate degradation it is necessary to determine kinetic parameters and expressions for autohydrogenotrophic perchlorate degradation in the presence of nitrate concentrations typical of those found in nature. These kinetic parameters and expressions are required input to design and predict long-term performance of autohydrogenotrophic perchlorate treatment systems.

Both hydrogen or perchlorate could be rate-limiting. Hydrogen is expected to be limiting as a result of its limited aqueous solubility. While perchlorate is expected to be limiting because its concentration in contaminated ground water is typically in the low hundreds of µg/L and most drinking water source concentrations less than 20 µg/L (Urbansky, 1998; Gullick et al., 2001; Hatzinger, 2005; Wang et al., 2002). Accordingly, kinetic parameters under hydrogen- and perchlorate-limiting conditions are necessary to develop kinetic models that can account for this dual substrate limitation.

All of the reported autohydrogenotrophic perchlorate parameters were estimated using simple Monod or Michaelis-Menten kinetics, without taking into account the

19

potential inhibitory/competitive effects of nitrate. Most are for pure cultures (Miller and Logan, 2000; Nerenberg et al., 2006; Yu et al., 2006) with typical initial concentrations in the mg/L range (Tables 2.3 and 2.4). Miller and Logan (2000) determined perchlorate- and hydrogen-limiting Michaelis-Menten ales-Menton kinetic parameters in the presence of perchlorate for the pure-culture *Dechloromonas* sp. JM (Table 2.4); however, strain JM is not autotrophic, as it cannot fix carbon dioxide directly and therefore needs an organic substrate for growth.

Table 2.3 Summary of autohydrogenotrophic perchlorate Monod kinetic parameters for different perchlorate-reducing strains/consortia

Isolate	Initial perchlorate concentration (mg/L)	k (mg/mg dry weight-day)	K_s (mg/L)	Electron donor	Reference
Microbial consortium	0.050 – 0.040	3.08×10^{-2}	7.2×10^{-2}	Hydrogen	Sanchez (2003)
PC1	250 – 800	3.1	0.14	Hydrogen	Nerenberg et al. (2006)
HZ	0.2 – 15	0.22	8.9	Hydrogen	Yu et al. (2006)

Table 2.4 Hydrogen and perchlorate Michaelis-Menten kinetic parameters for *Dechloromonas* sp. JM

Conditions	Initial H_2 (g) concentrations (%)	Initial ClO_4^- concentration (mg/L)	Vmax (mM/hr)	K_s (mM)
Hydrogen kinetic parameters	1.09 - 10.4	-	0.006 ± 0.001 (Liquid H_2 mM/hr)	0.036 ± 0.014
Perchlorate kinetic parameters	-	10 - 550	0.055 ± 0.004	0.15 ± 0.06

In our laboratory, Sanchez (2003) determined autohydrogenotrophic perchlorate-limiting Monod kinetic parameters for a microbial consortium (Table 2.3). The perchlorate kinetic parameters determined by Sanchez (2003) demonstrated the potential for autohydrogenotrophic perchlorate biodegradation using a microbial consortium taking into consideration typical low level µg/L concentrations of perchlorate contamination. The microbial kinetics work presented in the following chapters provides an extension of the microbial consortium work of Sanchez (2003) by presenting the first kinetic models and parameters to account for dual substrate limitation and the potential inhibitory/competitive effects of nitrate co-contamination for autohydrogenotrophic perchlorate degradation.

2.4.5. Autohydrogenotrophic biological reactors engineered to reduce perchlorate

The treatment systems described below demonstrate the feasibility and limitations of biological reactors engineered to treat perchlorate-contaminated water using hydrogen

gas as the electron donor. Systems are described in which hydrogen is injected directly or produced from the corrosion of ZVI. In general, the treatment systems were successful, but the presence of nitrate slowed perchlorate removal.

2.4.5.1 Direct injection of hydrogen gas

Giblin et al. (2000) was able to reduce perchlorate and nitrate simultaneously using a packed-bed bioreactor and an anaerobic autohydrogenotrophic consortium. Perchlorate concentrations of 0.740 mg/L and nitrate concentrations of 25 mg/L in ground water were reduced to below their respective detection limits. One factor influencing the rate of perchlorate removal was the non-uniform distribution of biomass. The bulk of the biomass was found near the column inlet. However, hydrogen was added to the reactor feed via the gas phase and therefore the low aqueous solubility of hydrogen prevented much of the electron donor from reaching the biomass near the column outlet.

Nerenberg et al. (2002) demonstrated an improved method of hydrogen gas delivery for perchlorate biodegradation by use of a hollow-fiber membrane bioreactor (HFMBR), in which dissolved hydrogen gas is delivered directly to the biofilm. The bioreactor was originally used in a denitrification study and was seeded with *Ralstonia eutropha* and non-sterile tap water. The HFMBR was fed ground water with concentrations of perchlorate up to 100 µg/L and concentrations of nitrate at 2.6 – 3 mg/L as N. Although overall the reactor was successful, achieving greater than 99% removal of both perchlorate and nitrate, Nerenberg et al. (2002) concluded that in the HFMBR, nitrate slowed perchlorate removal and perchlorate had no effect on denitrification rates. A different HFMBR, treating synthetic ion-exchange spent brine, was also able to successfully reduce perchlorate in the presence of nitrate (van Ginkel et al., 2008).

However, perchlorate reduction rates were higher when nitrate loadings were lower, demonstrating competition for available hydrogen gas.

Logan and Miller (2000) were able to remove $38 \pm 9\%$ of perchlorate from the influent (740 µg/L) using a mixed culture packed-bed biofilm reactor operated in unsaturated-flow mode. The column was continuously fed water containing a gas mixture of 5% hydrogen and carbon dioxide. Logan and LaPoint (2002) used the same reactor as Logan and Miller (2000) to test two water sources, an artificial ground water and perchlorate-contaminated ground water. Perchlorate removal in the synthetic ground water without nitrate was $29 \pm 3\%$ and $17 \pm 3\%$ with nitrate. For the perchlorate-contaminated ground water, similar rates of perchlorate removal were found with and without the presence of nitrate at a concentration three orders of magnitude greater than that of perchlorate ($25 \pm 5\%$). However, Logan and LaPoint (2002) noted that nitrate removal in the perchlorate-contaminated ground water column seemed to increase the longer the column was exposed to nitrate, indicating the column might require time to adapt to elevated levels of nitrate and eventually negatively affect perchlorate removal.

The above discussion of reactors using direct injection of hydrogen demonstrate not only does the presence of nitrate have potentially negative impacts on perchlorate removal, but the bioavailability of hydrogen due to its low solubility in water is a crucial factor for successful treatment.

2.4.5.2 Chemical hydrogen gas generation

The above bioreactors have been able to degrade perchlorate using direct injection of hydrogen gas. Although for in-situ treatment, like in a permeable reactive barrier (PRB), direct injection of hydrogen gas is not practical due to its low aqueous solubility and explosion hazards. PRBs are a passive ground water remediation technology that

places a porous barrier in the path of a contaminated ground water plume. Barriers contain either an adsorptive or reactive media, such as ZVI, that remove contaminants from the ground water plume as the water flows through the barrier. Typical field-scale PRBs consist of 100% iron as the reactive media and have dimensions varying from 2 – 50 m long, <1 – 5 m wide, <1 – 10 m deep (Henderson and Demond, 2007; TAPRBI, 2002).

Chemical generation of hydrogen gas would make autotrophic treatment a more attractive technology for both ex- and in-situ perchlorate treatment. Hydrogen can be generated chemically from the corrosion of ZVI under anaerobic conditions (Equation 2.2).

$$4Fe^0 + 8\ H^+ \rightarrow 4Fe^{2+} + 4H_2 \qquad\qquad \text{Equation 2.2}$$
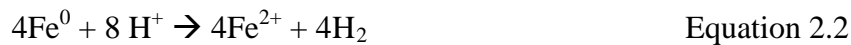
Electrochemical corrosion occurs when metal is submerged in an aqueous salt solution. Electrons are transferred from the anode to the cathode. There, the electrons react with H^+ to form hydrogen gas, with O_2 and H^+ to form water and OH^-, or with other oxidized species.

As seen in Equation 2.2, ZVI corrosion under anaerobic conditions consumes hydrogen ions, which increases the pH of the system. Liang et al. (2000) noted, at some installed ZVI PRBs the effluent pH rose more than 3 units, while in other barriers the rise in pH was small. If the pH is high, meaning the concentration of H^+ ions is low, the driving force for iron corrosion theoretically decreases. However, Reardon (1995) and Whitman et al. (1924) showed at the pH range of interest (pH 4 – 10), pH is not a major factor in determining anaerobic hydrogen production rates.

A survey of hydrogen production rates for ZVI under various water chemistries and types and preparations of iron can be seen below in Table 2.5. All rates were adjusted based on their reported units and specific surface area.

Table 2.5 Hydrogen production rates by ZVI

Hydrogen production rate $mol/m^2 Fe^0$-day	Media	Iron brand	Iron particle size	Iron specific surface area m^2/g	Reference
1.1×10^{-6} to 2.2×10^{-6}	Millipore	Maier Metallpulver GmbH, Germany	0.3 – 3 mm	0.5	Bokermann et al. (2000)
1.7×10^{-7} to 8.5×10^{-6}	carbonate	Maier Metallpulver GmbH, Germany	0.3 – 3 mm	0.5	Bokermann et al. (2000)
1.66×10^{-6}	unknown	Peerless Metals and Abrasives, MI	unknown	1.12[a]	Yu et al. (2007)
$\sim 4 \times 10^{-7}$	carbonate	Master Builders, OH	microscale	1.5	Reardon (1995)
$\sim 2 \times 10^{-7}$	Millipore	Master Builders, OH	microscale	1.5	Reardon (1995)
5.8×10^{-4}	phosphate	International Steel Wool	steel wool	0.091	Sanchez (2003)

a: specific surface area assumed based on iron brand

26

Table 2.5 indicates that ZVI has the potential to provide the necessary hydrogen concentrations needed for biodegradation of perchlorate if the environmental conditions are favorable.

2.4.5.3 ZVI-supported biodegradation of perchlorate

Sanchez (2003) provided proof of concept for ZVI (steel wool)/biotic perchlorate treatment with an initial perchlorate concentration of 1 mg/L and utilizing a microbial consortium. The laboratory columns received a synthetic feed with a relatively high phosphate buffer concentration to maintain a stable pH. The perchlorate concentration decreased over time after an initial lag period, attributed to the start-up of the biological process. Perchlorate removal deteriorated after 70 days due to the passivation of the iron surface by iron phosphate precipitates, resulting in decreased hydrogen production.

Son et al. (2006) was able to build upon Sanchez's (2003) proof of concept of a ZVI/biotic perchlorate treatment system, albeit with perchlorate concentrations one to two orders of magnitude greater than typical contaminated ground and drinking water perchlorate concentrations. Perchlorate was reduced from an influent concentration of 16 mg/L to below 20 µg/L using a microbial consortium and a column packed with ZVI filings and glass beads. The rate of perchlorate reduction in the system using hydrogen produced via ZVI corrosion for the electron donor was comparable to that of systems fed hydrogen through the gas-phase (5%) or acetate.

Nitrate has also negatively affected microbial perchlorate reduction in ZVI/biotic systems. Again building upon Sanchez's (2003) proof of concept, Yu et al. (2006) found in batch experiments with the pure culture *Dechloromonas* sp. HZ, the presence of nitrate slowed, but did not completely inhibit microbial perchlorate reduction (1000 µg /L

perchlorate, 5 – 20 mg/L as N nitrate). Perchlorate reduction was not initiated until most, if not all, of the nitrate present was degraded.

Yu et al. (2007) also studied the performance of flow-through columns packed with ZVI filings. In long residence time experiments, the reactor was inoculated with *Dechloromonas* sp. HZ. Tap water was amended with 500 - 700 µg /L of perchlorate and had a natural nitrate concentration of 4.7-5.9 mg/L as N. Greater than 99% removal of perchlorate (< 4 µg/L) was seen as long as the influent pH was less than 7.5. If the influent pH was greater than 7.5, the effluent pH was found to be greater than 10.0 and perchlorate removal decreased to $60 \pm 5\%$. Little perchlorate removal was found near the inlet end of the column, which was later discovered to be coated with vivianite, a Fe^{2+} phosphate precipitate.

Yu et al. (2007) also ran several short residence time flow-through columns packed with ZVI filings. The columns were inoculated with *Dechloromonas* sp. HZ or alternatively contained soil from a rapid infiltration tertiary wastewater treatment plant. Various influent concentrations of perchlorate (20 - 1000 µg/L) at a fixed flow-rate were analyzed. At influent concentrations less than 150 µg/L, near complete perchlorate removal was achieved in all test columns. At higher influent perchlorate concentrations, lower removal efficiencies were observed and attributed to hydrogen gas limitation, although no hydrogen gas concentrations were reported. At an influent perchlorate concentration of 30 µg/L and a nitrate concentration of 5.9 mg/L as N, perchlorate removal decreased from near complete removal to between 8 – 50 percent. No hydrogen or nitrate effluent concentrations were reported, making it difficult to assess the relationship between perchlorate and nitrate reduction and associated biotic and abiotic processes.

The highest removal (50%) was in the column inoculated with soil rather than the pure-culture *Dechloromonas* sp. HZ. Therefore, in the presence of nitrate, a ZVI/biotic system treating perchlorate-contaminated water, use of a microbial consortium may have a competitive advantage over those systems inoculated with a pure culture. For an in-situ system, exploiting the naturally occurring microbial communities would not have the additional cost or regulatory issues associated with bioaugmentation of a PRB. Communities of autohydrogenotrophic perchlorate- and nitrate-degrading microorganisms would likely form in and around the PRB. Studies have shown a natural increase in bacterial concentration in and around ZVI PRBs as compared to the background concentration (Belay and Daniels, 1990; Gerlach et al., 2000; Till et al., 1998; van Nooten et al., 2008; Yu et al., 2007). The population shifts when ZVI PRBs are installed, such that metabolic niches are exploited (Da Silva et al., 2007; Gu et al., 2002b).

The above reactors demonstrate the potential of ZVI/biotic systems to treat perchlorate-contaminated water in the presence of nitrate and the potential advantages of using microbial consortia. Results indicate ZVI/biotic perchlorate treatment systems should operate similarly or better than treatment systems in which hydrogen gas is injected directly. Although, hydrogen gas production by ZVI must be sustained or the system designed to account for hydrogen production deficiencies. However, there lacks a predictive tool to aid in the design of pilot- and eventually full-scale zero-valent/iron biotic perchlorate treatment systems. To develop and validate such a tool, further experimentation to quantify hydrogen production rates and assess the long-term viability of ZVI/biotic treatment systems are needed. This is in addition to the need for autohydrogenotrophic microbial kinetic models and parameters in the presence of nitrate. Therefore, a laboratory-scale study of a long-term ZVI/microbial consortium treatment

system, treating perchlorate concentrations typical of contaminated ground water, subject to increasing concentrations of nitrate, and monitored for hydrogen, nitrate, and perchlorate concentrations should be studied.

2.5. ENHANCEMENT AND INHIBITION OF H_2 GAS PRODUCTION FROM ZVI CORROSION

Sustained hydrogen production from the corrosion of ZVI is a critical component in ZVI/biotic treatment systems regardless of the presence of nitrate. The reactivity of the ZVI is likely a complex function of the surrounding aqueous chemistry of the ground water. Some ions in solution may promote iron corrosion, while others may inhibit or decrease the rate of corrosion (Klausen et al., 2003), thus affecting hydrogen production in ZVI treatment/biotic systems.

Rates of corrosion may be increased by the action of aggressive ions via pitting corrosion. Pitting corrosion occurs when the aggressive ions increase the surface defects of the metal or by breaking down the passive film (Gotpagar et al., 1999; Klausen et al., 2003; Scherer et al., 1998).

The thermodynamic instability of ZVI immersed in water in addition to the environmental conditions present can lead to the formation of a surface layer of corrosion products. Passivation of the iron surface occurs when the surface becomes saturated with these products, thus limiting the transfer of electrons from the ZVI. Passivation of the iron surface may affect the proposed treatment process by decreasing the reactivity of the iron surface, thereby creating a hydrogen-deficient environment as seen in the perchlorate ZVI/biotic systems of Sanchez (2003) and Yu et al. (2007). Passivation of the iron surface can occur either by amorphous oxide films forming on the surface of the iron, by precipitates forming and being deposited on the iron surface, or a mixture of the two (Klausen et al., 2003).

2.5.1 Inhibition of biodegradation by ZVI

Shrout et al. (2005b) found that ZVI inhibited perchlorate reduction using an anaerobic mixed culture. The mixed culture was provided 5 mg/L perchlorate and lactate in excess as an electron donor, in addition to 20 g/L of ZVI filings (Fisher Scientific 3.82 m^2/g). The inhibition was theorized to be a result of the encapsulation of microorganisms by iron precipitates or the inactivation of microorganisms from the production of free radicals by Fe(II) which could act on the oxygen produced during chlorite dismutation. However, the concentrations of phosphate and carbonate were several orders of magnitude greater than typically found in ground water. The additional carbonate and phosphate species could have led to greater than typical precipitation and thus greater than typical encapsulation.

2.6. ABIOTIC REDUCTION OF PERCHLORATE BY ZVI

Chlorinated compounds and heavy metals are able to be reduced chemically by ZVI (Gillham and O'Hannesin, 1994; Johnson et al., 1996). Therefore multiple studies to investigate the ability of ZVI to abiotically reduce perchlorate have been performed.

Moore et al. (2003) studied the rate and extent of perchlorate reduction at the surface of several different types and preparations of iron metal. The highest levels of perchlorate removal were at near-neutral or slightly acidic pHs. Initial drops in aqueous perchlorate concentration were attributed to sorption to the iron surface rather than chemical reduction. After this sorption period, aqueous chloride concentrations increased progressively, indicating that perchlorate reduction was taking place. The lack of reduction in experiments with soluble Fe^{2+} and the similarity of the specific reaction rate constants for three different iron sources, suggested that the reduction of perchlorate is a surface mediated reaction. The degree of perchlorate removal in all experiments was dependent upon the amount of iron surface area in the reactor.

31

The specific reaction rate constant (k_{sa}) for all iron types and pH conditions was on the order of 10^{-7} L m^{-2} h^{-1}. As a comparison, Johnson et al. (1996) found the specific reaction rate constant for several different chlorinated organics at the surface of zero-valent iron. The k_{sa} values ranged from 1.2 x 10^{-1} L m^{-2} h^{-1} for carbon tetrachloride to 6.1 x 10^{-6} L m^{-2} h^{-1} for trichlorpropane. In the end, Moore et al. (2003) concluded that the rate of abiotic perchlorate reduction at the surface of ZVI is too slow for use in remediation. Multiple subsequent studies saw similar results for micro-scale ZVI (Cao et al., 2005; Huang and Sorial, 2007; Schaefer et al., 2007; Son et al., 2006). Therefore, abiotic perchlorate reduction will likely not be an important component of a predictive design tool for ZVI/biotic systems. However, as discussed in the following section, prediction of abiotic reduction of nitrate will be relevant.

2.7. ABIOTIC/BIOTIC REDUCTION OF NITRATE USING ZVI

As discussed previously, nitrate contamination is of concern in ZVI/biotic perchlorate treatment systems because of the possibility of electron acceptor competition or inhibition. Nitrate itself is a health concern. Nitrate ingestion can cause low levels of oxygen in the blood of infants, and, like perchlorate, it can also block the uptake of iodide to the thyroid (De Groef et al., 2006). The EPA maximum contaminant level for nitrate in drinking water of 10 mg/L as N (USEPA, 1992). Many research groups have studied the abiotic reduction of nitrate by ZVI and some have looked at combined abiotic/biotic reduction of nitrate using ZVI.

Researchers have been unable to reach a consensus on the reaction mechanism responsible for nitrate reduction by ZVI (Mishra and Farrell, 2005; Rodríguez-Maroto et al., 2009). When nitrate is reduced by ZVI abiotically, the typical end product is the ammonium ion (Cheng et al., 1997; Choe et al., 2004; Ginner et al., 2004;

Ruangchainikom et al., 2006; Schlicker et al., 2000; Su and Puls, 2007); however, some researchers have reported nitrite as an end product or intermediate (Dejournett and Alvarez, 2000; Mishra and Farrell, 2005; Siantar et al., 1996).

The results of the effect of pH on abiotic nitrate reduction vary. Reduction at low pH is faster (Alowitz and Scherer, 2002; Ginner et al., 2004), though the results vary as to the effects of neutral pH. In *un*buffered solutions, Huang and Zhang (2002) and Zawaideh and Zhang (1998) found that at neutral pH, reduction of nitrate by ZVI did *not* take place, while Choe et al. (2004) and Alowitz and Scherer (2002) found nitrate reduction by ZVI *did* occur at neutral pH. In buffered solutions, Siantar et al. (1996), Cheng et al. (1997), and Zawaideh and Zhang (1998) found that nitrate reduction at neutral pH in was possible. Zawaideh and Zhang (1998) found at neutral pH, the addition of HEPES buffer to a ZVI system significantly increased nitrate reduction. This increase in nitrate reduction was not directly a result of the addition of HEPES buffer, as HEPES buffer was *not* shown to reduce nitrate. Conversely, Alowitz and Scherer (2002) found that buffer type (MES, MOPS, PIPES, HEPES) had little effect on the reduction rates of nitrate and concluded that pH was primarily responsible for the differences in rate, not buffer type. Alowitz and Scherer (2002) also found that at a pH of 7, there was only a modest difference in the rate of nitrate reduction when using different brands of ZVI (Peerless and Connelly). Ideally ZVI/biotic perchlorate treatment systems will operate at neutral pH to prevent inactivation of the microorganisms. The above results indicate some nitrate reduction will take place in ZVI/biotic perchlorate treatment systems if the pH is buffered at neutral pH.

In microbial denitrification the end product is typically $N_2(g)$ which is a more innocuous product than ammonium or nitrite. In ZVI/biotic systems, when growth conditions were not optimal for autohydrogenotrophic denitrification, abiotic removal of

nitrate has been the dominant removal mechanism (Till et al., 1998; Su and Puls 2007). Accordingly, Ginner et al. (2004) found that with sufficient buffering capacity, by inoculating their abiotic system with autotrophic microorganisms they were able to improve nitrate removal. Moreover, Gandhi et al. (2002) found in a ZVI column treating Cr(VI), NO_3^-, SO_4^{2-}, and trichloroethylene that the addition of *Shewanella algae* BRY enhanced nitrate removal over iron alone from 15% to 80%. The enhanced removal was attributed in part to the ability of *Shewanella algae* BRY to use nitrate as an electron acceptor and in part due to its ability to dissolve passivated iron oxide layers.

The presence of microorganisms has been shown to enhance ZVI corrosion by removing the passivated cathodic hydrogen layer and increasing the flow of electrons via cathodic depolarization (Belay and Daniels, 1990; Gerlach et al., 2000; Till et al., 1998; van Nooten et al., 2008). Even without the presence of nitrate, this could be advantageous in ZVI/biotic perchlorate treatment systems with respect to passivation and hydrogen production.

2.8. MODELING OF ZVI/BIOTIC SYSTEMS

The computer program AQUASIM can be used to model biofilm systems, such as those expected in ZVI/biotic perchlorate treatment systems. AQUASIM is a computer program designed for the analysis of aquatic systems (Reichert, 1994; 1995). AQUASIM extended the existing mass balance equations designed to mathematically model mixed-culture biofilms. Extensions included adding flexibility and additional components related to the transport of dissolved and particulate compounds in and out of the biofilm, as well as allowing for changes in porosity and detachment of cells from the biofilm. Additionally, AQUASIM allows for pseudo-two-dimensional modeling of plug-flow in the biofilm (Reichert, 1994; 1995). Therefore, an AQUASIM based model could be

developed based on experimental results from a laboratory-scale ZVI treatment system and used as a predictive design tool.

2.9. SUMMARY

Perchlorate contamination is widespread. Perchlorate, a water contaminant, disrupts the uptake of iodide to the thyroid, inhibiting growth and mental development. Autohydrogenotrophic treatment of perchlorate-contaminated water, especially in treatment systems using hydrogen gas produced from the corrosion of ZVI, is a promising technology. It is clear that, for the successful treatment of perchlorate-contaminated water, the potential inhibitory/competitive effects of nitrate co-contamination must be taken into consideration. Research presented in the following chapters was used to develop models to describe (1) nitrate inhibition/competition on autohydrogenotrophic perchlorate degradation kinetics and (2) function as a design tool that predicts long-term system performance of ZVI/biotic perchlorate treatment systems in the presence of nitrate.

Chapter 3: Kinetics of an Autohydrogenotrophic Microbial Consortium in the Presence of Nitrate[1]

3.1. INTRODUCTION

Concern regarding the presence of perchlorate (ClO_4^-) in drinking water has increased dramatically over the past decade and at least 35 states have known perchlorate contamination (USEPA, 2005a). Perchlorate is of particular concern because of its ability to inhibit thyroid functionality, potentially affecting growth, mental development, and metabolism (NRC, 2005). Perchlorate tends to persist in the aqueous environment under typical ground and surface water conditions because it sorbs weakly to most soil minerals, is highly soluble, and nonreactive (Urbansky, 1998; 2002). Perchlorate contamination is frequently attributed to its use as a propellant in the defense and aerospace industries and in products such as fireworks and road flares (Gullick et al., 2001). Additionally, it has been hypothesized that naturally-occurring perchlorate in the environment is a result of atmospheric deposition. (Dasgupta et al., 2005; Rajagopalan et al., 2006; Rao et al., 2007). Furthermore, perchlorate has also been found in the drinking water disinfectant sodium hypochlorite (Greiner et al., 2008), as well as produce, milk (both dairy and breast) (USFDA, 2004; Kirk et al., 2005), and powdered infant formula (Schier et al., 2009).

Contaminated ground water perchlorate concentrations are typically in the low hundreds of µg/L (Gullick et al., 2001; Urbansky, 1998) and most drinking water source concentrations are less than 20 µg/L (Hatzinger, 2005; Wang et al., 2002). Federal regulation of perchlorate is still under consideration by the EPA; in the interim the EPA

issued a health advisory level for perchlorate in drinking water of 15 µg/L, based on the National Academy of Science's recommended reference dose (USEPA, 2008). However, some states, such as California and Massachusetts, have set their own maximum contaminant levels for perchlorate in drinking water at 6 µg/L and 2 µg/L respectively (CDEP, 2008; MDEP, 2009).

Microorganisms capable of degrading perchlorate are ubiquitous in the environment (Coates and Achenbach, 2004), and autohydrogenotrophic microbial reduction of perchlorate to chloride has proven effective in the treatment of perchlorate-contaminated ground and drinking water (Giblin et al., 2000; Logan and LaPoint, 2002; Nerenberg et al., 2002; Sanchez, 2003; Yu et al., 2007). However, to fully take advantage of these systems for perchlorate-contaminated water, nitrate co-contamination must be taken into account.

Nitrate co-contamination is of considerable concern for biological perchlorate treatment because perchlorate degradation may be inhibited by nitrate (Coates and Achenbach, 2004). Nitrate is often a co-contaminant with perchlorate, is usually present at concentrations several orders of magnitude greater than that of perchlorate (Gu et al., 2002b; Kimbrough and Parekh, 2007; van Ginkel et al., 2008), and can also be degraded autotrophically using hydrogen gas as the electron donor (Kurt et al., 1987; Liessens et al., 1992). Nitrate has been shown to inhibit biological perchlorate reduction in autohydrogenotrophic treatment systems (Nerenberg et al., 2002; van Ginkel et al., 2008; Yu et al., 2006). Although research suggests separate pathways are responsible for perchlorate and nitrate reduction, the potential exists for shared enzymes in the reduction pathway of perchlorate and nitrate for some perchlorate-reducing bacteria (Chaudhuri et al., 2002; Kengen et al., 1999; Rikken et al., 1996; Xu et al., 2004).

Both hydrogen and perchlorate could be rate-limiting and nitrate co-contamination is likely. Therefore, suitable kinetic models and parameters that incorporate hydrogen, perchlorate, and nitrate utilization must be identified to predict performance of and aid in the design of effective autohydrogenotrophic perchlorate treatment systems. Nearly all of the reported hydrogen-oxidizing, perchlorate-limiting kinetic parameters are for pure cultures (Miller and Logan, 2000; Nerenberg et al., 2006; Yu et al., 2006) with initial perchlorate concentrations in the mg/L range. Miller and Logan (2000) determined hydrogen-limiting kinetic parameters in the presence of perchlorate for the pure culture *Dechloromonas* sp. JM. However, strain JM cannot grow in the absence of an organic substrate because it cannot fix carbon directly. Most importantly, all of the aforementioned parameters were estimated using simple Monod or Michaelis-Menten kinetics without taking into account potential inhibitory/competitive effects of nitrate.

In our laboratory, Sanchez (2003) demonstrated the potential for autohydrogenotrophic perchlorate biodegradation using a microbial consortium by determining perchlorate-limiting kinetic parameters with typical perchlorate concentrations in the µg/L range. This work extends the previous research by developing a model to account for the impact of nitrate co-contamination on autohydrogenotrophic perchlorate degradation, with the aim of facilitating and enhancing autohydrogenotrophic treatment technologies for perchlorate-contaminated water.

3.2. MATERIALS AND METHODS

3.2.1. Bacterial strain and culture conditions

Originally, seed cultures were taken from raw wastewater and activated sludge at the Walnut Creek Wastewater Treatment Plant (WWTP) in Austin, Texas, an anaerobic

digester at the Horsby Bend WWTP also in Austin, Texas, and from a dormant perchlorate-degrading microbial consortium (stored at -80°C) previously cultured by Sanchez (2003). All three cultures were maintained in the laboratory and were capable of degrading perchlorate anaerobically using hydrogen gas as the electron donor. Because all three cultures behaved similarly and provided good perchlorate degradation, the three cultures were mixed together. The resultant microbial consortium was maintained in the laboratory for use in the kinetic experiments.

Initially, cultures were grown in autoclaved 250-mL amber glass bottles capped with Mininert valves (VICI, TX). Bottles were stored in a Plexiglas housing (Bellco Biotechnology, NJ) under a $N_2(g)$ atmosphere on top of a lateral shaker. Bottles were monitored and fed both $H_2(g)$ (5%) and ClO_4^- (50 mg/L, $NaClO_4$, reagent grade) in fresh deaerated buffer medium (6.4×10^{-4} M NH_4Cl, 6.0×10^{-3} M $NaHCO_3$, 2.3×10^{-2} M KH_2PO_4, 2.3×10^{-2} M K_2HPO_4, 1 mL/L trace mineral solution (0.0367 g/L $CuSO_4$, 0.2880 g/L $ZnSO_4 \cdot 7H_2O$, 0.0232 g/L $NiCl_2 \cdot 7H_2O$, 0.7016 g/L $FeCl_2 \cdot 4H_2O$, 0.2000g/L $AlCl_3 \cdot 6H_2O$, 0.2807 g/L $MnCl_2 \cdot 4H_2O$, 0.0382 g/L $CoCl_2 \cdot 6H_2O$, 0.0254 g/L $Na_2MoO_4 \cdot 2H_2O$, 0.0382 g/L H_3BO_4, 0.1420 g/L Na_2SO_4), all reagent grade).

To produce large amounts of bacteria, a Bio-Flo 3000 or Bio-Flow III Batch/Continuous Bioreactor (New Brunswick Scientific, NJ) with a 2.5-L working volume was operated in batch mode using deaerated bioreactor buffer medium (3.2×10^4 M NH_4Cl, 8.9×10^{-4} M $NaHCO_3$, 2.9×10^{-3} M KH_2PO_4, 2.9×10^{-3} M K_2HPO_4, 0.1 - 1 mg/L $NaClO_4$, 1 mL/L trace mineral solution, all reagent grade). Temperature was regulated at 28°C and agitation was set to 300 RPM. The bioreactor diffuser tube was exploited for use in delivering $H_2(g)$ and $CO_2(g)$ to provide the energy source and maintain anaerobic conditions, respectively. Gas flow was regulated by external flow meters and mixed before entering the diffuser tube. An oxygen trap (Agilent, CA) was

used on the $CO_2(g)$ line to remove any impurities. The bioreactor was inoculated from the bottle cultures, typically fed up to 2.5 mg/L of perchlorate (as needed), and both pH and DO were monitored.

3.2.2. Phylogenetic characterization

Terminal restriction fragment length polymorphism (T-RFLP) was performed to aid in characterizing the microbial consortium. DNA was extracted from samples of the bioreactor inoculum using the UltraClean™ Soil DNA Isolation Kit (Mo Bio Laboratories, CA). T-RFLP was conducted according to previously developed protocols (Egert and Friedrich, 2005; Marsh, 1999). Briefly, the 16S rRNA gene was amplified using a set of PCR primers that can amplify all bacteria (8F and 1492R); the forward primer was fluorescently labeled with 5-carboxyfluorescein (FAM). DNA samples were PCR-amplified for 16 cycles. For all samples, two replicate PCR reactions were combined and subjected to post-amplification treatment with Klenow to fill in partially single-stranded amplicon (Egert and Friedrich, 2005). The PCR amplicon was digested with one of three restriction enzymes: HhaI, MspI, or RsaI. Restriction fragments were separated by size on an ABI 3130 DNA analyzer. Individual T-RFs were putatively identified using the TAP T-RFLP software (Marsh et al., 2000).

3.2.3. Batch microbial kinetic experiments

A series of batch kinetic experiments were performed to model autohydrogenotrophic perchlorate degradation in the absence and presence of nitrate. The conditions for the experiments were:

(1) perchlorate was provided in excess relative to hydrogen (hydrogen-limiting)

(2) hydrogen was provided in excess relative to perchlorate (perchlorate-limiting)

(3) hydrogen was provided in excess relative to nitrate (nitrate-limiting)

(4) hydrogen was provided in excess relative to perchlorate and nitrate; the nitrate concentration was several orders of magnitude greater than the perchlorate concentration (perchlorate-in-the-presence-of-nitrate)

Kinetic experiments were conducted in bottles (condition 1 above) or in a 2.5-L bioreactor (conditions 2, 3, 4 above), and in each set of experiments all microbial nutritional requirements were provided in excess except for the limiting substrate under study. Although Sanchez (2003) performed perchlorate-limiting kinetic experiments using a microbial consortium from a similar source under similar conditions, new perchlorate-limiting experiments were conducted to minimize any differences owing to the consortium's provenance.

3.2.3.1 Hydrogen-limiting

During the hydrogen-limited experiments, perchlorate was provided in excess at a concentration of 50 mg/L (hundreds of orders of magnitude greater than the perchlorate half-saturation coefficient determined in the perchlorate-limiting experiments described later). A modified deaerated buffer media was used as follows: 6.4×10^{-4} M NH_4Cl, 6.0×10^{-4} M $NaHCO_3$, 1.7×10^{-4} M KH_2PO_4, 1.7×10^{-4} M K_2HPO_4, 1 mL/L trace mineral solution, all reagent grade. The initial hydrogen gas concentration in the headspace was 1%, 2%, or 3% by volume. Each experiment included a non-inoculated control and was performed in duplicate. Glass amber vials (125-mL) with Teflon septa and purged with $N_2(g)$ were seeded with microorganisms from the bioreactor. Experiments lasted less than 12 hours, and 1-mL samples were taken from the vial head space using a 1-mL gas-tight syringe.

41

Liquid samples were taken at the beginning and end of each hydrogen-limiting experiment (and all subsequent experiments outlined in the following sections), to determine the biomass concentration (i.e., total suspended solids [TSS]). The initial and final biomass concentration values in these and subsequent experiments were always found to be within 10% of one another. Therefore, the biomass concentration was considered constant throughout each experiment.

3.2.3.2 Perchlorate-limiting, nitrate-limiting, perchlorate-in-the-presence-of-nitrate

Perchlorate-limiting, nitrate-limiting, and perchlorate-in-the-presence-of-nitrate , kinetic experiments were each conducted in the bioreactor buffer medium described previously. Hydrogen gas was provided to the bioreactor in excess (the initial aqueous hydrogen gas concentration was several orders of magnitude greater than the hydrogen half-saturation coefficient determined in the hydrogen-limiting experiments) and was continually replenished. The experiment duration varied from 1 to 268 hours. Initial perchlorate and nitrate concentrations varied. For the perchlorate-limiting experiments, initial perchlorate concentrations were 80, 195, and 340 µg/L. For the nitrate-limiting experiments, nitrate concentrations varied between 2.7 and 3.6 mg/L as N. Finally, for the perchlorate-in-the-presence-of-nitrate experiments, perchlorate concentrations varied between 220 and 230 µg/L and nitrate concentrations varied between 2.2 and 4.6 mg/L as N. Samples for perchlorate and nitrate analysis were taken from the bioreactor through septa using an 8-inch long needle and 10-mL syringe. Samples were filtered immediately through a 0.2-µm filter (Pall Life Sciences, NY) and the first 4 mL of the filtrate were discarded. After filtration, any sample not immediately analyzed was stored at 4°C.

3.2.3.3 Determination of kinetic parameters

Microbial kinetic parameters were estimated by nonlinear regression using the kinetic models shown in Table 3.1. For each hydrogen-limiting, perchlorate-limiting, and nitrate-limiting kinetic experiment, the half-saturation coefficient (K_s) and maximum substrate utilization rate (k) were estimated simultaneously using the Solver routine in Excel. In Excel, a fourth-order Runge-Kutta numerical approximation of the microbial kinetic rate expression was fit to the data by minimizing the normalized residual sum of squares between predicted and measured concentrations. Normalization was achieved by dividing the residual sum of squares by the measured concentration at that time (Aziz et al., 1999). Additional adjustable parameters included the initial concentration of hydrogen, perchlorate, and nitrate.

Error in the parameter estimates were determined by approximating 95% joint confidence limits (CL) for all experimental scenarios (Aziz et al., 1999; Berthouex and Brown, 2002). The critical sum of squares value (S_c) that bounds the joint confidence region was calculated according to Equation 3.1. A Visual BASIC program in Excel was used to vary the kinetic parameters near the best-fit values and calculate the resulting sum of normalized squares. The S_c value was then used to approximate the upper and lower bounds for each parameter.

$$S_c = S_R \left(1 + \frac{p}{n-p} F_{p,n-p,\alpha}\right)$$ Equation 3.1

where:

S_c = critical sum of squares

S_R = minimized residual normalized sum of squares

p   = number of parameters estimated

n   = number of observations

$F_{p,n-p,\alpha}$ = upper α% value of the F distribution with p and n-p degrees of freedom

Table 3.1 Kinetic models for hydrogen, perchlorate, nitrate, and perchlorate-in-the-presence-of-nitrate biodegradation

Chemical	Model	Rate equation
Hydrogen	Modified Monod[a]	$r_{H_2} = \dfrac{\left(K_{S_{H_2}} + S_{H_2}\right) S_{H_2} H \beta \varphi + k_{H_2} X S_{H_2}}{\left(K_{S_{H_2}} + S_{H_2}\right)(1 + H\beta)}$
Perchlorate	Monod	$r_{ClO_4} = \dfrac{k_{ClO_4} X S_{ClO_4}}{K_{S_{ClO_4}} + S_{ClO_4}}$
Nitrate	Monod	$r_{NO_3} = \dfrac{k_{NO_3} X S_{NO_3}}{K_{S_{NO_3}} + S_{NO_3}}$
Perchlorate-in-the-presence-of-nitrate	Modified competitive inhibition[b]	$r_{ClO_4} = \dfrac{k_{ClO_4} X S_{ClO_4}}{K_{S_{ClO_4}}\left(1 + \dfrac{S_{NO_3}}{K_{S_{NO_3}}}\right) + S_{ClO_4}}$

H	=	hydrogen Henry's constant (dimensionless)
β	=	ratio of the volume of gas to the volume of liquid
φ	=	volumetric flow fraction representing the mass of hydrogen lost during sampling; product of the volume of sample and the number of samples taken, divided by product the of elapsed experimental time and the headspace volume [1/t]
X	=	biomass concentration [M/L^3]
k_{ClO_4}	=	perchlorate maximum substrate utilization rate [M/M-T]
k_{H_2}	=	hydrogen maximum substrate utilization rate [M/M-T]
k_{NO_3}	=	nitrate maximum substrate utilization rate ([M/M-T]
$K_{S_{ClO_4}}$	=	perchlorate half-saturation coefficient [M/L^3]
$K_{S_{H_2}}$	=	hydrogen half-saturation coefficient [M/L^3]
$K_{S_{NO_3}}$	=	nitrate half-saturation coefficient [M/L^3]
S_{ClO_4}	=	perchlorate concentration µg ClO_4^-/L) ([M/L^3]
S_{H_2}	=	aqueous hydrogen concentration [M/L^3]
S_{NO_3}	=	nitrate concentration [M/L^3]

a: Sanchez, 2003; b: adapted from Rittmann and McCarty, 2001

A modified competitive inhibition model (Table 3.1) was used to predict perchlorate degradation in the presence of nitrate. The modified competitive inhibition model uses the perchlorate and nitrate concentrations, the single-component perchlorate K_s and k values, and the single component nitrate K_s value to predict perchlorate degradation.

3.2.4. Analytical methods

Hydrogen gas concentrations were analyzed on a Gow-Mac, Series 580 gas chromatograph equipped with a thermal conductivity detector and a Suppelco molecular sieve 13X column. Column, injector, and detector were all set at 60°C. The method detection limit (MDL) for hydrogen gas was 3.8×10^{-5} atm. Perchlorate concentrations were analyzed (EPA Method 314) using a 1000-μL loop injection on a Dionex DX-600 ion chromatograph (IC) equipped with a Dionex AMMS III 2-mm conductivity detector suppressor, Dionex AS-16 2 x 250 mm column, Dionex AG-16 2 x 50 mm guard column, Dionex EGC II KOH eluent cartridge, and Dionex AS-40 auto-sampler. The column was regenerated using 50 mN sulfuric acid and the MDL was 1.2 μg/L (EPA Method 314).

An Agilent 8453 UV-visible spectrophotometer was used to measure NO_3^--N during the perchlorate-in-the-presence-of-nitrate experiments at a wavelength of 410 nm using the HACH Test 'N Tube Reactor/Cuvette Tubes with NitraVer X Reagent (Chromotropic Acid method). Alternatively, NO_3^--N during the nitrate-limiting experiments was measured (EPA Method 300) using a 500-μL loop injection on a Dionex DX-600 IC, equipped with a Dionex ASRS Ultra II 4-mm conductivity detector suppressor, Dionex AS-11 4 x 250 mm column, Dionex AG-11 4 x 50 mm guard column, Dionex EGC II KOH eluent cartridge, and Dionex AS-40 auto-sampler. To avoid nitrate peak interference from phosphate, iron (III) chloride was used to precipitate out the

phosphate. OnGuard II H cartridges (Dionex, IL) were used to remove soluble iron from solution prior to IC analysis. The MDL was 0.0065 mg/L nitrate as N.

A Perkin-Elmer Lambda 3b UV-visible spectrophotometer at a wavelength of 600 nm and analysis of TSS (Clesceri et al., 1998) were used to measure the concentration of biomass. DO was measured with an YSI 5905 probe on an YSI 54ARC oxygen meter. pH was measured with an Orion 9157 electrode on an Orion Model 920A pH/ISE meter.

3.3. RESULTS AND DISCUSSION

3.3.1. Hydrogen-limiting kinetics

Hydrogen-limiting kinetic parameters were determined after the microbial consortium had acclimated to autohydrogenotrophic degradation of perchlorate for several months. Kinetic parameters and 95% joint CL for hydrogen-limited degradation were determined for experiments conducted at 1%, 2%, and 3% hydrogen gas by volume, simultaneously fitting the Monod model to the experimental results (Table 3.1). The modified Monod model (Sanchez, 2003) incorporates two corrections to the general Monod equation to account for (a) losses of hydrogen gas due to sampling; and (b) mass transfer of hydrogen between the aqueous and gas phases.

Figure 3.1 presents the simultaneous fit to the results of the three experiments using the modified Monod model. Table 3.2 lists the best-fit K_s value and associated 95% joint CL. The mean K_s value from the simultaneous fit was found to be 2.26 x 10^{-6} M, approximately two orders of magnitude lower than the solubility of hydrogen in water. Additionally, narrow 95% joint CL were found. The 95% joint CL were determined to examine the range of error of the simultaneous kinetic parameter fitting procedure.
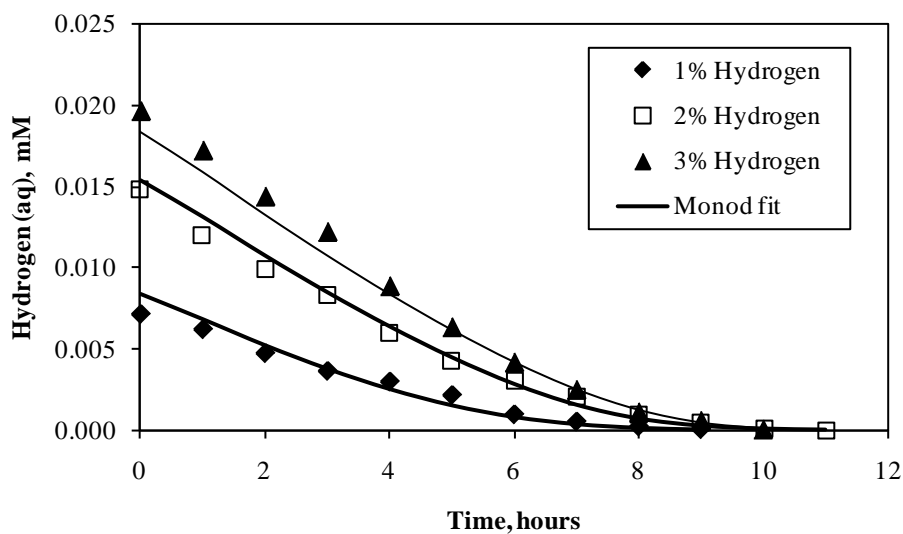
Figure 3.1 Hydrogen-limiting batch kinetic experiments using the modified Monod model simultaneously fit to all three data sets

(initial perchlorate concentration of 50 mg/L; initial hydrogen concentrations: 7.21 x 10^{-6} M H_2 (aq) (1%), 1.49x 10^{-5} M H_2 (aq) (2%), 1.97 x 10^{-5} M H_2 (aq) (3%); biomass concentrations: 14.6 mg TSS/L (1%), 18.3 mg TSS/L (2%), 19.3 mg TSS/L (3%))

Table 3.2 Half-saturation coefficients (K_s), maximum substrate utilization rates (k), and 95% joint confidence limits for the hydrogen-limiting, perchlorate-limiting, and nitrate-limiting batch kinetic experiments

Chemical	Units	K_s		
		Lower 95%	Mean	Upper 95%
Hydrogen	M (aq)	1.50×10^{-6}	2.26×10^{-6}	3.26×10^{-6}
Perchlorate	µg/L	23.3	28.4	34.4
Nitrate	mg/L as N	0.0385	0.153	0.388
		k		
Hydrogen	mol/mg TSS-hr	4.45×10^{-6}	4.94×10^{-6}	5.61×10^{-6}
Perchlorate	µg/mg TSS-hr	1.73	1.81	1.89
Nitrate	mg as N/mg TSS-hr	0.0125	0.0139	0.0167

Miller and Logan (2000) found the hydrogen K_s value for the hydrogen-oxidizing, perchlorate-reducing culture *Dechloromonas* sp. JM (JM) to be $3.6 \times 10^{-5} \pm 0.014$ M. The maximum concentration of hydrogen in water is 7.8×10^{-4} M at 25 °C and 1 atm (Lide, 1994). The K_s value for the consortium used in this research and for JM are at least one order of magnitude lower than the solubility concentration of hydrogen. In scenarios where the hydrogen concentration is well below the saturation value, the microbial consortium may have a competitive advantage over JM because the K_s value of the consortium is an order of magnitude less than that of JM.

The best-fit k value and corresponding 95% joint CL for the hydrogen-limited experiments are listed in Table 3.2. The mean value of k was found to be 4.94 x 10^{-6} mol H_2/mg TSS-hr. It was not possible to compare the k value to the work of Miller and Logan (2000) because only a maximum uptake rate (V_{max}) was reported. V_{max} is not normalized by the biomass concentration, and the biomass concentration was not reported.

3.3.2. Perchlorate-limiting kinetics

Perchlorate-limiting kinetic parameters were determined after the autohydrogenotrophic microbial consortium had become acclimated to perchlorate concentrations of 1 mg/L or less over a period of several months. Biological perchlorate reduction to chloride was not confirmed because low initial perchlorate concentrations and background chloride concentrations made mass balance closure difficult. However, complete perchlorate reduction was assumed, as a single enzyme reduces both perchlorate and chlorate, and it has been shown that chlorite does not typically accumulate in solution if perchlorate-reducing microorganisms are present (Rikken et al., 1996 Logan, 2001). Because chlorite is toxic to microorganisms (De Groot and Stouthamer, 1969), if chlorite had built up in solution, the chlorite would have likely killed the microbial population and no further reduction of perchlorate would have been observed.

The Monod model (Table 3.1) was fit to the three experiments shown in Figure 3.2 simultaneously. Table 3.2 lists the K_s value and 95% joint CL. The mean K_s value was found to be 28.4 µg/L. A narrow 95% joint CL was obtained. The mean K_s value is on the same order of magnitude of that found by Sanchez (2003) for a microbial consortium from a similar source (mean: 72.2 µg/L, 95% joint CL: 49.6 – 86.8 µg/L).
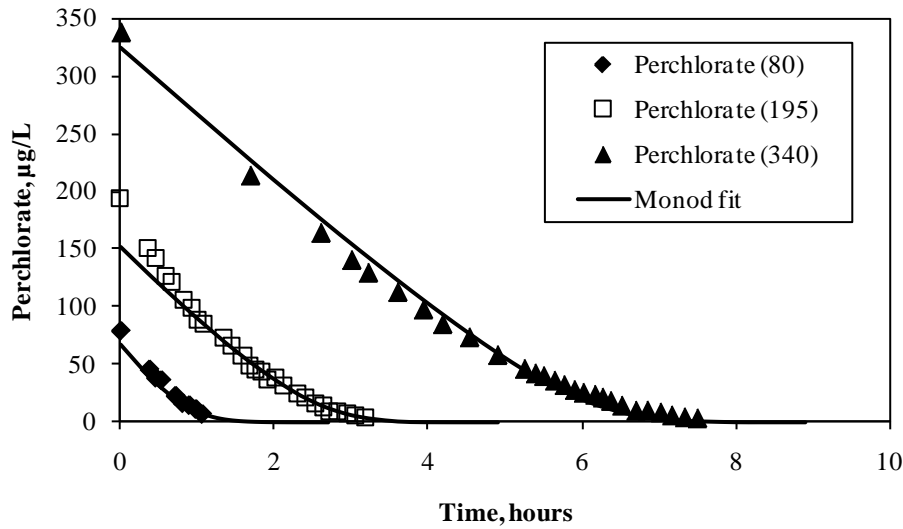
Figure 3.2 Perchlorate-limiting batch experiments using the Monod model fit simultaneously to all three experimental data sets

(biomass concentrations: 58.4 mg TSS/L (80 µg/L), 42.2 mg TSS/L (195 µg/L), 34.7 mg TSS/L (340 µg/L))

A low µg/L perchlorate K_s value indicates the microorganisms are able to reach their maximum degradation rate at low µg/L perchlorate concentrations. Therefore, a low µg/L K_s value for perchlorate is desirable for the treatment of perchlorate-contaminated waters with initial perchlorate concentrations in the low hundreds of µg/L or lower and the existing/expected µg/L perchlorate regulations. The perchlorate K_s value found for the microbial consortium was approximately an order of magnitude less than that found by Nerenberg et al. (2006) for the hydrogen-oxidizing pure culture *Dechloromonas* sp. PC1 (PC1) (140 µg/L), around two orders of magnitude less than that found by Yu et al. (2006) (8,900 µg/L) for the hydrogen-oxidizing pure culture *Dechloromonas* sp. HZ (HZ), and approximately three orders of magnitude less than that found by Miller and Logan (2000) (15,000 µg/L) for the hydrogen-oxidizing pure culture *Dechloromonas* sp.

51

JM (JM). The lower value of K_s for the consortium, especially compared to those of HZ and JM, indicates that the consortium has a greater affinity for perchlorate and could provide a competitive advantage when perchlorate concentrations are in the low µg/L range, as is the case with most contaminated waters (Hatzinger, 2005; Wang et al., 2002) and regulations (CDPH, 2008; MDEP, 2009).

Correspondingly, the k values and 95% joint CL for the perchlorate-limited experiments are presented in Table 3.2. The mean k value was found to be 1.81 µg/mg TSS-hr. The mean k value is on the same order of magnitude of that found by Sanchez (2003) (1.29 µg/mg TSS-hr) for a microbial consortium from a similar source. The k values reported by Nerenberg et al. (2006) and Yu et al. (2006) for their hydrogen-oxidizing pure cultures were 130 (PC1) and 9.2 (HZ) µg/mg dry weight-hr respectively. Because the k values of the consortium and HZ are approximately two orders of magnitude less than that reported for PC1, the consortium and HZ may degrade perchlorate more slowly than PC1.

Because of the differences in kinetic parameters, the software package AQUASIM (Reichert, 1994; 1995) was used to determine if the consortium would have a competitive advantage over the hydrogen-oxidizing pure cultures PC1 and HZ at a perchlorate concentration of 100 µg/L. An initial biomass concentration of 100 mg TSS/L was assumed. Biodegradation of perchlorate by each consortium/species using the corresponding set of Monod kinetic parameters can be seen in Figure 3.3. Figure 3.3 shows the microbial consortium and PC1 are predicted to require less time to completely degrade perchlorate as compared to HZ. Whereas it takes less than 1.5 hours for the microbial consortium and PC1 to completely degrade the perchlorate, it takes HZ 45 hours to achieve the same. As expected, based on the k values and evidenced by Figure

3.3, PC1 is able to completely degrade perchlorate slightly faster than the microbial consortium.
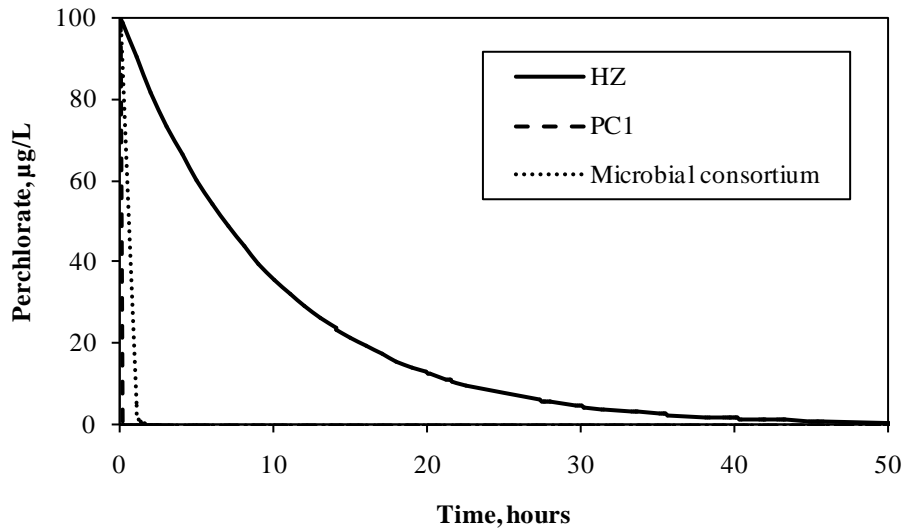
Figure 3.3 Predictions of perchlorate biodegradation using Monod model and kinetic parameters for various autohydrogenotrophic strains/consortium

(initial perchlorate concentration = 100 μg/L; biomass concentration = 100 mg TSS/L , hydrogen available in excess; Monod kinetic parameters for microbial consortium studied here, Dechloromona*s sp. HZ (Yu et al., 2006),* Dechloromonas *sp. PC1 (Nerenberg et al., 2006)*

3.3.2.1 Phylogenetic characterization

Because the hydrogen and perchlorate kinetic parameters for the microbial consortium were one to three orders different than that of previously-documented, pure culture, perchlorate-reducing, hydrogen-oxidizing microorganisms (*Dechloromonas* spp. HZ, JM, and PC1 strains), it was hypothesized that genera other than *Dechloromonas* may be present and responsible for perchlorate reduction in the bioreactor. T-RFLP was

performed to describe the microbial community present in the consortium. The microbial community present in the kinetic experiments appeared to contain strains related to previously documented perchlorate-reducing microorganisms. Restriction fragments for the perchlorate-reducing bacteria *Dechloromonas* sp. and the chlorate-reducing bacteria *Ideonella dechloratans* were putatively identified. Other restriction fragments were present that may be associated with unknown perchlorate-reducing bacteria or non-perchlorate-reducing bacteria.

Since T-RFLP indicated *Dechloromonas* sp. strains were present in the bioreactor and *Dechloromonas* sp. strains are known perchlorate-reducers, it follows that *Dechloromonas* sp. strains were most likely responsible for at least a portion of the perchlorate reduction seen in the kinetic experiments. However, because of the differences in kinetic parameters, it is possible that the microbial consortium contains *Dechloromonas* sp. strains other than HZ, JM, and PC1. The different enrichment conditions for the three hydrogen-oxidizing pure cultures and the microbial consortium may have led to the selection of different strains, which in turn could have led to the variations among the four sets of kinetic parameters.

The perchlorate concentration (~ 300 mg/L) used to isolate HZ could have led to the selection of a pure culture that has an advantage at higher initial perchlorate concentrations. The presence of nitrate in the reactor from which PC1 was isolated and the use of different growth media (R2A) could have led to the selection of a pure culture that degrades perchlorate at faster rates. Furthermore, the selection of JM using a rich media containing acetate and yeast and a perchlorate concentration, likely led to the selection of a pure culture that could not fix carbon dioxide directly. The microbial consortium studied in this research, and thus the kinetic parameters, are more representative of what would develop in full-scale in- or ex-situ treatment system,

without bioaugmentation. This is because of the typical low hundreds of µg/L or lower concentrations of perchlorate found in ground and drinking water and even lower perchlorate regulations (2 – 6 µg/L). Because the hydrogen and perchlorate kinetic parameters for the consortium represent similar or better perchlorate degradation performance over the pure cultures characterized by others, further characterization of the microorganisms present in the microbial community is recommended. Further characterization could identify more precisely which strains of *Dechloromonas* and other microorganisms are present. Strains of previously documented or novel perchlorate-reducing microorganisms that are best-suited for environments with low hundreds of µg/L or lower levels of perchlorate contamination could be identified.

3.3.3. Nitrate-limiting kinetics

Since nitrate typically is a co-contaminant present at concentrations several orders of magnitude greater than that of perchlorate, the potential for competition or inhibition was explored for the consortium. To quantify the impact of nitrate on perchlorate, it was necessary to determine kinetic parameters for nitrate at concentrations typical of those found in contaminated water. Nitrate-limiting kinetic parameters were estimated after the microbial consortium had been acclimated to a nitrate concentration of 5 mg/L as N for a period of several months. During this period no perchlorate was fed to the microbial consortium.

Nitrate-limiting kinetic experiments were fit to the Monod model (Table 3.1); a typical experiment can be seen in Figure 3.4. Table 3.3 lists the mean nitrate-limiting K_s (0.153 mg/L as N) and k (0.0139 mg as N/mg TSS-hr) values and their 95% joint CL, respectively.
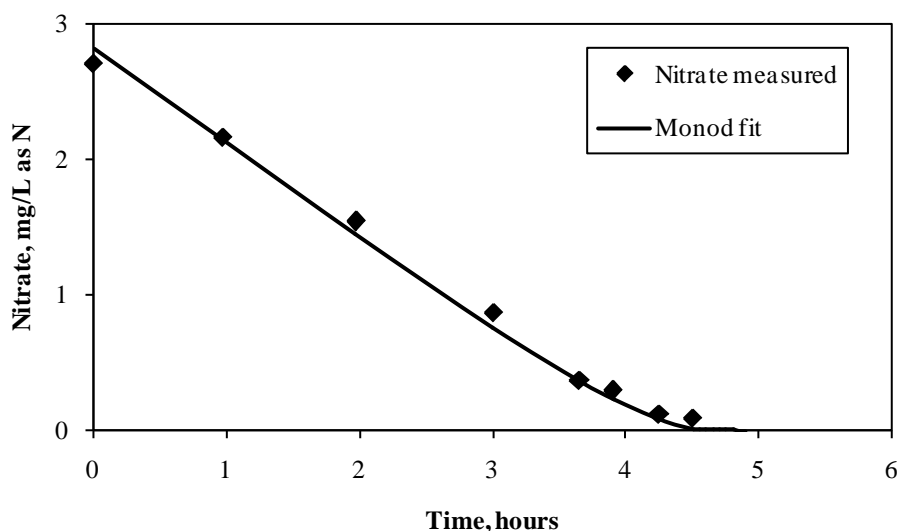
Figure 3.4 Typical nitrate-limiting batch kinetic experiment using Monod model fit

(initial nitrate concentration: 2.71 mg/L as N; biomass concentration: 53.2 mg TSS/L)

3.3.4. Perchlorate kinetics in the presence of nitrate

The impact of nitrate on perchlorate degradation was examined in batch experiments in which both nitrate and perchlorate were present. Prior to the perchlorate-in-the-presence-of-nitrate kinetic experiments, the autohydrogenotrophic microbial consortium had been consistently degrading perchlorate (1 mg/L or less) for several months and was exposed to nitrate (5 mg/L as N) in addition to perchlorate for a short period. Typical results can be seen in Figure 3.5. During the course of the experiment, when perchlorate was present, nitrate exhibited zero-order degradation kinetics, with a rate constant of 0.0207 mg/L-hr.
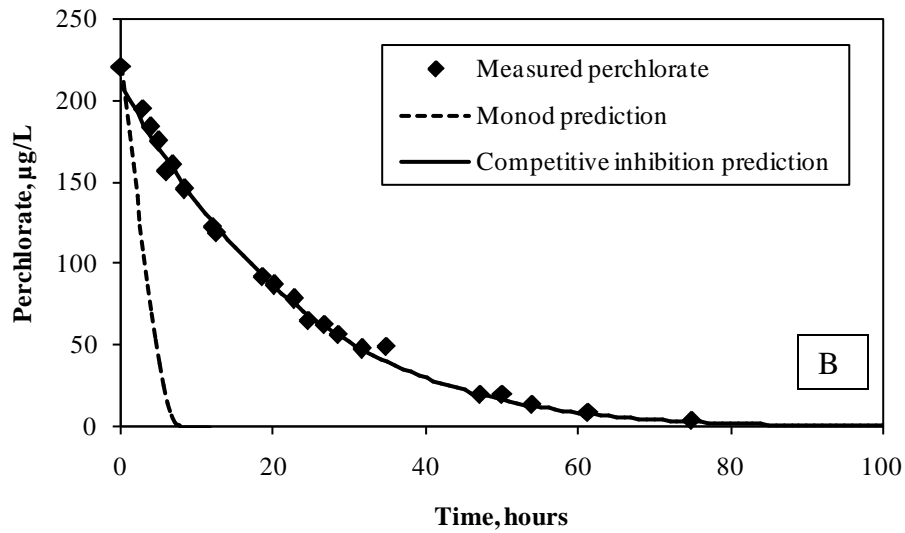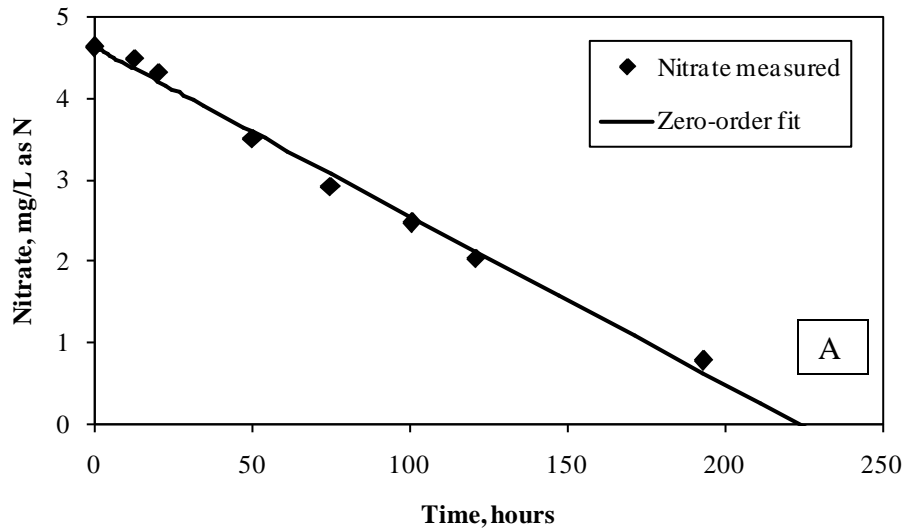
Figure 3.5 (a) Typical nitrate degradation and zero-order fit during a perchlorate-in-the presence-of-nitrate kinetic experiment (b) Typical perchlorate degradation and modified competitive inhibition and Monod model predictions during a perchlorate-in-the-presence-of-nitrate kinetic experiment

(Note: different time scales; initial nitrate concentration 4.6 mg/L as N; initial perchlorate concentration 221 µg/L; biomass concentration 25.1 mg TSS/L)

57

The modified competitive inhibition model was able to successfully predict perchlorate degradation in the presence of nitrate (Figure 3.5a). The modified competitive inhibition model used the perchlorate, biomass, and nitrate concentrations, as well as the single-component perchlorate K_s and k values and the single-component nitrate K_s value to predict perchlorate degradation in the presence of nitrate. Although the competitive inhibition model is an enzyme competition model, it is used here more empirically, as no mechanistic basis for applying the model has been demonstrated.

The perchlorate-in-the-presence-of-nitrate experiments demonstrated the significant competitive/inhibitory effect of nitrate on perchlorate degradation by the microbial consortium. The dashed line in Figure 3.5b shows the predicted perchlorate degradation profile by the Monod model in the absence of nitrate. In the absence of nitrate, complete perchlorate degradation would be expected in approximately 10 hours, whereas approximately 90 hours were actually required at the nitrate concentrations present in these experiments. However, despite the additional time required for completely perchlorate removal, the consortium demonstrated it is capable of significant perchlorate reduction while the bulk of nitrate is still present.

Additional model predictions using the modified competitive inhibition model were conducted for perchlorate concentrations between 25 and 100 µg/L. An initial biomass concentration of 25 mg TSS/L was assumed, and biomass decay and yield were accounted for using the coefficients listed below. These model runs considered biomass decay and growth because of the additional growth expected as a result of the presence of nitrate concentrations several orders of magnitude greater than that of perchlorate.

    (1) perchlorate-reducing, hydrogen-oxidizing microbial consortium endogenous
        decay coefficient: 0.008 1/d (Sanchez, 2003)

(2) perchlorate-reducing, hydrogen-oxidizing microbial consortium yield

coefficient perchlorate – 0.3 mg/mg (Sanchez, 2003)

(3) microbial yield coefficient nitrate – 0.7 mg/mg (Rittmann and McCarty, 2001)

Effectively, in the modified competitive inhibition model, the single-component perchlorate K_s value is altered by the presence of nitrate. The larger the ratio of the nitrate concentration to the single-component nitrate K_s value, the greater its impact on the effective K_s value for perchlorate. Therefore, rates of perchlorate degradation were compared for increasing ratios of the initial nitrate concentration to the single-component nitrate K_s value (ratio). As seen in Figure 3.6, the time required to achieve 99% perchlorate removal (initial perchlorate concentration of 100 µg/L) for ratios of 0.16, 0.33, and 1.6, increased by 15%, 43%, and 295% relative to the time required for 99% perchlorate removal in the absence of nitrate (ratio = 0), respectively. For initial concentrations of 25 µg/L and 50 µg/L, the time required to achieve 99% removal at a ratio of 0.16 increased by 17% and 13% relative to the time required for a ratio of zero. Hence, at a ratio of 0.16 (or possibly lower) the presence of nitrate could become important with respect to perchlorate biodegradation rates.
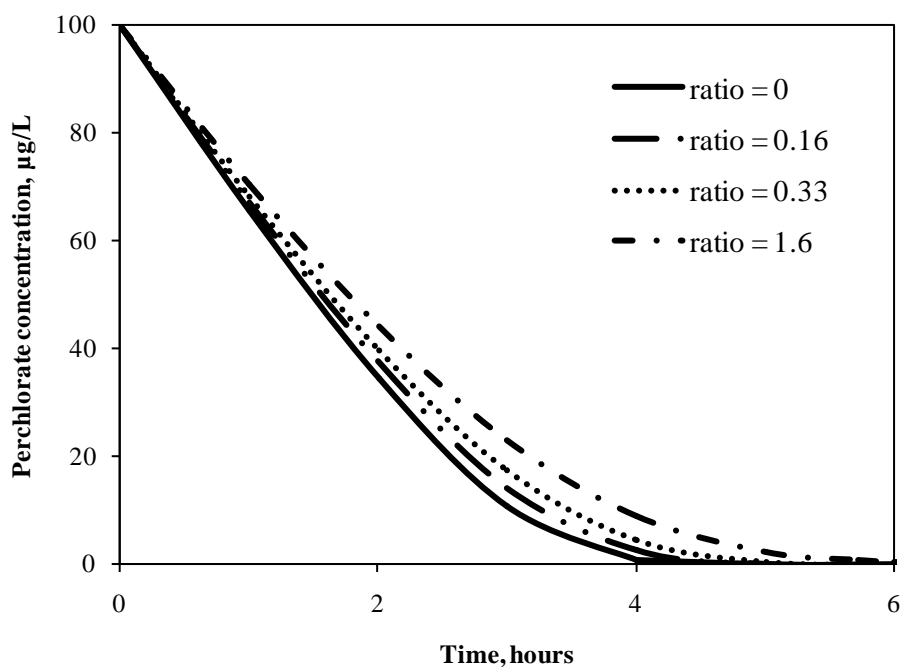
Figure 3.6 Effect of the ratio of initial nitrate concentration to nitrate single-component half-saturation coefficient on rates of perchlorate biodegradation in the presence of nitrate

(initial perchlorate concentration 100 µg/L; initial biomass concentration of 25 mg TSS/L; initial nitrate concentration 4.6 mg TSS/L)

3.3.5. Practical implications of kinetic parameters

The kinetic parameters and models determined could be used to aid in the design of autohydrogenotrophic perchlorate treatment systems, such as biofilm reactors or ZVI permeable reactive barriers (PRB). In practice, in different parts of the reactor or barrier, different substances could be limiting. Hydrogen is expected to be limiting as a result of its limited aqueous solubility, while perchlorate is expected to be limiting because its concentration in contaminated ground and drinking water is typically in the low hundreds of µg/L and 20 µg/L, respectively (Urbansky, 1998; Gullick et al., 2001; Hatzinger, 2005; Wang et al., 2002). The simplest way to account for dual substrate limitation is use of a

multiplicative term. Equations 3.2 and 3.3 below are a multiplicative Monod model for autohydrogenotrophic perchlorate degradation and a multiplicative modified competitive inhibition model for autohydrogenotrophic perchlorate degradation in the presence of nitrate, respectively.

$$r_{ClO_4} = \frac{k_{ClO_4} XS_{ClO_4}}{K_{S_{ClO_4}} + S_{ClO_4}} \frac{S_{H_2}}{K_{S_{H_2}} + S_{H_2}} \qquad \text{Equation 3.2}$$

$$r_{ClO_4} = \frac{k_{ClO_4} XS_{ClO_4}}{K_{S_{ClO_4}} \left(1 + \frac{S_{NO_3}}{K_{S_{NO_3}}}\right) + S_{ClO_4}} \frac{S_{H_2}}{K_{S_{H_2}} + S_{H_2}} \qquad \text{Equation 3.3}$$

3.4. CONCLUSIONS

Kinetic coefficients were successfully determined for an autohydrogenotrophic microbial consortium using the Monod model (or a modified version) under hydrogen-limiting, perchlorate-limiting, and nitrate-limiting conditions. The kinetic parameter values obtained indicate that the microbial consortium may have a competitive advantage over some pure cultures when treating perchlorate-contaminated water with initial concentrations of perchlorate in the low hundreds of μg/L or less and in states with perchlorate treatment goals in the low μg/L range.

Perchlorate-contaminated water is often co-contaminated with nitrate. Results demonstrated the significant competitive/inhibitive effect of nitrate on autohydrogenotrophic perchlorate degradation by the microbial consortium; however, the consortium demonstrated it is capable of significant perchlorate reduction while the bulk

of nitrate is still present. A means to account for and model perchlorate biodegradation in the presence of nitrate was determined. Analysis showed that a modified competitive inhibition model was able to successfully predict autohydrogenotrophic degradation of perchlorate by the consortium in the presence of nitrate using the perchlorate, biomass, and nitrate concentrations, as well as the single-component K_s value for nitrate and the single-component K_s and k values for perchlorate. The modified competitive inhibition model suggests that, for typical perchlorate concentrations less than 100 μg/L, the presence of nitrate will slow perchlorate reduction by the microbial consortium by at least 13% at a value of 0.16 for the ratio of the initial nitrate concentration to the nitrate single-component K_s. As part of a larger design tool, the modified competitive inhibition model and kinetic parameters presented here could aid in predicting performance and enhancing designs of autohydrogenotrophic perchlorate treatment systems.

Chapter 4: Modeling of a ZVI/biotic treatment system for perchlorate-contaminated water

4.1. INTRODUCTION

Perchlorate, ClO_4^-, contamination of ground and surface waters throughout the United States is of significant environmental concern. Perchlorate tends to persist in the aqueous environment under typical ground and surface water conditions because it sorbs weakly to most soil minerals, is highly soluble, and nonreactive (Urbansky, 1998, 2002). Human exposure to perchlorate is of particular concern as it disrupts the uptake of iodide to the thyroid gland and consequently inhibits growth, mental development, and metabolism (NRC, 2005). Most perchlorate-contamination has been attributed to its use as a propellant in the defense and aerospace industries (Gullick et al., 2001); however, naturally-occurring perchlorate, hypothesized to be a result of atmospheric deposition, has also been found in the environment (Dasgupta et al., 2005; Rajagopalan et al., 2006; Rao et al., 2007).

Contaminated ground water perchlorate concentrations are typically in the low hundreds of µg/L (Gullick et al., 2001; Urbansky, 1998) and most drinking water source concentrations are less than 20 µg/L (Hatzinger, 2005; Wang et al., 2008). Federal regulation of perchlorate is still under consideration by the EPA; in the interim the EPA has issued a health advisory level for perchlorate in drinking water of 15 µg/L (USEPA, 2008). However, some states, such as California and Massachusetts, have set their own maximum contaminant levels for perchlorate in drinking water at 6 µg/L and 2 µg/L respectively (CDPH, 2008; MDEP, 2009).

Microorganisms capable of degrading perchlorate are ubiquitous in the environment (Coates and Achenbach, 2004) and autohydrogenotrophic reduction of

perchlorate to chloride has proven effective in the treatment of perchlorate-contaminated water ground and drinking water (Giblin et al., 2000; Logan and LaPoint, 2002; Nerenberg et al., 2002; Sanchez, 2003; Yu et al., 2007). Autohydrogenotrophic systems are particularly well-suited for perchlorate treatment, because of the decreased potential for additional cost, clogging, and contamination issues associated with use of an organic substrate (Giblin et al., 2000; Miller and Logan, 2000). However, the low aqueous solubility of hydrogen has limited the application of autohydrogenotrophic degradation systems.

In-situ generation of hydrogen gas from ZVI corrosion circumvents many of the limitations associated with external gas feeds including explosion and mass transfer concerns. Under anaerobic conditions, iron corrodes and produces hydrogen gas according to Equation 4.1. Previous research has shown that the rate of this reaction is dependent on both the surface area of the iron and the pH of the system (Gould, 1982; Reardon, 1995).

$$Fe^0 + 2H_2O \rightarrow Fe^{2+} + 2OH^- + H_2(g) \qquad \text{Equation 4.1}$$
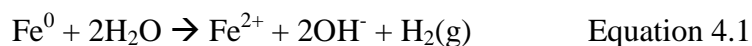
ZVI/biotic treatment systems have proven effective in the treatment of perchlorate-contaminated water in both batch and column studies (Sanchez, 2003; Son et al., 2006; Yu et al., 2006; 2007). Previous research has demonstrated the importance of quantifying the hydrogen production rates and microbial kinetics to assess the long-term viability of a ZVI/biotic treatment system for perchlorate reduction.

In this research, column experiments were conducted using ZVI and a microbial consortium to determine whether perchlorate degradation could be maintained for extended periods. To effectively design ZVI/biotic perchlorate treatment systems, a tool

that can predict long-term system performance is necessary. A biofilm based model was formulated using AQUASIM (Reichert, 1994; 1995) to examine whether the biokinetics determined from batch experiments could be used to describe non-steady-state and steady-state operation of the column. A batch version of the model was initially tested using data from ZVI/biotic experiments conducted by Sanchez (2003). To develop the AQUASIM model; perchlorate- and hydrogen-limiting biodegradation kinetics determined previously for an autohydrogenotrophic microbial consortium (Chapter 3) were used. In addition, hydrogen production rates by ZVI for representative water chemistries and the rate of abiotic perchlorate reduction by ZVI were determined.

4.2. MATERIALS AND METHODS

4.2.1. ZVI hydrogen production kinetics

Hydrogen evolution from ZVI corrosion was studied to investigate the effect of water chemistry on hydrogen production kinetics. Iron was obtained from Peerless Metals and Abrasives (MI) and sieved to retain the -30/+40 fraction. The external surface area of the iron particles (1.1124 +/- 0.0027 m^2/g) was determined by BET analysis (Micrometrics BET Model 2010, nitrogen absorbing gas, 77 K). Batch hydrogen gas production was examined at room temperature under anaerobic conditions in the presence of three different water chemistries: (1) Millipore water (Milli-Q UV Plus 18Ω), (2) phosphate mineral medium (235 mg/L KH_2PO_4, 301 mg/L K_2HPO_4, all reagent grade), and (3) carbonate mineral medium (494 mg/L $NaHCO_3$, 247 mg/L NaCl, all reagent grade). NaCl was added to the carbonate mineral medium to obtain a similar ionic strength to the phosphate mineral medium.

A custom Teflon reactor with a total volume of 660-mL was constructed and leak tested to allow for headspace sampling. A pH of 7 was maintained by addition of 0.1 or 0.5 N HCl (reagent grade) using a pH stat (Titralab 90, Radiometer Analytical). To

continuously mix the solution and avoid magnetic attachment of iron (~ 2.2 m^2) to the stir bar, a polycarbonate frame sieve with polyester mesh (Global Gilson, OH) was used. Prior to each experiment, the medium and reactor components were autoclaved or treated with 70% ethanol. Both the medium and headspace were vigorously purged with high purity nitrogen gas prior to the start of each experiment. Hydrogen gas production was monitored via headspace samples through Teflon-lined septa. Preliminary testing of the system without ZVI demonstrated that losses of hydrogen were less than 2.3×10^{-5} moles over a six-day period.

4.2.2. Abiotic perchlorate reduction by ZVI

A series of batch tests was performed to characterize abiotic-only reduction of perchlorate by the -30/+40 fraction of the Peerless iron filings. Experiments was modeled after those conducted by Moore et al. (2003) in which multiple samples of the filings, background water, and solutes were placed in 20-mL amber glass vials with Teflon-lined septa, placed on a tumbler, and sacrificed periodically. Experiments were conducted at ambient temperature (22°C), and the tumbler was maintained in an anaerobic glove chamber (Labconco, MO). All supplies, including the glove chamber, were autoclaved or by rinsed with 70% ethanol. Triplicate samples were sacrificed at 0, 6, 18, 24, 48, 169, and 338 hours. A variety of background waters were used:

(1) HEPES buffer, perchlorate, and iron

(2) HEPES buffer and iron

(3) HEPES buffer and perchlorate

(4) Millipore water and iron

Each headspace-free vial contained ~8.8 m^2 of iron. The initial perchlorate concentration was 8.5 µM ($NaClO_4^-$, reagent grade), the HEPES (4-(2-hydroxyethyl)-1-piperazineethanesulfonic acid, reagent grade) concentration was 4.2 x 10^{-4} M, and pH was adjusted to 7.48 (the pKa of HEPES buffer at 25°C) using reagent grade NaOH. Perchlorate and its degradation products were monitored.

Each vial was sampled using a sterile syringe. Vials were opened in the anaerobic chamber and filtered through a 0.2-µm membrane filter (Pall Life Sciences, NY) and passed through an On-Guard II H cartridge (Dionex) to remove soluble iron. Any sample not immediately analyzed was stored at 4°C.

4.2.3. Long-term laboratory-scale ZVI/biotic column system

A continuous-flow, ZVI/biotic system to treat perchlorate-contaminated water was built and studied in the laboratory over a period of more than one year. A 5-cm x 30-cm glass column (Ace Glass, NJ) with Teflon end caps was wet packed with the -30/+40 fraction of the ZVI fillings and housed in an anaerobic glove box (Labconco, MO). Table 4.1 details the column characteristics and parameters.

Table 4.1 Laboratory-scale continuous-flow ZVI/biotic column parameters

Parameter	Units	Laboratory-scale ZVI/biotic column
Darcy velocity	m/d	2.2
Column volume	m^3	5.9 x 10^{-4}
Column depth	m	0.30
Empty bed contact time	hrs	3.3
Media size (US stnd. sieve size)	-	30 x 40
Temperature	°C	22

The column was inoculated from a laboratory-maintained microbial consortium previously shown to reduce perchlorate using hydrogen gas as the electron donor (Chapter 3). After addition of a concentrated inoculum, the column feed was re-circulated with a perchlorate concentration of 1000 µg/L for several days. Column feed consisted of Millipore water (Milli-Q UV Plus 18Ω) supplemented with perchlorate, nutrients, and a carbonate/phosphate buffer to simulate natural ground waters as follows: NaClO$_4^-$ (~105 µg/L ClO$_4^-$), 8 mg/L NH$_4$Cl, 10 mg/L KH$_2$PO$_4$, 10 mg/L K$_2$HPO$_4$, 700 mg/L H$_2$CO$_3$, (all reagent grade) and 1 mL/L mineral solution (Chapter 3). Initially, the feed was deoxygenated by vigorous sparging with high purity nitrogen gas and was subject to a continuous slow nitrogen purge; however; lack of sustained oxygen control led to a slight re-design in feed deoxygenation. Instead, deoxygenation was accomplished via a

vigorous purge with high purity nitrogen gas and the feed was maintained under a constant nitrogen pressure of 4 – 5 psi. Additionally, pH control issues led to an adjustment of the feed composition after 220 days of operation.

After 220 days, the column was re-inoculated and re-circulated with a perchlorate concentration of 1000 µg/L for several days. The main adjustment to the composition of the column feed was the addition of the organic buffer HEPES and the adjusted feed composition was as follows: $NaClO_4^-$ (~105 ± 9 µg/L ClO_4^-), 0.01M HEPES (4-(2-hydroxyethyl)-1piperazineethanesulfonic acid), 8 mg/L NH_4Cl, 25 mg/L KH_2PO_4, 25 mg/L K_2HPO_4, 700 mg/L H_2CO_3, (all reagent grade) and 1 mL/L mineral solution.

Column influent and effluent were monitored over time for perchlorate, pH, hydrogen, iron, phosphate, and DO. Headspace-free sampling was accomplished using 50-mL glass barrel syringes. As appropriate, samples were filtered using a 0.2-µm membrane filter (Pall Life Sciences, NY) and passed through a Dionex On-Guard II H cartridge for soluble iron removal. Samples for perchlorate analysis not immediately analyzed were stored at 4°C.

Hydrogen production rates (Equation 4.2) in the column were calculated based on perchlorate, oxygen, and hydrogen mass balances, as well as the column flow rate, mass of iron in the column, and reaction stoichiometry calculated using McCarty's microbial energetic approach (McCarty, 1975). It was assumed that the difference between the influent and effluent oxygen concentrations and the difference between the influent and effluent perchlorate concentrations were a result of autohydrogenotrophic consumption by the microorganisms. The rate was normalized by the mass of ZVI in the column.

$$r_{H_2} = \frac{-QS_{I,H_2} + QS_{E,H_2} + Q(S_{I,O_2} - S_{E,O_2})\gamma_{O_2} + Q(S_{I,ClO_4} - S_{E,O_2})\gamma_{ClO_4}}{M_{ZVI}}$$ Equation 4.2

where:

r_{H_2} = hydrogen production rate in column [$M_{H2}/M_{Fe(0)}T$]

Q = volumetric flow rate of column [L^3/T]

S_{I,O_2} = influent concentration of oxygen [M/T]

S_{I,ClO_4} = influent concentration of perchlorate [M/T]

S_{I,H_2} = influent concentration of hydrogen gas [M/T]

S_{E,O_2} = effluent concentration of oxygen [M/T]

S_{E,ClO_4} = effluent concentration of perchlorate [M/T]

S_{E,H_2} = effluent concentration of hydrogen [M/T]

γ_{O_2} = stoichiometric ratio H_2/O_2 [M_{H2}/M_{O2}]

γ_{ClO_4} = stoichiometric ratio H_2/ClO_4^- [M_{H2}/M_{ClO4}]

M_{ZVI} = mass of ZVI in column [M]

4.2.4. Analytical methods

Hydrogen gas concentrations were analyzed on a Gow-Mac, Series 580 gas chromatograph equipped with a thermal conductivity detector and a Suppelco molecular sieve 13X column. A Henry's constant of 7.9035 x 10^{-4} M/atm at 298.15 K (Lide, 2005) was used for conversion of gas sample concentrations to aqueous phase concentrations in the samples.

Perchlorate, chlorate, chlorite, and chloride concentrations were analyzed using a 1000-µL loop injection on a Dionex DX-600 ion chromatograph equipped with an AMMS III 2-mm conductivity detector suppressor, AS-16 2 x 250 mm column, Dionex

AG-16 2 x 50 guard column, Dionex EGC II KOH eluent cartridge, and AS-40 auto-sampler. The column was regenerated using 50 mN sulfuric acid. DO was measured with an YSI 5905 probe on an YSI 54ARC oxygen meter with a detection limit of 1 mg/L.

4.2.5. Model development

The computer simulation package AQUASIM, was used to model the nonlinear biofilm system (Reichert, 1994; 1995). Biofilm reactor compartments (BRC) were used to simulate biofilm growth dynamics, constant-volume mixed reactor compartments (MRC) were used to simulate hydrogen production from ZVI corrosion, and diffusive links simulated mass transfer of hydrogen from MRCs into the biofilm of the BRCs (Ortiz de Montellano, 2006; Reichert, 1994; 1995; Wanner and Morgenroth, 2004). A mass exchange coefficient between MRCs and BRCs was set at a large value to ensure that mass transfer would not be the rate-limiting step (Table 4.2) (Ortiz de Montellano, 2006).

Table 4.2 Model parameters summary

Model Parameter	Unit	Value	Source
Diffusivity of ClO_4^- in water	m^2/day	1.55×10^{-4}	a
Diffusivity of H_2 (g) in water	m^2/day	4.40×10^{-4}	b
Diffusivity of O_2 (g) in water	m^2/day	2.16×10^{-4}	b
Biofilm to water diffusion coefficients ratio	-	0.80	c
Endogenous decay coefficient	1/d	0.008	d
Volatile suspended to total suspended solids ratio	mg VSS/mg TSS	0.80	c
Cell yield coefficient ClO_4^-	g VSS/g ClO_4^-	0.30	d
Cell yield coefficient O_2	g VSS/g O_2	0.22	e
Number of reactors in series	-	10	
Stoichiometric ratio H_2/ClO_4^-	g H_2/g ClO_4^-	0.134	d
Stoichiometric ratio H_2/O_2	g H_2/g O_2	0.164	e
Maximum bacterial cell density in biofilm	g VSS/m^3	50,000	c
Exchange coefficient – diffusive link	m^3/day	1×10^{11}	
Initial biofilm thickness (fitting parameter)	m	1×10^{-7}	
Initial porosity	-	0.6	

a: Lide, 1994; b: Perry and Green, 2008; c: Rittmann and McCarty, 2001; d: Sanchez, 2003; e: based on calculations using McCarty, 1975

The number of BRC in series was determined by a Li tracer test (1 mg/L, analysis by Perkin-Elmer AA Analyst 600 Atomic Absorption Spectrometer) run at the

completion of the experiment. The actual column porosity at steady-state was determined to be approximately 0.55. The initial column porosity in the model was set at 0.6, so that the porosity calculated at steady-state matched the actual column porosity (i.e., the porosity calculated in the model decreased as the biofilm was established). Measured perchlorate influent concentrations were used as model inputs and interim influent concentrations between measurements were calculated by AQUASIM using linear interpolation.

Each BRC in AQUASIM was selected to be confined, the pore volume set to contain only the liquid phase, and the biofilm matrix characterized as rigid. The geometric mean of the US standard sieve sizes for the ZVI filings was used as the particle radius in AQUASIM's calculation of the biofilm area (Wahman et al., 2007). Biofilm loss was not controlled by the functionality associated with the BRC, and instead a biofilm specific loss rate, b' (Rittmann and McCarty, 2001; Wahman et al., 2007), was used. The biofilm specific loss rate uses biofilm thickness, the endogenous decay coefficient, and shear stress to calculate an overall loss rate. The shear stress expression used to calculate the biofilm specific loss rate differs from the original derivation of Rittmann (1982). The basic difference between the two shear stress expressions is the application of the pressure force. Based on the work of Leva (1959), it was assumed the pressure force acted only on the pore volume. The shear stress derivation of Rittmann (1982) assumes the pressure force acts on the total volume. By assuming the pressure force acts on the total volume, the shear stress expression of Rittmann (1982) overpredicts the shear stress by a factor of porosity^{-1} and b' by a factor of porosity$^{-0.58}$. Table 4.2 summarizes the remaining model inputs necessary to characterize transport equations, growth and of the biofilm, and hydrogen and perchlorate concentrations within AQUASIM.

Multiplicative Monod models for perchlorate and oxygen reduction were incorporated into the model (Table 4.3). The hydrogen and perchlorate half-saturation coefficients (K_s) and maximum substrate utilization rates (k) used in the model were determined previously for the microbial consortium inoculum (Chapter 3) and are reported in Table 4.4. Oxygen kinetic parameters (Table 4.1) were assumed to be identical to the values obtained for nitrate for this microbial consortium (Chapter 3), based on the similarity of kinetic parameters reported for heterotrophic denitrifiers and aerobic heterotrophs (Chen et al., 1989; Goner and Henze, 1991; Rittmann and McCarty, 2001; Tchobanoglous et al., 2003). In previous experiments with a microbial consortium from a similar source, reduction of perchlorate was slowed in the presence of oxygen in a ZVI/biotic continuous-flow column (Sanchez, 2003). Since most oxygen is expected to be degraded prior to perchlorate, an oxygen inhibition term (K_{O2}) (Table 4.4) (Grady et al., 1999) was included in the perchlorate rate expression (Table 4.3). Incorporation of these kinetic expressions and a zero-order hydrogen production rate (Equation 4.2) into AQUASIM allowed prediction of the effluent hydrogen, oxygen, and perchlorate concentrations over time.

74

Table 4.3 Rate expressions for perchlorate and oxygen biodegradation

Chemical	Model	Rate equation
Perchlorate	Multiplicative Monod	$r_{ClO_4} = \dfrac{k_{ClO_4} X S_{ClO_4}}{K_{S_{ClO_4}} + S_{ClO_4}} \; \dfrac{K_{O_2}}{K_{O_2} + S_{O_2}} \; \dfrac{S_{H_2}}{K_{S_{H_2}} + S_{H_2}}$
Oxygen	Multiplicative Monod	$r_{O_2} = \dfrac{k_{O_2} X S_{O_2}}{K_{S_{O_2}} + S_{O_2}} \; \dfrac{S_{H_2}}{K_{S_{H_2}} + S_{H_2}}$

r_{ClO_4}	=	perchlorate utilization rate [M/T]
r_{O_2}	=	oxygen utilization rate [M/T]
r_{H_2}	=	hydrogen production from ZVI corrosion rate [M/T]
k_{ClO_4}	=	perchlorate maximum substrate utilization rate [M/M-T]
X	=	biomass concentration [M/L^3]
$K_{S_{ClO_4}}$	=	perchlorate half-saturation coefficient [M/L^3]
S_{ClO_4}	=	perchlorate concentration [M/L^3]
K_{O_2}	=	oxygen inhibition coefficient [M/L^3]
S_{O_2}	=	oxygen concentration [M/L^3]
S_{H_2}	=	aqueous hydrogen concentration [M/L^3]
$K_{S_{H_2}}$	=	hydrogen half-saturation coefficient [M/L^3]
$K_{S_{O_2}}$	=	oxygen half-saturation coefficient [M/L^3]
k_{O_2}	=	oxygen maximum substrate utilization rate [M/M-T]

Table 4.4 Estimated and assumed microbial kinetic parameters for hydrogen, oxygen, and perchlorate

Parameter	Units	Lower 95%	Mean	Upper 95%
$K_{S_{H_2}}$ [a]	M (aq)	1.50×10^{-6}	2.26×10^{-6}	3.26×10^{-6}
$K_{S_{ClO_4}}$ [a]	µg/L	23.3	28.4	34.4
k_{ClO_4} [a]	µg/mg TSS-hr	1.73	1.81	1.89
$K_{S_{O_2}}$ [b]	mg/L	-	0.28	-
k_{O_2} [b]	mg/mg TSS-hr	-	0.48	-
K_{O_2} [c]	mg/L	-	0.75	-

a: Chapter 4; b: assumed to be same as nitrate parameters from Chapter 3; c: Grady et al., 1999

4.2.6. Sensitivity analysis

Sensitivity analyses were conducted in AQUASIM on the perchlorate, oxygen, and hydrogen microbial kinetic parameters, as well as on the hydrogen production rate, endogenous decay coefficient, initial biofilm thickness, and oxygen inhibition coefficient. Because the parameters undergoing sensitivity analysis were not estimated by the model, a value of 10% for their standard deviation was used as recommended by Reichert (1998). Of the four sensitivity functions available in AQUASIM, the absolute-relative sensitivity function (SENS AR) was utilized. For a 100% change in a model parameter, the SENS AR function calculated the absolute change in the effluent perchlorate concentration.

4.3. RESULTS AND DISCUSSION

4.3.1. Batch hydrogen production kinetic experiments

Batch hydrogen production kinetic experiments were performed to quantify hydrogen production rates from micro-scale ZVI corrosion for varying background water chemistries (carbonate mineral medium, phosphate mineral medium, Milllipore water) and fixed pH. The phosphate and carbonate mineral mediums allowed investigation of the relative impacts of phosphate and carbonate for promoting corrosion and passivating the ZVI surface. The choice of pH and water chemistries were made based on typical ground waters that contain significant carbonate concentrations, as well as interest in using phosphate buffers to control PRB pH.

Although hydrogen concentrations were measured in the gas phase, equivalent aqueous hydrogen production normalized by the total surface area of iron was calculated assuming that Henry's law was valid. The results presented in Figure 4.1 demonstrate two phases of hydrogen gas production were present. An initial rapid hydrogen gas production period was followed by cessation of hydrogen gas production, or, in the case of the carbonate mineral medium, a slower hydrogen production rate. Table 4.5 summarizes the approximate duration of hydrogen production and initial hydrogen production rates by ZVI under each of the different water chemistries.

Table 4.5 Batch ZVI hydrogen production rates under varying water chemistries at a constant pH of 7

Medium	Approximate time to $H_2(g)$ production cessation or rate reduction	Initial $H_2(g)$ production rate
	days	mols H_2/m^2 Fe^0-day
Millipore water	18	6.43×10^{-6}
Carbonate mineral medium	10.5	6.05×10^{-5}
Phosphate mineral medium	3	3.94×10^{-5}
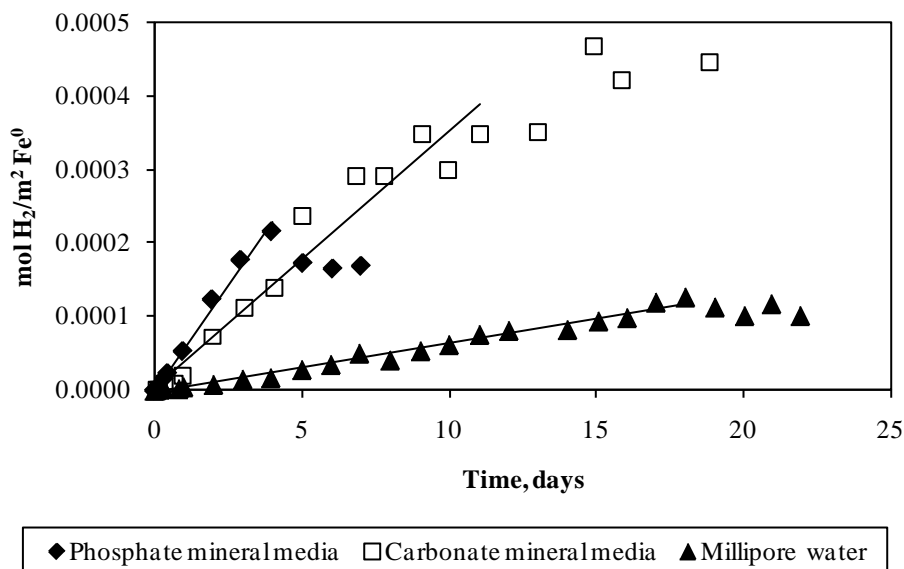
Figure 4.1 Effect of solutes on batch hydrogen production

(lines represent initial hydrogen production rates, equivalent aqueous hydrogen concentration ([mols of H_2 in gas phase + mols of H_2 in liquid phase]/liquid volume)

The observed cessation or slow-down of hydrogen production was hypothesized to be caused by the formation of passivating layers on the surface of the ZVI, preventing further corrosion. To test this hypothesis, scanning electron microscopy images of ZVI from the phosphate medium experiments showed a relatively uniform build up of material on the surface of the iron. Prior to passivation, first-order hydrogen gas production rates in the carbonate and phosphate mineral medium were approximately 6 and 9.5 times faster, respectively, than hydrogen production in Millipore water, and initial hydrogen production in the phosphate mineral medium was approximately 1.5 times faster than initial production in the carbonate mineral medium. Similar patterns of enhanced corrosion of iron metal followed by passivation has been observed for other systems containing carbonate (Agrawal et al., 2002; Gu et al., 1999; Reardon, 1995).

A literature survey of hydrogen production rates for ZVI revealed a large range of values of normalized initial hydrogen gas production rates. The values were on the same order of magnitude as observed in these experiments to more than two orders of magnitude higher and lower than the rates presented in Table 4.5 (Bokermann et al., 2000; Reardon, 1995; Sanchez, 2003).

Based on typical ground water flow rates, reaction stoichiometry, and PRB size, the results indicate that these ZVI filings have the potential to provide the necessary hydrogen concentrations needed for biodegradation of perchlorate if the environmental conditions are favorable. However, concerns associated with passivation must be addressed for long-term operation.

4.3.2. Abiotic reduction of perchlorate

Abiotic experiments were performed to confirm that ZVI is unable to appreciably reduce perchlorate abiotically. Samples containing HEPES buffer, perchlorate, and iron were monitored for perchlorate and its degradation products over time.

Figure 4.2 shows the ratio of perchlorate concentration to the initial perchlorate concentration for solutions containing HEPES buffer/perchlorate and those containing ZVI/HEPES buffer/perchlorate.
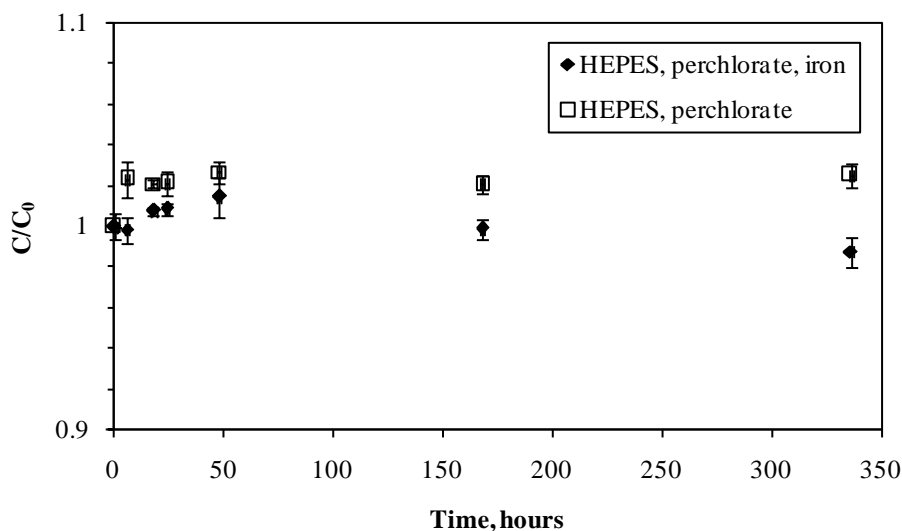
Figure 4.2 Abiotic reduction of perchlorate by ZVI

(error bars represent one standard deviation about the mean for replicate experiments)

The 95% confidence interval for the mean perchlorate concentration at time zero overlapped the 95% confidence interval for the mean concentrations at every other time point. Therefore, no statistically significant degradation was observed, as random

measurement error cannot be rejected as a plausible explanation for any differences in concentration throughout the experiment. These results are consistent with other studies that concluded abiotic reduction of perchlorate by micro-scale ZVI is unfavorable (Moore et al., 2003; Cao et al., 2005; Huang and Sorial, 2007; Son et al., 2006; Schaefer et al., 2007).

4.3.3. Combined ZVI/biotic experiments

Previous research has demonstrated the bioavailability of hydrogen produced from ZVI corrosion for a perchlorate-degrading microbial consortium (Sanchez, 2003), and biokinetic parameters were previously determined for autohydrogenotrophic perchlorate reduction using a microbial consortium from a similar source with an external hydrogen gas feed (Chapter 3). The applicability of the biokinetic parameters determined in Chapter 3 were tested to determine if they could predict perchlorate degradation by the consortium used by Sanchez (2003) when ZVI was used for in-situ hydrogen gas production. Figure 4.3 demonstrates that the rate of degradation of perchlorate is not dependent on the source of hydrogen. The biokinetic parameters reported in Chapter 3 able to successfully predict perchlorate degradation under perchlorate-limiting conditions with excess hydrogen. Hence, the parameters presented in Table 4.4 can be used in a model for zero-valent/biotic perchlorate treatment system design.

Additionally, it should be noted that a period of several years elapsed between the batch experiments of Sanchez (2003) and the studies conducted in Chapter 3, suggesting stability of the consortium over the long-term. Prior to use in the current experiments, the consortium used by Sanchez (2003) was stored at -80°C.
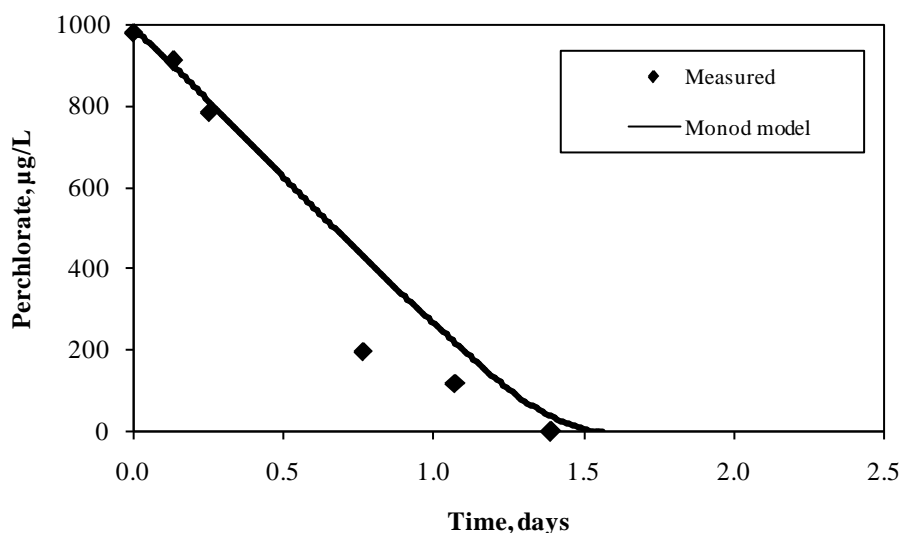
Figure 4.3 Batch ZVI/biotic perchlorate degradation

(Hydrogen produced in excess from corrosion of steel wool (Sanchez, 2003), Monod kinetic parameters from batch perchlorate-limiting experiments with external hydrogen gas feed (Chapter 3))

4.3.4. Long-term laboratory-scale ZVI/biotic column system

A continuous-flow, laboratory-scale column packed with micro-scale ZVI filings and seeded with a microbial consortium previously shown to degrade perchlorate using hydrogen gas (Chapter 3) was used to simulate application of the ZVI/biotic treatment technology. The influent perchlorate concentration was based on typical values in the low hundreds of µg/L (Gullick et al., 2001; Urbansky, 1998) reported for perchlorate-contaminated ground water sites.

The column was operated initially for a period of over 220 days without significant perchlorate reduction. Lack of significant perchlorate reduction is believed to be a result of inactivation of the microbial consortium due to high pH. The average value of the influent pH was 7.9, and the effluent pH had an average value of 9.0. Yu et al.

(2007) noted perchlorate removal efficiency dropped when the influent pH was greater than 7.5 in a ZVI laboratory-scale column inoculated by the pure culture *Dechloromonas* sp. HZ. Effluent hydrogen concentrations over the 220-day period were relatively constant (1.25×10^{-4} M – 6.55×10^{-4} M) with an average aqueous effluent hydrogen concentration of 2.3×10^{-4} M. Based on calculations using the effluent hydrogen concentration, flow rate, and perchlorate biodegradation stoichiometry, excess hydrogen was available for perchlorate degrading microorganisms in the column. The hydrogen production rate in the column was calculated to be at least an order of magnitude greater than what was required to biologically reduce perchlorate in the column. The production rate calculation also revealed hydrogen was produced in excess of what was required to biologically reduce *both* the influent perchlorate and oxygen in the column. Thus, while perchlorate degradation was inhibited, it was apparent that the ZVI media in the column was still operative.

The column was re-inoculated after the pH of the column feed was stabilized (by addition of the organic buffer HEPES). HEPES buffer was selected as it is stable and does not form precipitates or complexes with ferrous iron (Good et al., 1966; Zawaideh and Zhang, 1998). After a start-up period of approximately 60 days, the column achieved excellent removal of perchlorate. The average effluent perchlorate concentration was 7 µg/L (Figure 4.4), the effluent pH was 7.4, the effluent total iron concentration was 11 mg/L, and the effluent DO concentration was typically below the detection limit. Table 4.6 summarizes the apparent steady state performance data for the column. For clarity, data from the acclimation period (0 – 60 days of the second period of column operation) are omitted from Table 4.6.

Hydrogen production (Figure 4.4) did not appear to diminish throughout the entire 230-day operating period following re-inoculation. Aqueous hydrogen concentrations in

the effluent were relatively constant and averaged 4.4×10^{-4} M $\pm 1.3 \times 10^{-4}$ M , as can be seen in Figure 4.4. An F-test was used to determine if the variance in hydrogen concentrations was the same before (initial 220 days) and after the column was actively degrading perchlorate (following 230 days). The 'before' sample was assumed to represent the uncertainty in the hydrogen sampling and measurement process. The 'after' sample represents a system that degrades perchlorate. The F-test showed that the variances were not different at the 5% level. This result implies that variation in the hydrogen concentration under perchlorate degrading conditions falls within the uncertainty of the sampling and measurement process.
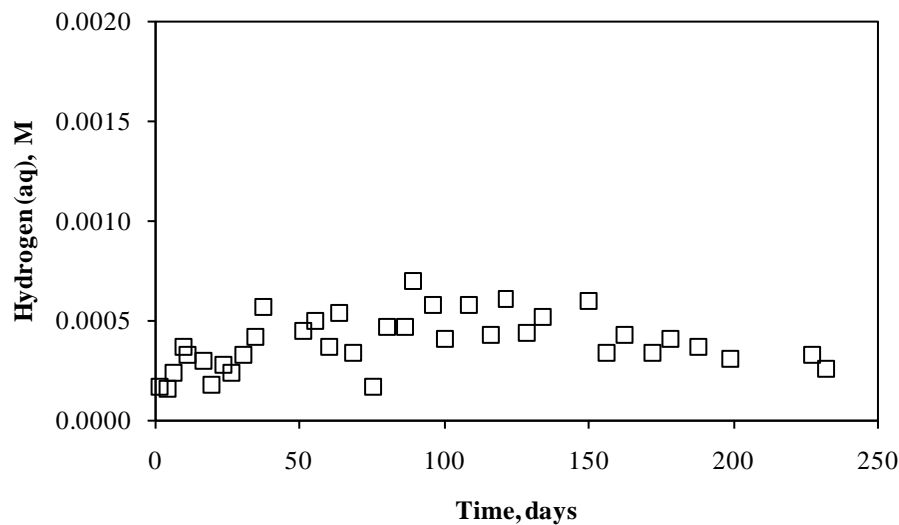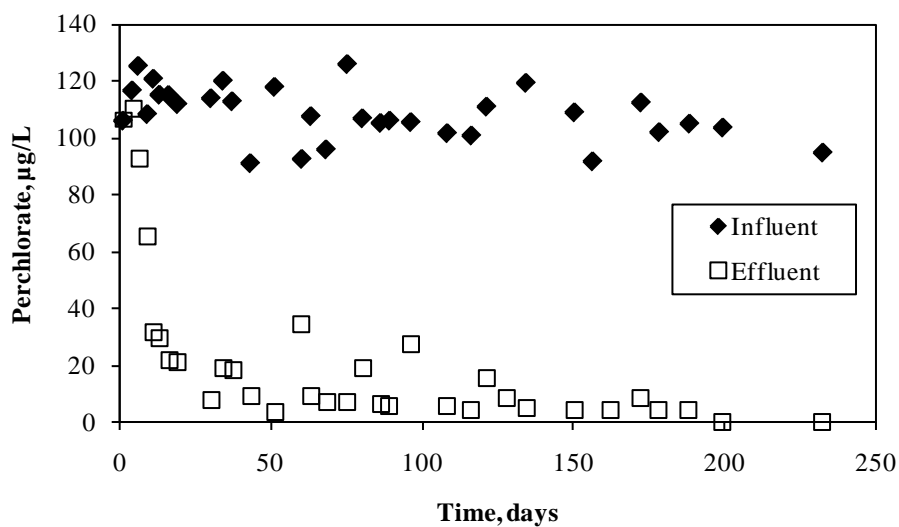
Figure 4.4 Influent and effluent perchlorate concentrations and effluent hydrogen concentrations in the laboratory-scale ZVI/biotic column

(Day 0 corresponds to the day in which the column was re-inoculated and HEPES buffer was introduced in the feed).

85

Table 4.6 Summary of apparent steady-state performance data for ZVI/biotic column system from second period of operation

Parameter	Units	Laboratory-scale ZVI/biotic column
Influent pH	—	7.0 ± 0.2
Effluent pH	—	7.4 ± 0.2
Influent dissolved O_2	mg/L	1.3 ± 0.2
Effluent dissolved O_2	mg/L	below detection limit
Effluent H_2 (aq)	M	$4.4 \times 10^{-4} \pm 1.3 \times 10^{-4}$
Influent ClO_4^-	µg/L	105 ± 9
Effluent ClO_4^-	µg/L	7 ± 7

Hydrogen production was sustained throughout the 450 days of operation of the column. The average effluent hydrogen concentration remained on the order of 10^{-4} M, regardless of whether perchlorate degradation was operative. The average hydrogen production rate in the column was estimated to be 7×10^{-7} mol H_2 (aq)/m^2 Fe^0-day. This production rate is consistent with rates found by other researchers (Bokermann et al., 2000; Reardon, 1995; Yu et al., 2007), but one to two orders of magnitude less than the initial rates obtained in the batch hydrogen production experiments in the phosphate and carbonate mineral media at neutral pH. The concentration of phosphate in the column feed was approximately an order of magnitude lower than in the phosphate mineral

medium and the concentration of carbonate was approximately 1.5 times greater than in the carbonate mineral medium. The presence of greater quantities of phosphate in the phosphate mineral media likely allowed for higher initial hydrogen production in the batch experiments, while the presence of greater quantities of carbonate in the column feed could have decreased the hydrogen production rate in the column feed via passivation of the iron surface.

Zawaideh and Zhang (1998) observed immediate corrosion of iron when HEPES was added to a ZVI/water system. In contrast, hydrogen production rates observed with and without HEPES addition did not vary significantly at neutral pH in this research.

The column performance and hydrogen production data obtained during operation were used to calibrate a model to aid in the design of ZVI/biotic perchlorate treatment systems.

4.3.5. Model verification

An AQUASIM-based model was developed to simulate the non-steady and steady-state behavior of the continuous-flow ZVI/biotic laboratory-column system. The model was created based upon laboratory experiments in an effort to provide a design tool for future treatment systems that can predict the performance of a full-scale system under typical conditions. Abiotic degradation of perchlorate was not accounted for in the model, as it was assumed to be negligible, per the results of the abiotic- perchlorate reduction batch experiments (Section 4.3.2).

The performance of the column was simulated using the parameter values presented in Tables 4.2 and 4.4 and the hydrogen production rate (Section 4.3.4) determined for the column. The initial biofilm thickness was used as a fitting parameter. Figure 4.5 compares the modeled effluent perchlorate and aqueous hydrogen concentrations to experimental observations. The measured and modeled effluent

concentrations closely match one another for both the start-up period and steady-state operation of the column. In both the model and experimental observations, complete removal of perchlorate was seen around day 55. Additionally, the measured and modeled effluent oxygen concentrations closely matched. Effluent oxygen concentrations were typically below analytical detection limits (data not shown).

Intermediate concentrations along the length of the column were not measured. In the model, 80 to 95 percent of the influent perchlorate is biodegraded in the first third of the column (data not shown). Accordingly, in the model the bulk of the biomass is also in the first third of the column. Therefore based on modeling, the column should be able to degrade increased influent perchlorate concentrations.
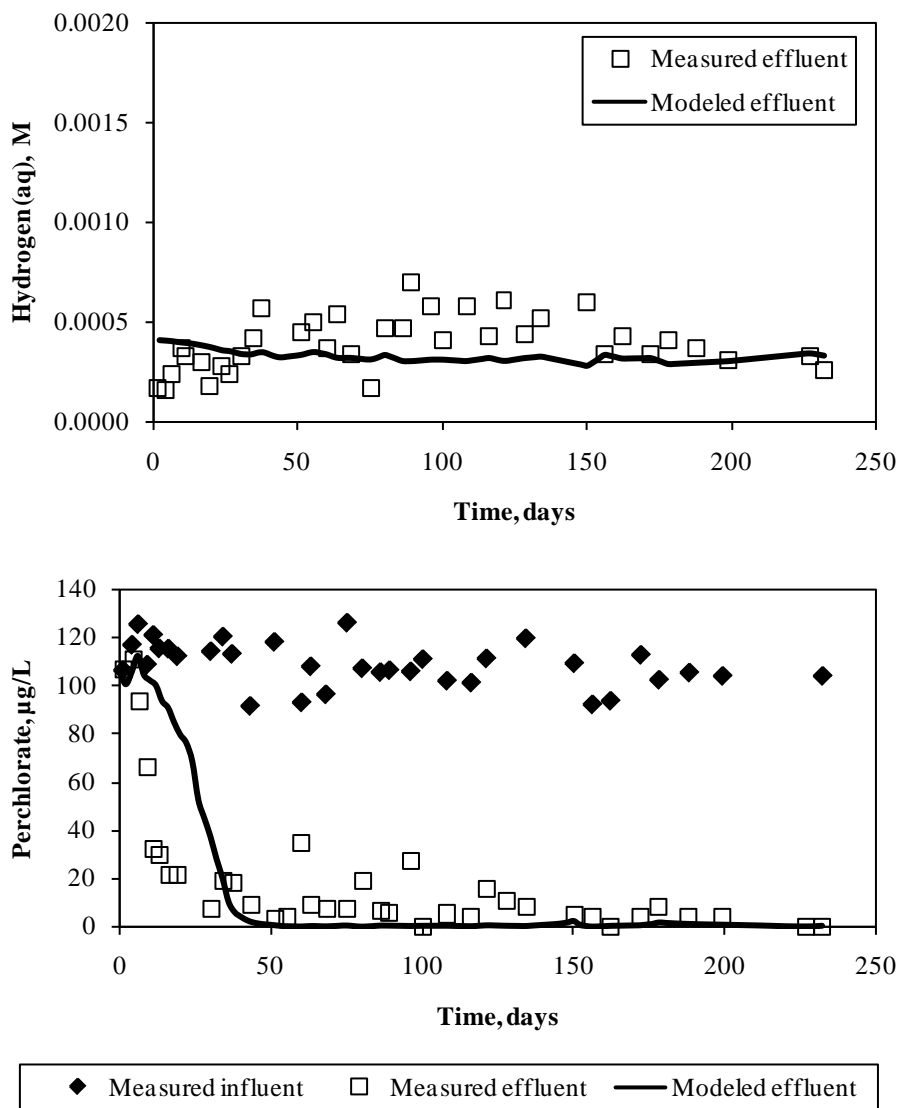
Figure 4.5 Modeled effluent hydrogen and perchlorate concentrations in laboratory-scale ZVI/biotic column

4.3.1.1 Sensitivity Analysis

The impact of each biokinetic parameter on the effluent perchlorate concentration is summarized in Table 4.7. As expected, increasing the perchlorate and oxygen

maximum substrate utilization rates, initial biofilm thickness, oxygen inhibition coefficient, or hydrogen production rate, decreased the effluent perchlorate concentration, whereas increasing the perchlorate and oxygen half-saturation coefficients or the endogenous decay coefficients increased the effluent perchlorate concentration. The half-saturation coefficient and maximum substrate utilization rate are determined simultaneously through fits to experimental data, and their effect on effluent perchlorate concentrations are inversely correlated; changes induced in effluent perchlorate concentrations by one can be balanced by appropriate changes in the other.

The maximum substrate utilization rates of perchlorate and oxygen and the initial biofilm thickness had the largest effect on the predicted effluent perchlorate concentration. The sensitivity of the model to the k value of oxygen is noteworthy given that the biokinetic parameters for oxygen were assumed. Nonetheless, the impact of changing either the perchlorate or the oxygen maximum substrate utilization rates by 100 percent had less than an 11% impact on the effluent perchlorate concentrations throughout the entire period of column operation. Additional analyses were performed varying the oxygen k value by an order of magnitude. The impact of increasing the oxygen k value by an order of magnitude did not significantly affect the effluent perchlorate concentration beyond the impact observed during the original sensitivity analysis.

The minimal impact of the hydrogen production rate can be explained by the excess hydrogen that was produced in the column during the entire period of column operation. Under alternate conditions, such as those in which hydrogen is the limiting substrate instead of perchlorate, the sensitivity of the model to the hydrogen production rate could become significant.

Table 4.7 Average absolute-relative sensitivity values for laboratory-scale column

Parameter	Variable effect value
	ClO_4^- (µg/L)
Maximum substrate utilization rate perchlorate	-10.4
Maximum substrate utilization rate oxygen	-9.7
Initial biofilm thickness	-6.8
Oxygen inhibition coefficient	-3.4
Half-saturation coefficient perchlorate	4.6
Half-saturation coefficient oxygen	1.3
Hydrogen production rate	-1.9
Endogenous decay	2.3
Half-saturation coefficient hydrogen	0.39

negative values indicates effluent perchlorate concentration decreases when parameter increases, positive values indicates effluent perchlorate concentration increases when parameter increases

4.3.1.2 Application of model to other ZVI/biotic perchlorate treatment systems

Yu et al. (2007) ran a column experiment (63-hour empty bed residence time) to simulate in-situ perchlorate treatment using ZVI in a PRB. The bed was inoculated with the known autohydrogenotrophic pure culture *Dechloromonas* sp. HZ. Biodegradation in the column was simulated by the model developed here. Model parameter values were changed to reflect the column geometry and flow conditions, and initial biofilm thickness was used as a fitting parameter since no initial period of column re-circulation was detailed.

First, best-fit Monod kinetic parameters for the Yu et al. (2007) column start-up period (~15 days) were estimated in AQUASIM using non-linear regression for varying values of initial biofilm thickness. In AQUASIM, non-linear regression was performed using the secant algorithm (Ralston and Jennrich, 1978; Reichert, 1998) to minimize the normalized residual sum of squares between predicted and measured concentrations. Normalization was achieved by dividing the residual sum of squares by the measured concentration squared at that time.

The overall best-fit Monod kinetic parameters estimated using AQUASIM were: K_s equal to 8.2 µg/L and k equal to 33.8 µg/mg TSS-hr. While these parameters simulated the effluent perchlorate data reasonably well for the Yu et al. (2007) column start-up period (Figure 4.6), the values are not consistent with the Monod kinetic parameters determined for *Dechloromonas* sp. HZ (HZ) in batch reactors: K_s equal to 8900 µg/L and k equal to 9.2 µg/mg-hr (Yu et al., 2006). This is not surprising given that the initial perchlorate concentration in the column (500 – 700 µg/L) was significantly less than the reported half-saturation coefficient of HZ.

Accordingly, using the same initial biomass thickness associated with the overall best-fit HZ kinetic parameters estimated for the Yu et al. (2007) column start-up period, additional simulations were performed using the Monod kinetic parameters of an autohydrogenotrophic microbial consortium (Table 4.1) (Chapter 3) and an autohydrogenotrophic pure-culture *Dechloromonas* sp. PC1 (PC1) (K_s: equal to 140 µg/L, k: equal to 130 µg/mg-hr) (Nerenberg et al., 2006). These parameter values are more consistent with the best-fit values determined using AQUASIM for the Yu et al. (2007) column start-up period.

However, as can be seen in Figure 4.6, the rate of perchlorate degradation during the start-up period of the column was not sufficiently predicted by either the microbial consortium or PC1. The rate of perchlorate degradation was either too slow (microbial consortium) or too fast (PC1). These results are consistent with the earlier sensitivity analysis performed on the model that determined the model is most sensitive to the maximum substrate utilization rate value for perchlorate

The simulations demonstrate, for successful prediction of system performance and design tool functionality, reliable microbial kinetic parameters for the biotic component of ZVI/biotic treatment systems are necessary. For the system described by Yu et al. (2007), microbial kinetic parameters for HZ at initial concentrations more consistent with the influent perchlorate concentration of the column would need to be determined to model the system effectively.
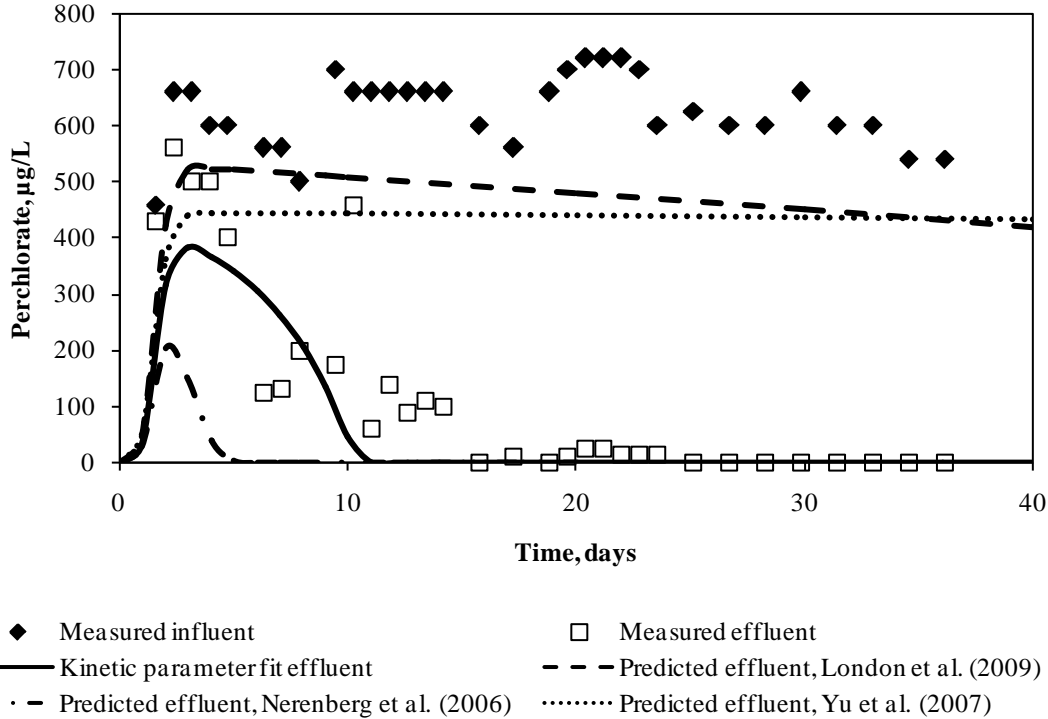
Figure 4.6 Modeled perchlorate biodegradation in ZVI/biotic laboratory-scale column
(Yu et al., 2007), using various Monod kinetic parameters

*(Fit: Monod kinetic parameters for start-up period and initial biofilm
thickness estimated; Predictions: each used initial biofilm thickness estimated
during fit)*

4.3.1.3 Full-scale model runs

Following model verification, multiple full-scale simulations of the ZVI/biotic

treatment process were run to demonstrate that the model could be used as a design tool.

Additionally, simulations were conducted to demonstrate that a full-scale system could

remove typical levels of perchlorate contamination (low hundreds of µg/L) in the

presence of varying oxygen concentrations at neutral pH. The full-scale simulations were

performed for a conservative scenario (Table 4.5) in which a small ZVI PRB (Henderson

94

and Demond, 2007: typical PRB 2 – 50 m long, <1 – 5 m wide, <1 – 10 m deep) was operated at with a 2-day detention time. Operating conditions were varied for the full-scale model runs to determine design requirements such as barrier composition. The model was adjusted such that the barrier could be filled with ZVI only or a mixture of ZVI and other media (e.g., sand/silica). The operating conditions for the full-scale model runs can be seen in Table 4.8. The microbial kinetic parameters determined for the microbial consortium in Chapter 3 were used in the model.

Table 4.8 Full-scale ZVI/biotic model simulation parameters

Parameter	Units	Full-scale ZVI/biotic simulations
Darcy velocity	m/d	1
Volume	m^3	2 (2-m x 1-m x 1-m)
Initial porosity	-	0.6
Media size (Fe^0 and sand/silica) (US standard sieve size)	-	30 x 40
Dissolved oxygen	mg/L	1 – 6
% Fe^0	%	10, 30, 100
Perchlorate concentration	µg/L	100 – 2000

The model predicted complete removal of 100 µg/L of perchlorate at all oxygen concentrations and for a range of ZVI/alternative media. However, the simulations for several of the scenarios exhibited an initial start-up period prior to achieving low effluent concentrations. Figure 4.7 displays effluent perchlorate concentrations for the scenarios with 10% iron with an initial perchlorate concentration of 100 µg/L for all DO concentrations simulated. The model also predicted removal of elevated concentrations of perchlorate (1000 µg/L) to below the EPA perchlorate health advisory level (15 µg/L) for influent DO concentrations as high as 6 mg/L. Thus, this technology should be feasible for contaminated ground waters with typical concentrations of perchlorate and oxygen.

Additional simulations were run to obtain effluent perchlorate concentrations that exceeded the EPA perchlorate health advisory level to determine the maximum perchlorate concentration that could be treated by the conservative PRB simulated. As expected, the smallest initial perchlorate concentration at which breakthrough of perchlorate was predicted was when 10% iron was added with alternative media and the DO concentration was 6 mg/L. For the aforementioned scenario, breakthrough was predicted when the initial perchlorate concentration was increased to 1800 µg/L (effluent hydrogen concentration 3.6×10^{-4} M).
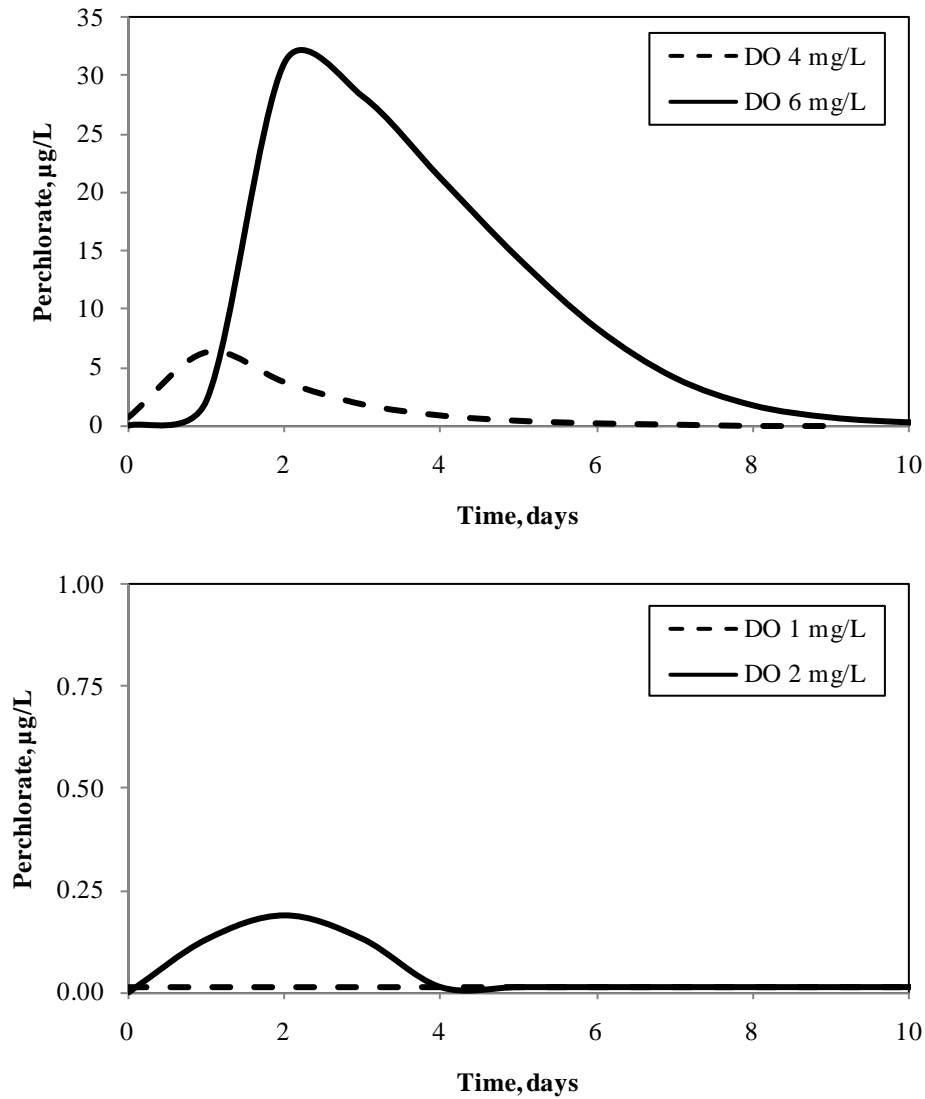
Figure 4.7 Full-scale model runs of a permeable reactive barrier

(Effluent; note different concentration scales; barrier dimensions 2-m x 1-m x 1-m; influent perchlorate concentration of 100 µg/L)

Excess hydrogen was predicted for all scenarios modeled. In fact, when the iron content was 30% or 100% by volume, the predicted effluent hydrogen concentrations

were often greater than the aqueous solubility of hydrogen gas. Predicted excess hydrogen gas concentrations in the effluent may be advantageous in real systems by providing a factor of safety. Theoretically, the rate of hydrogen production is dependent on the pH of the system. However, Reardon (1995), Whitman et al. (1924), and the hydrogen production rates determined in this research indicate that in the pH range of interest (pH 4 – 10) pH is not a major factor in determining anaerobic hydrogen production rates.

Because production of hydrogen by corrosion of ZVI consumes hydrogen ions, in an unbuffered system, excess hydrogen production could cause a pH rise that would inhibit microbial activity. The laboratory-scale ZVI/biotic column was buffered at neutral pH. Therefore, the model developed assumes neutral pH is maintained. Although most current full-scale ZVI PRBs are composed of 100% iron, the full-scale simulations indicate ZVI PRBs can be designed with a small percentage of iron mixed with other materials. Using oxide-based media (e.g. aluminosilicates) is advantageous as it has been shown that protons generated from dissolution of these aluminosilicate materials can help mediate pH rise and enhance corrosion in ZVI systems (Dejournett and Alvarez, 2000; Oh et al., 2007; Powell and Puls, 1997; Powell et al., 1995). Moreover the alternative materials can be used to adsorb precipitates (Oh et al., 2007), reducing passivation of the iron surface.

4.4. CONCLUSIONS

Perchlorate degradation using ZVI and a microbial consortium was maintained in a laboratory-column for over 230 days. Furthermore, relatively constant hydrogen production from ZVI corrosion in column system was sustained over the long-term in the presence of varying pH and both an inorganic buffer (simulated carbonate/phosphate ground water conditions) and subsequently the organic buffer HEPES. These results

suggest that for anaerobic corrosion of ZVI, HEPES buffer does not appear to influence the rate of hydrogen gas production by ZVI.

Experimentation confirmed, as expected, that abiotic reduction of perchlorate by ZVI under typical environmental conditions is negligible. Experimental evidence also supports that pH control is essential for successful operation of the treatment system to maintain an active culture capable of degrading perchlorate.

A biofilm model using AQUASIM was developed to simulate long-term performance of a laboratory-scale continuous-flow ZVI/biotic treatment system for perchlorate-contaminated water. The model was able to successfully integrate physical parameters, hydrogen production from ZVI corrosion, and microbial consortium degradation kinetics. The full-scale model simulations of a PRB in ground water suggest that a barrier that includes 10% by volume of ZVI and an additional media capable of pH buffering would be able to remove up to 1800 µg/L of perchlorate to below the EPA health advisory limit in the presence of 6 mg/L of DO for this microbial consortium.

Modeling of another ZVI/biotic systems described in the literature indicated that reliable kinetic parameters for the biotic component of ZVI/biotic systems are necessary for successful prediction of system performance. It was also shown that perchlorate kinetic parameters obtained for a microbial consortium are valid regardless of hydrogen source (addition through gas phase or from ZVI corrosion).

Chapter 5: Modeling of a ZVI/biotic treatment system for perchlorate-contaminated water in the presence of nitrate

5.1. INTRODUCTION

Perchlorate (ClO_4^-) contamination of ground and surface water is a continually-growing water quality concern throughout the United States. Perchlorate tends to persist in the aqueous environment under typical ground and surface water conditions because it sorbs weakly to most soil minerals, is highly soluble, and nonreactive (Urbansky, 1998, 2002). Most perchlorate contamination has been attributed to its use as a propellant in the defense and aerospace industries (Gullick et al., 2001), though recent studies have hypothesized that perchlorate in the environment is also a result of atmospheric deposition (Dasgupta et al., 2005; Rajagopalan et al., 2006; Rao et al., 2007). Exposure to perchlorate can interfere with the uptake of iodide by the thyroid gland, potentially affecting thyroid hormone production (NRC, 2005). This is of particular concern because thyroid hormones are crucial for fetal and neonatal development (Charnley, 2008).

Federal regulation of perchlorate is still under consideration by the EPA; in the interim the EPA has issued a health advisory level for perchlorate in drinking water of 15 µg/L (United States Environmental Protection Agency, 2008). However, some states, like California and Massachusetts, have set their own maximum contaminant levels for perchlorate in drinking water at 6 µg/L and 2 µg/L respectively (CDPH, 2008; MDEP, 2009).

Autotrophic microbial reduction of perchlorate to chloride utilizing hydrogen gas has proven effective in the treatment of perchlorate-contaminated water (Giblin et al., 2000; Logan and LaPoint, 2002; Nerenberg et al., 2002; Sanchez, 2003; Yu et al., 2007).

Under anaerobic conditions, hydrogen gas can be produced via the corrosion of ZVI according to Equation 5.1.

$$Fe^0 + 2H_2O \rightarrow Fe^{2+} + 2OH^- + H_2(g) \qquad \text{Equation 5.1}$$
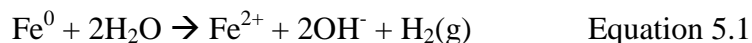
In-situ generation of hydrogen gas via a ZVI corrosion process was previously shown to provide sufficient hydrogen to maintain perchlorate reduction in column studies (Sanchez, 2003; Son et al., 2006; Yu et al., 2007). For example, Yu et al. (2007) evaluated the effects of operational variables, such as residence time and influent pH, on laboratory-scale, ZVI/biotic columns. In Chapter 4 a non-linear biofilm model was developed that was able to successfully fit long-term performance data of a laboratory-scale, continuous-flow ZVI/biotic treatment system for perchlorate-contaminated water and simulate examples of full-scale system performance. The model successfully integrated physical parameters, hydrogen production from ZVI corrosion, and batch microbial consortium degradation kinetics.

While previous studies support the development of ZVI treatment systems for perchlorate remediation, few studies have quantified the impact of competing electron acceptors (e.g., nitrate) on the bioreduction of perchlorate. Nitrate is often a present as a co-solute in perchlorate-contaminated waters as a result of extensive applications of fertilizer (Nolan et al., 1997), and it is usually present at concentrations several orders of magnitude greater than that of perchlorate (Gu et al., 2002a; Kimbrough and Parekh, 2007). Nitrate co-contamination is of considerable concern because it has been shown to inhibit biological perchlorate reduction in autohydrogenotrophic systems (Nerenberg et al., 2002; van Ginkel et al., 2008; Yu et al., 2006; Yu et al., 2007).

Another factor that must also be considered in treating waters containing both perchlorate and nitrate using ZVI is the potential for abiotic reduction. Multiple researchers have demonstrated that abiotic reduction of perchlorate by ZVI is not favorable (Cao et al., 2005; Huang and Sorial, 2007; Moore et al., 2003; Schaefer et al., 2007; Son et al., 2006). Conversely, successful reduction of nitrate to ammonium or nitrite by ZVI for ground water applications has been demonstrated under a variety of conditions (e.g., Siantar, 1996; Alowitz and Scherer 2002), and combined ZVI/biotic systems have shown higher nitrate removal than ZVI-only systems (Dejournett and Alvarez, 2000; Gandhi et al., 2002; Ginner et al., 2004). Thus, the contribution of abiotic reduction of nitrate should be considered during the design and operation of ZVI systems.

The research presented in this chapter extends the work of Chapter 4 by incorporating the impact of nitrate on perchlorate reduction in a ZVI/biotic laboratory column. To this end, increasing concentrations of nitrate were added to the influent of a ZVI column reactor that had been treating µg/L concentrations of perchlorate for over seven months. The effect of nitrate was assessed based on its impact on perchlorate reduction and hydrogen availability. Furthermore, the role of hydrogen availability was assessed by simulating results using the column model developed in Chapter 4. The model was expanded to include abiotic and biotic nitrate reduction and the modified competitive inhibition microbial kinetic model. Model simulations of perchlorate, nitrate, and hydrogen effluent concentrations were performed to characterize the complex relationship between perchlorate and nitrate reduction and associated biotic and abiotic processes in zero-valent iron/biotic perchlorate treatment systems.

5.2. MATERIALS AND METHODS

5.2.1. Long-term laboratory-scale ZVI/biotic column system

The effect of nitrate on ZVI/biotic treatment of perchlorate-contaminated water was studied using the laboratory column system first utilized by. A 5-cm x 30-cm glass column (Ace Glass, NJ) with Teflon end caps was originally wet-packed with sieved ZVI fillings (30 x 40 mesh, Peerless Metals and Abrasives, MI) and housed in an anaerobic glove box (Labconco, MO). The surface area of the iron particles, as determined by BET analysis (Micrometrics BET Model 2010, N_2 adsorbing gas, 77 K), was $1.1124 +/- 0.0027$ m^2/g. The continuous-flow column was originally inoculated from a laboratory-maintained microbial consortium previously shown to reduce perchlorate and nitrate using hydrogen gas as the electron donor (Chapter 3). The column had been successfully treating synthetic perchlorate-contaminated ground water for a period of greater than 230 days prior to the addition of nitrate. Sustained, relatively constant hydrogen production in the column, was achieved for over 450 days prior to addition of nitrate. Table 5.1 summarizes the column and apparent steady-state performance parameters for the column system prior to the addition of nitrate.

Table 5.1 Summary of laboratory-scale ZVI/biotic column and apparent steady state performance parameters prior to the addition of nitrate

Parameter	Units	Laboratory-scale ZVI/biotic column
Darcy velocity	m/d	2.2
Volume	m^3	5.9×10^{-4}
Depth	m	0.30
Empty bed contact time	hrs	3.3
Media size (US standard sieve size)	—	30 x 40
Temperature	°C	22
Influent pH	—	7.0 ± 0.2
Effluent pH	—	7.4 ± 0.2
Influent dissolved O_2	mg/L	1.3 ± 0.2
Effluent dissolved O_2	mg/L	below detection limit
Effluent H_2 (aq)	M	$4.4 \times 10^{-4} \pm 1.3 \times 10^{-4}$
Influent ClO_4^-	µg/L	105 ± 9
Effluent ClO_4^-	µg/L	7 ± 7

Column feed consisted of Millipore water (Milli-Q UV Plus 18Ω) supplemented with perchlorate, nitrate, nutrients, HEPES buffer, and carbonate/phosphate concentrations typical of natural ground waters as follows: ClO_4^- (106 ± 12.6 µg/L ClO_4^-), $NaNO_3$ (0 – 8 mg/L as N), 0.01M HEPES (4-(2-hydroxyethyl)-1-piperazineethanesulfonic acid), 8 mg/L NH_4Cl, 25 mg/L KH_2PO_4, 25 mg/L K_2HPO_4, 700 mg/L H_2CO_3, all reagent grade; 1 mL/L mineral solution without Fe. The average influent pH was 7.1 ± 0.2 and the average influent DO concentration 1.6 ± 0.5 mg/L.

Nitrate was added to the influent feed of the existing column on Day 239 at a concentration of 2 mg/L as N and was increased progressively to a concentration of 8 mg/L as N on day 289 as described below.

(1) day 239 – 258: 2.0 ± 0.15 mg/L as N

(2) day 258 – 276: 3.8 ± 0.42 mg/L as N

(3) day 276 – 287: 7 mg/L as N

(4) day 287 – 330: 7.9 ± 0.26 mg/L as N

On day 330 nitrate was removed from the influent, and the column feed contained perchlorate at a concentration of approximately 100 µg/L.

Column influent and effluent were monitored over time for perchlorate, nitrate, pH, hydrogen, total iron, and DO. Headspace free sampling was accomplished using 50-mL glass barrel syringes. As appropriate, samples were filtered using a 0.2-µm membrane filter (Pall Life Sciences, NY) and passed through a Dionex On-Guard II H cartridge for soluble iron removal. Samples for perchlorate and nitrate analysis not immediately analyzed were stored at 4°C.

5.2.2. Surface analysis

To physically and chemically characterize the surface of the iron from the laboratory-scale column, Scanning Electron Microscopy and Electron Dispersive X-ray Spectroscopy (SEM/EDS) were performed. A LEO 1530 scanning electron microscope equipped with an IXRF Systems model 500 Energy Dispersive X-ray Spectrometer was used to obtain images of the iron particles at various magnifications (40X – 8000X) at an energy of 10kV, as well as elemental changes in the chemical composition of the surfaces at an energy of 20kV. A Gresham Sirius 10/7.5 x-ray detector and EDS 2008 software were also used**.**

SEM images were used qualitatively to study the morphological and topographical characteristics of the iron surface, while EDS was used to analyze the chemical composition of the different solids on the iron surface. Samples of virgin ZVI and samples taken from the column inlet and outlet were analyzed. Iron samples from the column inlet and outlet were collected inside the anaerobic glove chamber immediately after flow to the column was terminated (~750 days of column operation, ~200 days after nitrate was removed from column influent). Samples were freeze dried and stored under vacuum until analysis. Prior to analysis, samples were attached to an aluminum stub using colloidal graphite.

For each of the temporal and spatially different samples, three different regions of the sample were analyzed using EDS. Triplicate analyses were performed on each of these regions.

5.2.3. Model development

The ZVI/biotic perchlorate reduction model developed in Chapter 4 was expanded to account for the presence of nitrate. Table 5.2 summarizes the additional model inputs required to characterize biological growth, substrate utilization, and transport equations

within AQUASIM when nitrate is present. Multiplicative models for perchlorate, nitrate, and oxygen reduction were incorporated into the model (Table 5.3). A modified competitive inhibition model was used to simulate perchlorate biodegradation in the presence of nitrate (Chapter 3). In the absence of nitrate, the modified competitive inhibition model collapses to the Monod model for perchlorate biodegradation. Incorporation of these kinetic expressions and a zero-order hydrogen production rate into AQUASIM allowed prediction of the effluent hydrogen, oxygen, nitrate, and perchlorate concentrations over time. Additional model development details can be found in Chapter 4.

Table 5.2 Additional ZVI/biotic system parameters when nitrate is present

Model Parameter	Unit	Value	Source
Diffusivity of NO_3^- in water	m^2/day	1.64×10^{-4}	a
Cell yield coefficient NO_3^-	g VSS/g NO_3^--N	0.7	b
Stoichiometric ratio H_2/NO_3^--N	g H_2/g NO_3^--N	0.7	c
$K_{S_{NO_3}}$	mg as N/L	0.153 (0.0385 – 0.388)*	d
k_{NO_3}	mg as N/mg TSS-hr	0.0139 (0.0125 – 0.0167)*	d

a: Lide, 1994; b: based on calculations using McCarty, 1975 c: Sanchez, 2003; d: This work; *: 95% joint confidence limits

Table 5.3 Rate expressions for perchlorate, nitrate, and oxygen biodegradation and hydrogen production

Description	Model	Rate equation
Perchlorate Utilization Rate [M/T]	Multiplicative Modified Competitive Inhibition	$r_{ClO_4} = \dfrac{k_{ClO_4} \, XS_{ClO_4}}{K_{S_{ClO_4}}\left(1 + \dfrac{S_{NO_3}}{K_{S_{NO_3}}}\right) + S_{ClO_4}} \quad \dfrac{K_{O_2}}{K_{O_2} + S_{O_2}} \quad \dfrac{S_{H_2}}{K_{S_{H_2}} + S_{H_2}}$
Nitrate Utilization Rate [M/T]	Multiplicative Monod	$r_{NO_3} = \dfrac{k_{NO_3} \, XS_{NO_3}}{K_{S_{NO_3}} + S_{NO_3}} \quad \dfrac{S_{H_2}}{K_{S_{H_2}} + S_{H_2}}$
Oxygen Utilization Rate [M/T]	Multiplicative Monod	$r_{O_2} = \dfrac{k_{S_{O_2}} \, XS_{O_2}}{K_{S_{O_2}} + S_{O_2}} \quad \dfrac{S_{H_2}}{K_{S_{H_2}} + S_{H_2}}$
Hydrogen Production Rate [M/T]	Zero-order	$r_{H_2} = K_{H_2} M_{ZVI}$

X	=	biomass concentration [M/L^3]
k_{ClO_4}	=	perchlorate maximum substrate utilization rate [M/M-T]
k_{NO_3}	=	nitrate maximum substrate utilization rate [M/M-T]
k_{O_2}	=	oxygen maximum substrate utilization rate [M/M-T]
$K_{S_{ClO_4}}$	=	perchlorate half-saturation coefficient [M/L^3]
$K_{S_{NO_3}}$	=	nitrate half-saturation coefficient [M/L^3]
$K_{S_{O_2}}$	=	oxygen half-saturation coefficient [M/L^3]
$K_{S_{H_2}}$	=	hydrogen half-saturation coefficient [M/L^3]
S_{ClO_4}	=	perchlorate concentration [M/L^3]
S_{NO_3}	=	nitrate concentration [M/L^3]
S_{O_2}	=	oxygen concentration [M/L^3]
S_{H_2}	=	aqueous hydrogen concentration [M/L^3]
K_{O_2}	=	oxygen inhibition coefficient [M/L^3]
K_{H_2}	=	zero-order hydrogen production coefficient [M/M-T]
M_{ZVI}	=	mass of ZVI [M]

Abiotic degradation of perchlorate was not accounted for in the model, as it was assumed to be negligible, per results of abiotic perchlorate reduction experiments (Figure 4.2). A first order rate coefficient for abiotic nitrate reduction of 5.3 day^{-1} was adapted from data for Peerless brand iron (same brand and similar surface area iron used in this research) and MOPS buffer from Alowitz and Scherer (2002). While this value was obtained from experiments using MOPS buffer (50 mM) at a pH of 7, their results demonstrated that the impact of iron brand was greater than that of buffer type.

5.2.4. Sensitivity analysis

Sensitivity analyses were conducted for perchlorate, DO, nitrate, and hydrogen microbial kinetic parameters, as well as the hydrogen production rate, endogenous decay coefficient, abiotic nitrate reduction rate, and oxygen inhibition coefficient for the period immediately before, during, and immediately after nitrate addition. Since the parameters undergoing sensitivity analysis were not estimated by the model, a value of 10% for their standard deviation was used as recommended by Reichert, 1998). Of the four sensitivity functions available in AQUASIM, the absolute-relative sensitivity function (SENS AR) was utilized. For a 100% change in a model parameter, the SENS AR function calculated the absolute change in the effluent perchlorate concentration.

5.2.5. Analytical methods

Hydrogen gas concentrations, perchlorate concentrations, DO, and pH were measured using the methods described by Chapter 4. Nitrate was measured using a 500-µL loop injection on a Dionex DX-600 IC, equipped with a Dionex ASRS Ultra II 4-mm conductivity detector suppressor, Dionex AS-11 4 x 250 mm column, Dionex AG-11 2 x 50 mm guard column, Dionex EGC II KOH eluent cartridge, and Dionex AS-40 auto-sampler. OnGuard II H cartridges (Dionex, IL) were used to remove soluble iron from

109

solution prior to perchlorate and nitrate IC analysis. The detection limit is 0.0065 mg/L as N.

5.3. RESULTS AND DISCUSSION

5.3.1. Long-term laboratory-scale ZVI/biotic column system

The continuous-flow, laboratory-scale ZVI/biotic column previously treating synthetic perchlorate-contaminated ground water (Chapter 4) was used to study application of the treatment technology in the presence of nitrate. Over the period in which nitrate was present in the column feed, the average effluent pH and DO were 7.3 ± 0.1 and below the detection limit of 1 mg/L, respectively.

Prior to the addition of nitrate, complete removal of influent perchlorate was observed (Figure 5.1a, Phase I). In the presence of 2 mg/L nitrate as N, the column system was capable of simultaneously degrading all of the influent perchlorate and nitrate (Figure 5.1a, Phase II). As the influent nitrate concentration was increased up to 8 mg/L as N (Figure 5.1a, Phases III and IV), the column system lost its ability to completely degrade perchlorate in the presence of nitrate. The loss of perchlorate degradation was consistent with an increase in the effluent nitrate concentration from the column. The system failure was attributed to hydrogen gas limitations, as the effluent hydrogen gas concentrations began to decrease (Figure 5.1b, Phase III) and eventually fell below the detection limit (Figure 5.1b, Phase IV). After nitrate was removed from the influent, 100% removal of perchlorate was achieved (Figure 5.1a, Phase V). Effluent hydrogen concentrations (Figure 5.1b, Phase V) also returned to levels observed prior to the addition of nitrate (Figure 5.1b, Phase I), indicating that the reduction in effluent hydrogen during the period of nitrate addition was due to rate limitations rather than iron passivation.

The decrease in perchlorate degradation due to hydrogen limitations confirms that nitrate is the preferred electron acceptor for this consortium. Indeed, approximately 70% of the influent nitrate concentration was removed on average, while only approximately 27% of the influent perchlorate concentration was removed on average after day 294 (Phase IV) when the influent nitrate concentration was approximately 8 mg/L as N (Figure 5.1 (a & b), Phase IV). Batch microbial kinetic experiments (Chapter 3) also support the observation that nitrate, present at concentrations several orders of magnitude greater than that of perchlorate, inhibits perchlorate removal.
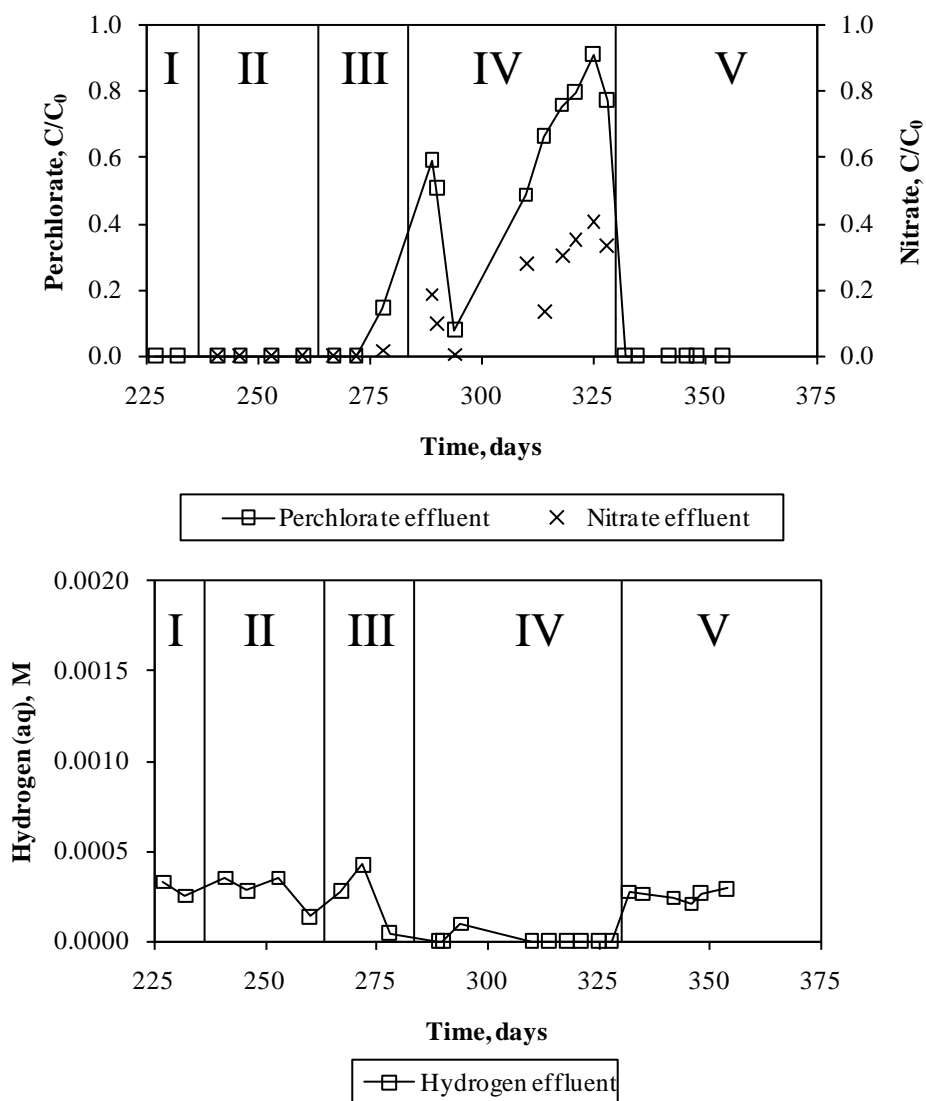
Figure 5.1 a) Perchlorate and nitrate removal and b) aqueous hydrogen gas effluent for ZVI/biotic column

(influent perchlorate concentration ~ 106 ± 12 µg/L throughout entire period; nitrate influent concentrations varied as follows – Phase I: 0 mg/L as N, Phase II: 2.0 ± 0.15 mg/L as N, Phase III: 3.8 ± 0.42 mg/L as N (last data point 7 mg/L as N), Phase IV: 7.9 ± 0.26 mg/L as N, Phase V: 0 mg/L as N)

112

5.3.2. Model results

The ZVI/biotic treatment system model developed and calibrated in Chapter 4 was run for all the nitrate feed phases to predict reactor performance. Figure 5.2a displays the measured and predicted aqueous hydrogen concentrations in the column effluent. Figures 5.2b and 5.2c show the measured and predicted effluent perchlorate and nitrate concentrations, respectively. Figure 5.2c also shows model predictions over the same period for strictly abiotic nitrate reduction by ZVI. Consistent with the measured data, predictions of effluent oxygen concentrations were below the detection limit (1 mg/L) throughout the experiment (data not shown).

Figure 5.2 demonstrates the predictive capabilities of the model. When effluent hydrogen concentrations are predicted well, the predicted effluent perchlorate and nitrate concentrations closely match observed concentrations (end of Phase IV, Figure 5.2). However, when the hydrogen concentration is not predicted well (underpredicted in Phases II, III, beginning of Phase IV), the model tends to overpredict effluent perchlorate and nitrate concentrations.

Although the observed effluent perchlorate concentrations were not affected by the initial addition of nitrate (beginning of Phase II), the model predicted a spike in the effluent perchlorate concentration when nitrate was added to the system. The spike in modeled perchlorate concentration on day 310 (Figure 5.2b, Phase IV) is a result of a concomitant spike in the influent perchlorate concentration of 149 µg/L, for which the model continued to overpredict effluent perchlorate concentrations. The model predicts that both abiotic and biotic degradation of nitrate are operative throughout the experiment (Figure 5.2c). On average, 41% of the influent nitrate removal (Phases II, III, IV) predicted by the model is from abiotic reduction.
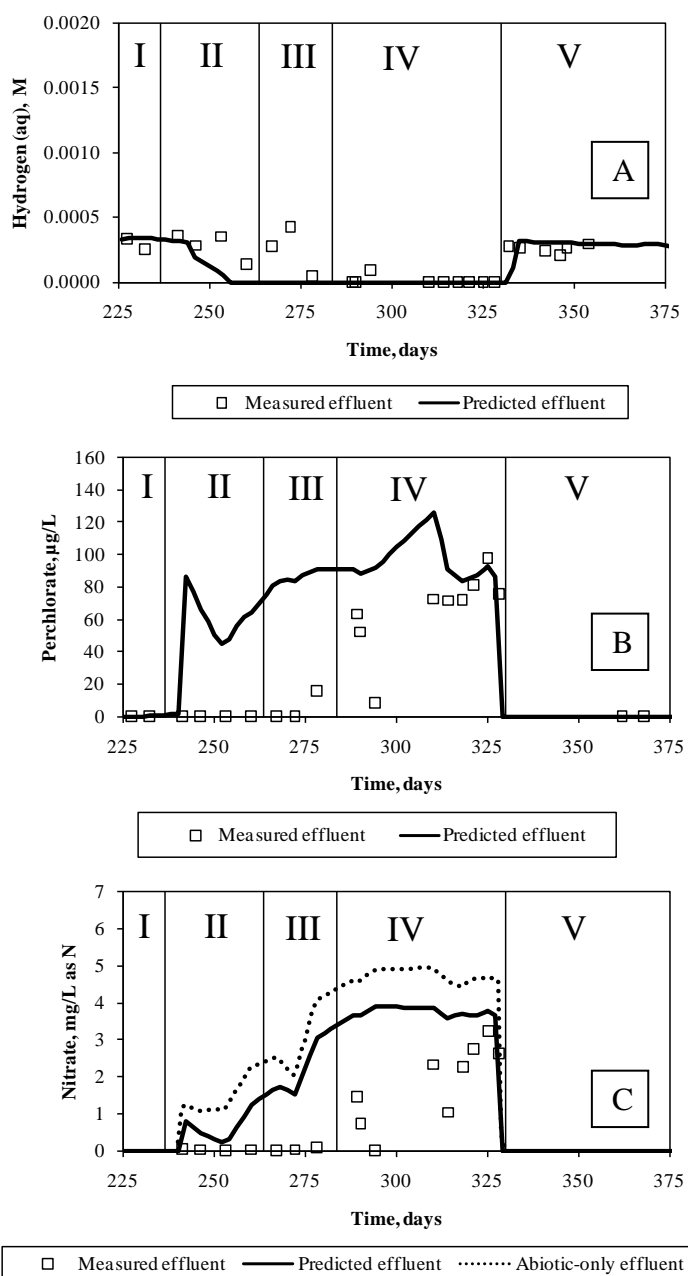
Figure 5.2 Predicted aqueous hydrogen gas, perchlorate, and nitrate effluent (with and without biotic reduction) from continuous flow ZVI/biotic column

(influent perchlorate concentration ~ 106 ± 12 μg/L throughout entire time period; nitrate influent concentrations varied as follows – Phase I: 0 mg/L as N, Phase II: 2.0 ± 0.15 mg/L as N, Phase III: 3.8 ± 0.42 mg/L as N (last data point 7 mg/L as N), Phase IV: 7.9 ± 0.26 mg/L as N, Phase V: 0 mg/L as N)

Discrepancies between measured and predicted effluent perchlorate concentrations for nitrate removal could be attributed to an underestimation of the abiotic rate of nitrate reduction used in the model, underestimation of hydrogen gas generation predicted by the model, or both. The reaction mechanism responsible for nitrate reduction by ZVI is not adequately understood (Mishra and Farrell, 2005; Rodríguez-Maroto et al., 2009), and the rate of abiotic nitrate reduction by ZVI directly affects effluent nitrate concentrations and indirectly affects effluent perchlorate concentrations.

In addition, the actual hydrogen generation rate calculated in the reactor may have increased beyond the zero-order hydrogen production rate included in the model, leading to the additional perchlorate and nitrate degradation observed. Evidence for enhanced hydrogen production in the presence of biomass has been demonstrated in previous studies (Belay and Daniels, 1990; Till et al., 1998; van Nooten et al., 2008) and has been attributed to the destruction of the passivating cathodic H_2 layer, which in turn increases the flow of electrons via cathodic depolarization. The model predicts that the biofilm thickness in the last half of the column increases by an order of magnitude during the period of nitrate addition, thus potentially increasing the hydrogen generation rate because of the presence of additional biomass.

Figure 5.2a reveals the model predicts hydrogen is depleted in the reactor on approximately day 255, while actual observations indicate that hydrogen concentrations fall below detection limits on day 289. Simulations performed using increased hydrogen production rates demonstrate that increasing the hydrogen production rate when nitrate is present delays hydrogen depletion (Figure 5.3a) and the effluent hydrogen concentrations more closely match the observed concentrations in Phases II, III, and IV (no nitrate present in Phase I and V). Additionally, by increasing the hydrogen production rate the predicted perchlorate and nitrate profiles more closely match observed concentrations.

Thus, the hydrogen production rate in the model may need to be adjusted for scenarios in which perchlorate and nitrate are likely to be present in excess of hydrogen availability.
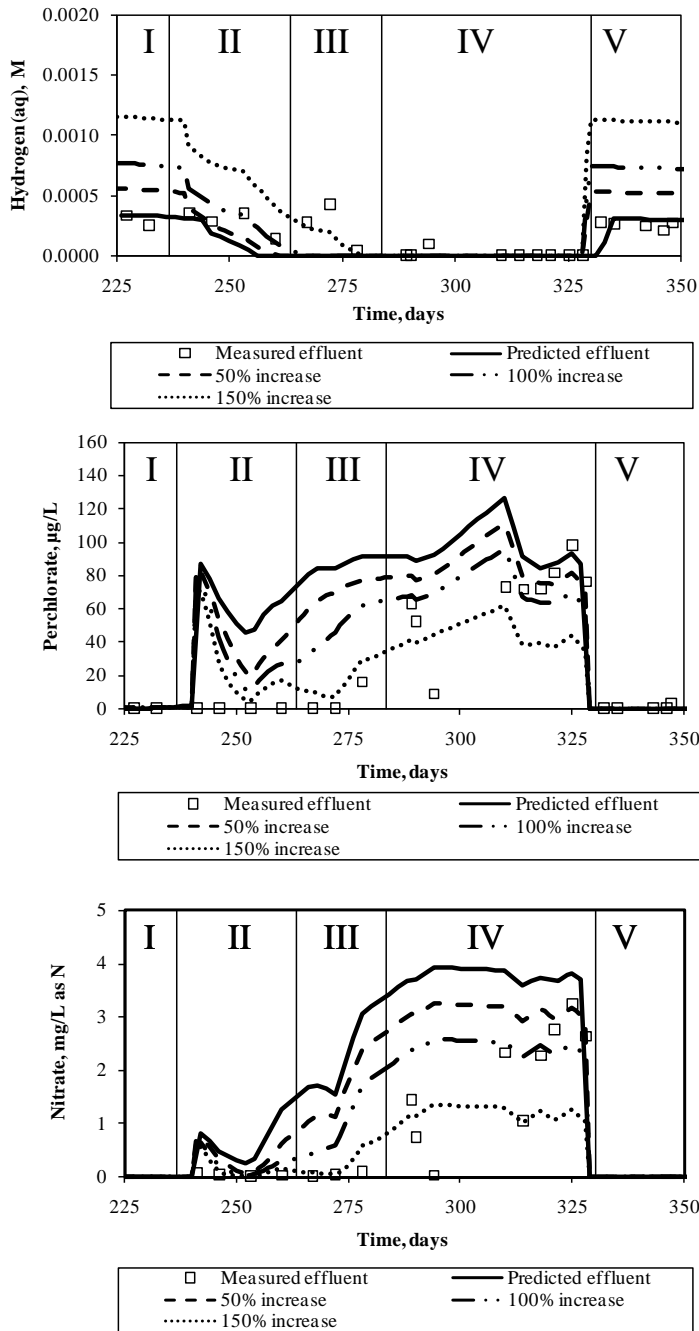
Figure 5.3 Predicted a) hydrogen b) perchlorate c) nitrate effluent from continuous flow ZVI/biotic column with increasing hydrogen production rate coefficients

(influent perchlorate concentration ~ 106 ± 12 μg/L throughout entire period; nitrate influent concentrations varied as follows – Phase I: 0 mg/L as N, Phase II: 2.0 ± 0.15 mg/L as N, Phase III: 3.8 ± 0.42 mg/L as N (last data point 7 mg/L as N), Phase IV: 7.9 ± 0.26 mg/L as N, Phase V: 0 mg/L as N)

5.3.2.1 Sensitivity analysis

The impact of each biokinetic parameter on the effluent perchlorate and nitrate concentrations is summarized in Table 5.4. The sensitivity analysis shows that oxygen inhibition becomes insignificant when nitrate is present at concentrations several orders of magnitude greater than perchlorate (e.g., perchlorate sensitivity < 1 μg/L and 0.05 mg/L as N, respectively). The sensitivity analysis results further illustrate the effect of the hydrogen production rate on predicted effluent perchlorate and nitrate concentrations. Effluent perchlorate concentrations are most sensitive to the hydrogen production rate followed by the microbial kinetic parameters for perchlorate and nitrate and the abiotic nitrate reduction rate. Effluent nitrate concentrations are most sensitive to the abiotic nitrate reduction rate and hydrogen production rate. In contrast, model predictions of the effluent perchlorate concentration were insensitive to the hydrogen production rate in the absence of nitrate (Chapter 4), when excess hydrogen was produced through the entire period of column operation.

Table 5.4 Average absolute-relative sensitivity values for laboratory-scale column

Parameter	Variable effect value	
	ClO_4^- (μg/L)	NO_3^- (mg/L as N)
Hydrogen production rate	-34.7	-1.1
Maximum substrate utilization rate perchlorate	-19.5	0.0034
Half-saturation coefficient perchlorate	15.8	-0.26
Maximum substrate utilization rate nitrate	14.5	-0.090
Half-saturation coefficient nitrate	-15.2	-0.016
Abiotic nitrate rate coefficient	-6.70	-1.48
Maximum substrate utilization rate oxygen	0.679	0.042
Oxygen inhibition coefficient	-0.902	-0.026
Half-saturation coefficient oxygen	-0.103	-0.0011
Half-saturation coefficient hydrogen	0.362	0.0039
Endogenous decay	0.124	0.0012

negative value indicates effluent perchlorate or nitrate concentration decreases when parameter increases, positive value indicates effluent perchlorate concentration increases when parameter increases

5.3.2.2 Application of model to other ZVI/biotic perchlorate treatment systems

To demonstrate the applicability of the model to general ZVI/biotic perchlorate/nitrate systems, the model was applied to a short residence time experiment (Column C) conducted by Yu et al. (2007). Column C was inoculated with soil to provide a microbial to degrade perchlorate and nitrate. Model parameters were changed to reflect the geometry and flow conditions of Column C. The column had already been in operation for 55 days prior to the addition of nitrate and therefore, the initial biofilm thickness was used as a fitting parameter. During the five days preceding the addition of nitrate, the column was able to achieve near complete removal of perchlorate. During nitrate addition, abiotic nitrate reduction was considered negligible because of the short column residence time (empty bed residence time equal to 17 minutes) as compared to the abiotic nitrate reduction rate in the model. Additionally, because the column contained a microbial consortium, the Monod kinetic parameters for a microbial consortium (Table 5.4) determined in Chapter 3 were used.

The influent perchlorate concentration was 30 µg/L throughout the entire period of nitrate addition, and influent nitrate concentrations were as follows (day 0 = start of nitrate addition, ~40 days total):

- day 0 – day 25: 0 – 0.34 mg/L as N
- day 25 – day 29: 0.45 – 1.1 mg/L as N
- day 29 – day 33: 2.3 – 2.9 mg/L as N
- day 33 – 40: 5.7 – 6.1 mg/L as N

From the results of Yu et al. (2007), effluent perchlorate concentrations were estimated at 6 µg/L or less over the first ~ 33 days of nitrate addition, and during the last 6 days of

nitrate addition the effluent perchlorate concentration was approximately 15 μg/L. Figure 5.4 demonstrates for a different ZVI/biotic treatment system, the model was able to successfully match observed effluent perchlorate concentrations in the presence of nitrate.
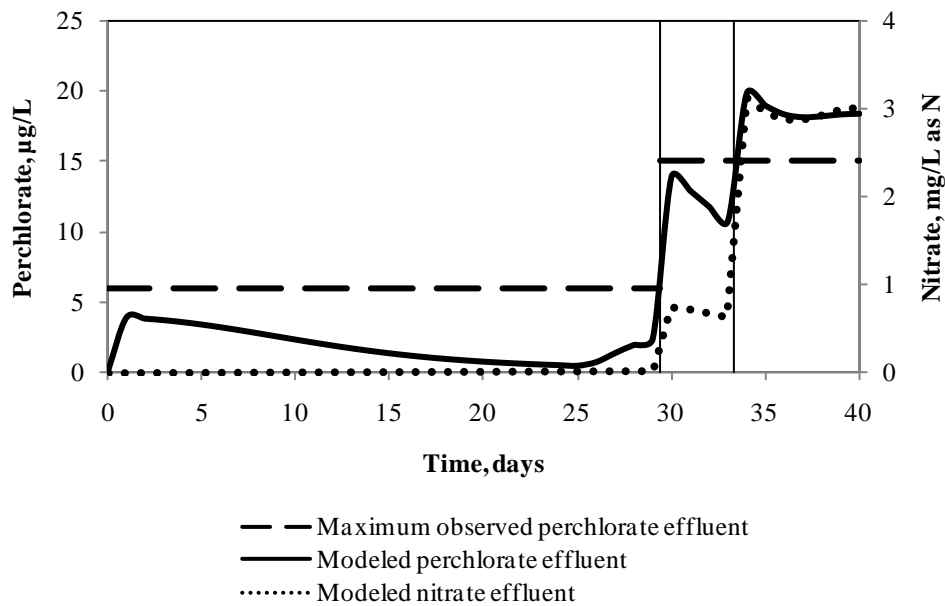
Figure 5.4 Modeled perchlorate and nitrate effluent for short-residence time column with microbial consortium (Column C) (Yu et al., 2007)

(no abiotic nitrate degradation assumed; initial biomass thickness used as a fitting parameter; Chapter 3 perchlorate and nitrate kinetic parameters; influent perchlorate concentration throughout entire time period ~30 μg/L; influent nitrate concentration Phase I: 0 – 1.13 mg/L as N, Phase II: 2.3 – 2.9 mg/L as N, Phase III: 5.7 – 6.1 mg/L as N; measured effluent perchlorate concentration Phase I: < 6 μg/L (9 data points), Phase II: no effluent concentration reported Phase III: 15 μg/L (1 data point); no nitrate effluent concentrations reported)

Although Yu et al. (2007) did not report effluent nitrate and hydrogen concentrations, model simulations were run for nitrate degradation (Figure 5.4) and

121

effluent hydrogen concentrations in Column C. After the influent nitrate concentration was increased above 2.3 mg/L as N, the effluent concentrations of both perchlorate and nitrate increased and the effluent concentrations of hydrogen decreased in the model. In the model, at the end of the 40-day nitrate addition period the column is hydrogen-limited (data not shown). The results of this modeling effort were consistent with the conclusion of Yu et al. (2007) that to achieve additional perchlorate removal in Column C at nitrate concentrations greater than 5.9 mg/L as N, longer detention times would be required.

5.3.2.3 Full-scale model runs

Multiple full-scale simulations of the ZVI/biotic treatment process were run to demonstrate the application of the model as a design tool. Additionally, simulations were conducted to assess whether a full-scale system could achieve adequate removal at typical levels of perchlorate contamination (low hundreds of µg/L) in the presence of varying oxygen and nitrate concentrations at neutral pH.

The full-scale simulations were performed for a conservative scenario (Table 5.5) in which a relatively small ZVI PRB (Henderson and Demond, 2007: typical PRBs are 2 – 50 m long, <1 – 5 m wide, <1 – 10 m deep) was operated with a 2-day detention time. The model predicted complete removal of 100 µg/L of perchlorate, for all nitrate and oxygen concentrations, as well as all mixtures of iron and alternative media. However, the simulations for several of the scenarios exhibited an initial start-up period prior to achieving low effluent concentrations.

Table 5.5 Full-scale ZVI/biotic model simulation parameters

Parameter	Units	Full-scale ZVI/biotic simulations
Darcy velocity	m/d	1
Volume	m^3	2 (2-m x 1-m x 1-m)
Initial porosity	-	0.6
Media size (Fe^0 and sand/silica) (US standard sieve size)	-	30 x 40
DO	mg/L	1 – 6
Nitrate concentration	mg/L as N	0 – 20
% Fe^0	%	10, 30, 100
Perchlorate concentration	µg/L	100 - 1000
Temperature	°C	22

Additional simulations using the minimal PRB design were run to obtain downstream perchlorate concentrations of greater than 15 µg/L (the current health advisory level for perchlorate set by the EPA) to determine the highest influent perchlorate concentration the PRB could potentially treat. As expected, the smallest initial perchlorate concentration at which breakthrough (> 15 µg/L) of perchlorate was predicted, was when 10% of iron was used and the initial DO and nitrate concentrations

were 6 mg/L and 20 mg/L as N, respectively. For the aforementioned scenario, breakthrough was predicted when the initial perchlorate concentration was increased to 600 μg/L (effluent hydrogen concentration 1.6×10^{-4} M). These conditions may represent a conservative estimate because the presence of nitrate may increase the hydrogen production rate coefficient above what is currently included in the model, as hypothesized for the laboratory column.

Because production of hydrogen by corrosion of ZVI consumes hydrogen ions, in an unbuffered system, excess hydrogen production could cause a large enough pH rise that would inhibit microbial activity. Furthermore, abiotic nitrate degradation by ZVI could be inhibited because the reaction rate is pH dependent. The laboratory-scale ZVI/biotic column was buffered at neutral pH and therefore the model developed assumes neutral pH is maintained. Although most current full-scale ZVI PRBs are composed of 100% iron, full-scale simulations indicate that PRBs with a small percentage of iron mixed with other materials is feasible. Using oxide-based media (e.g., aluminosilicates) is advantageous, as it has been shown protons generated from dissolution of these materials can help mediate pH rise and enhance corrosion in ZVI systems (Dejournett and Alvarez, 2000; Oh et al., 2007; Powell and Puls, 1997; Powell et al., 1995). Moreover the alternative media can be used to adsorb precipitates (Oh et al., 2007), reducing passivation of the iron surface and extending the life of the barrier.

5.4. SURFACE ANALYSES

Both the laboratory column data and subsequent modeling demonstrate that effective perchlorate degradation in the presence of nitrate over the long-term depends on adequate and sustained hydrogen concentrations. The presence of surface precipitates

could lead to eventual passivation of the iron surface, resulting in decreased hydrogen production and thus decreased treatment system performance.

For the laboratory column system, SEM analysis of virgin ZVI and inlet and outlet samples confirmed the presence of surface coatings (Figure 5.6). Inlet samples appear to be coated at least partially by a biofilm (Figure 5.6b). Column samples were collected approximately 200 days after nitrate had been removed from the influent feed. Accordingly, most of the biological perchlorate removal was assumed (and simulated by modeling) to have occurred well before the outlet of the column. Therefore, a biofilm was not expected on the surface of the iron at the column outlet.

The laboratory-column was able to sustain hydrogen production for over 750 days, indicating the iron surface was not subject to extensive passivation. The lack of extensive passivation over the entirety of the iron surface of the outlet samples was demonstrated by similar EDS elemental ratios. EDS ratios of Fe/O and Fe/C for both the virgin iron surface and some locations on the surface of the outlet samples were found to be approximately 1.0 and 5.4, respectively.

EDS analysis also revealed some precipitates on the surface of the outlet sample with an average Fe/P ratio of 1.8. Fe/P ratios of 1.8 are consistent with the formation of iron (III) phosphate solids. These iron (III) phosphate solids are likely an artifact from the initial 220 days of column operation when effluent dissolved oxygen concentrations were measured in the column effluent (Chapter 4). Effluent phosphate concentrations were below detection limits (0.15 mg/L). Using an influent phosphate concentration of 3.3×10^{-1} M PO_4^{3-} and an effluent total iron concentration of 2×10^{-4} M at neutral pH, the system was oversaturated with respect to iron phosphate.
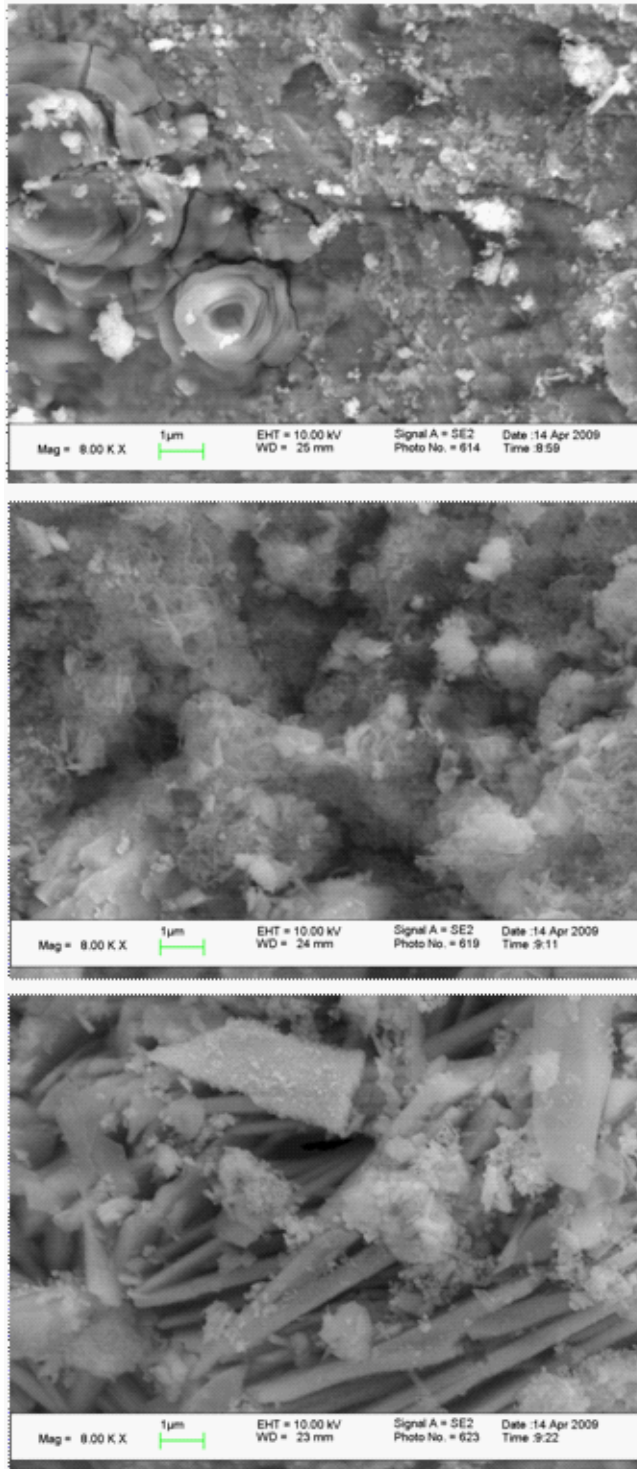
Figure 5.6 SEM images of iron surface at magnification 8,000x a)virgin iron b)column inlet c)column outlet

5.5. CONCLUSIONS

Experimentation performed to develop the model confirmed that perchlorate degradation is inhibited in the presence of nitrate. Sufficient residence time must be provided or sufficient hydrogen gas produced to ensure that adequate perchlorate removal will occur. Furthermore, hydrogen production from ZVI corrosion in the column system was sustained over the long-term (~750 days), and the presence of nitrate at concentrations several orders of magnitude greater than the perchlorate concentration, may have increased the zero-order hydrogen production rate observed in the column as compared to when only perchlorate was present.

If an adequate hydrogen production rate is used in the model, such that effluent hydrogen concentrations predicted match those concentrations observed, the biofilm model developed can successfully predict long-term performance of the laboratory-scale, continuous-flow ZVI/biotic treatment system for perchlorate-contaminated water in the presence of nitrate. The model was also successfully applied to another ZVI/biotic column discussed in the literature. The model was able to successfully integrate physical parameters, hydrogen production from ZVI corrosion, microbial consortium degradation parameters, and the modified competitive inhibition model for perchlorate degradation in the presence of nitrate.

The ability to predict long-term performance is essential in designing effective autohydrogenotrophic treatment systems for perchlorate-contaminated water that use hydrogen gas produced from ZVI corrosion. The model developed could be used as a design tool for pilot- and full-scale treatment systems. The full-scale model simulations of a ground water PRB, suggest for this microbial consortium that a PRB that includes 10% ZVI and an additional media capable of pH buffering would be able to remove up to

600 µg/L of perchlorate in the presence of oxygen and nitrate concentrations of 6 mg/L and 20 mg/L as N, respectively.

Chapter 6: Conclusions and Recommendations

The purpose of this research was to develop (1) models to describe dual substrate limitation from hydrogen and perchlorate, as well as nitrate inhibition/competition, on autohydrogenotrophic perchlorate degradation kinetics and (2) a model to function as a design tool to predict long-term system performance of ZVI/biotic perchlorate treatment systems in the presence of nitrate. The approach was to first perform a series of batch experiments to determine single-component biokinetic parameters under hydrogen-, perchlorate-, and nitrate-limiting conditions for an autohydrogenotrophic microbial consortium. This was followed by characterizing and modeling the effect of nitrate on perchlorate biodegradation by the consortium. Subsequently, laboratory column experiments were conducted to study perchlorate degradation and hydrogen production rates in ZVI/biotic treatment systems with and without the presence of nitrate. Finally, a biofilm-based model of ZVI/biotic treatment systems for perchlorate-contaminated water in the presence of nitrate was formulated and verified using biokinetic models and results from the experimental components.

6.1. CONCLUSIONS

- The kinetic parameter values determined for the microbial consortium along with model simulations predict the consortium should be able to successfully biologically treat perchlorate-contaminated water with initial perchlorate concentrations in the low hundreds of µg/L or lower and in states with perchlorate treatment goals in the low µg/L range.

129

- Nitrate at a concentration several orders of magnitude greater than that of perchlorate had a significant competitive/inhibitive on autohydrogenotrophic perchlorate degradation by the microbial consortium. However, the consortium demonstrated it is capable of significant perchlorate reduction while the bulk of nitrate is still present. A means to account for and model perchlorate biodegradation in the presence of nitrate was determined.

- A modified competitive inhibition model can successfully predict autohydrogenotrophic degradation of perchlorate by the microbial consortium in the presence of nitrate. The model describes perchlorate degradation as a function of the biomass, perchlorate, hydrogen, and nitrate concentrations, as well as the single-component perchlorate, hydrogen, and nitrate half-saturation coefficients and single-component perchlorate maximum substrate utilization rate.

- Long-term perchlorate degradation in the presence of nitrate in a laboratory-scale ZVI column system can be maintained if the pH is sufficiently buffered and sufficient hydrogen gas is available. pH control is essential for successful operation of the treatment system to maintain an active culture capable of degrading perchlorate. When hydrogen gas is limited, perchlorate reduction will be inhibited by the presence of nitrate.

- Hydrogen production from ZVI corrosion can be sustained over the long-term. Relatively consistent hydrogen production in the presence of varying pH and both an inorganic buffer and the organic buffer HEPES suggests, for

anaerobic corrosion of ZVI, that HEPES buffer does not influence the rate of hydrogen gas production.

- A non-linear biofilm model developed using AQUASIM was developed to simulate long-term performance of a laboratory-scale ZVI/biotic treatment system for perchlorate-contaminated water with and without the presence of nitrate. The model was able to successfully integrate physical parameters, hydrogen production from ZVI corrosion, and microbial consortium degradation kinetics. The model was also able to successfully applied to a ZVI/biotic system degrading perchlorate in the presence of nitrate reported in the literature by another research group (Yu et al., 2007).

- Model validation indicated that reliable kinetic parameters for the biotic component of ZVI/biotic systems are necessary to successful model system performance. It was also shown that perchlorate kinetic parameters obtained for a microbial consortium are valid regardless of hydrogen source (addition through gas phase or from ZVI corrosion).

- The hydrogen production rate from ZVI corrosion in the column system may have increased in the presence of nitrate because of the presence of additional biomass.

- Full-scale model simulations of a PRB in ground water suggest that a PRB that includes a small percentage of ZVI and additional media capable of pH buffering would be able to remove typical contaminated ground water concentrations of perchlorate in the presence of typical oxygen and nitrate concentrations.

6.2. RECOMMENDATIONS FOR FUTURE WORK

The most significant contributions of this research were the development of a model that accounts for dual limitation from hydrogen and perchlorate and predicts autohydrogenotrophic perchlorate degradation in the presence of nitrate, as well as development of a model to predict long-term performance of ZVI/biotic perchlorate treatment systems in the presence of nitrate. Most of the recommendations for future work outlined below are related to the refinement of the ZVI/biotic model inputs. Additional recommended future work could potentially improve overall process performance and identify novel perchlorate-reducing microorganisms.

6.2.1. Molecular biology

Based on kinetic parameters, the microbial consortium may have a competitive advantage over some autohydrogenotrophic pure cultures in systems with lower initial perchlorate concentrations and/or when perchlorate regulatory limits are in the low µg/L range. Therefore, further characterization of the microorganisms present in the microbial consortium inoculum is recommended. Genera or strains of previously documented or novel perchlorate-reducing microorganisms could be identified that are best suited for environments with low-levels of perchlorate contamination. This could be accomplished

through the isolation of pure cultures, performing additional T-RFLP analyses, and/or generating clone libraries.

In any future ZVI/biotic perchlorate experiments, molecular analyses should be expanded to characterize not only the microbial consortium inoculum, but the initial communities established in the column, and the cultures present in the column under differing conditions such as with and without the presence of nitrate. Comparison of the microorganisms present in the inoculum and those present in the column, could provide insight into the apparent selection of hydrogen-oxidizing cultures that are most suited for perchlorate/nitrate degradation using hydrogen gas generated by the corrosion of ZVI.

Furthermore, in future column studies it is recommended molecular analyses (density of biomass, types of microorganisms) are also used to characterize the microorganisms with respect to reactor depth. Spatially distinct biomass measurements could improve the accuracy of the model by capturing the biomass distribution within the reactor.

6.2.2. Nitrate and oxygen inhibition

Microbial kinetic experiments should be performed to determine if the modified competitive inhibition model adequately describes perchlorate degradation in the presence of nitrate for other autohydrogenotrophic microbial consortia and pure cultures.

Similar to nitrate, oxygen may slow or inhibit perchlorate biodegradation. Batch and column experiments should be conducted to investigate the impact of the presence of varying oxygen concentrations on autohydrogenotrophic perchlorate degradation. The effect of oxygen on perchlorate biodegradation should be evaluated with and without the presence of nitrate.

Currently, the ZVI/biotic model uses an assumed oxygen inhibition coefficient and assumed oxygen Monod kinetic parameters. Model predictions could be improved if oxygen biodegradation coefficients and rates were determined experimentally for the consortium. Future batch kinetic experiments should be performed to estimate the single-component oxygen biodegradation kinetic parameters using hydrogen gas as the electron donor. Additional batch experiments should also be performed to develop a kinetic model for autohydrogenotrophic perchlorate reduction, accounting for the potential inhibitory/competitive effects of oxygen with and without the presence of nitrate.

6.2.3. Hydrogen gas production and concentration profiles

Determination of column concentration profiles for hydrogen, oxygen, perchlorate, and nitrate in future experiments could also improve model predictions. The concentration profiles could be used to improve the hydrogen production rate used in the ZVI/biotic model when nitrate is present and better understand electron acceptor competition/inhibition.

6.2.4. Reactive media and pH control

Addition of a chemical buffer for pH control in ZVI/biotic systems is undesirable; however, experimental evidence demonstrated pH control is essential for successful operation of ZVI/biotic perchlorate treatment systems. Others have shown that aluminosilicate materials can naturally buffer ZVI systems. Also, full-scale model predictions suggested that PRBs with less than 100% iron would easily be able to remove typical ground water concentrations of perchlorate, even in the presence of oxygen and nitrate. Future column studies should investigate the effects of varying ratios of iron and aluminosilicate materials on perchlorate removal and pH control. If chemical buffers are

134

necessary, future research should explore buffer delivery methods for in-situ treatment, such as the use of encapsulated buffers with pH sensitive coatings.

Appendix A: Headspace Sampling for the Analysis of Hydrogen Gas using Gas Chromatography

A GowMac Gas Partitioner Series 580 equipped with a thermal conductivity detector was used for gas chromatography analyses. Peak integration was performed by a Hewlett Packard HP3396 Integrator. A method was developed to optimize the detection of hydrogen at low levels using a Suppelco Molecular Sieve 13X column. Specifications for the GC and integrator can be seen in Table A1.

The total mass is detected, not the sample concentration, it was important to use the same injection volume for the sample as was used when making the calibration curve. Alternatively, the differences in the injection volume were accounted for by manipulating the calibration curve appropriately. The area value is unit less, so a reference base was established using a calibration curve. The standards to calibrate the GC were made by dilution of hydrogen gas. The GC method detection limit (MDL) determined was 3.766×10^{-5} atm or 0.003667% by volume. A typical calibration curve can be seen in Figure A1. The calibration curve gave a linear correlation R^2 value of 0.9992.

After a calibration curve for hydrogen was established the concentration of hydrogen was measured by injecting gas samples through the sample port on the GC. After every ten samples, or the last sample, a standard of a known concentration was run in order to determine if the calibration curve is still applicable. If the standard was within ten percent of the expected value the calibration curve was considered valid.

Table A1 Specifications for GC and integrator

GC Parameters	
Bridge Current	44 mA
Carrier Gas	Nitrogen
Flow Rate	45 mL/min
Column Temperature	60º C
Injector Temperature	60º C
Detector Temperature	60º C
Polarity	Negative (-)
Attenuation Factor	1
Injection Volume	1 mL (atmospheric pressure)
Integrator Parameters	
Attenuation Factor	0
Chart Speed	2
Threshold	-6
Peak Width	0.04
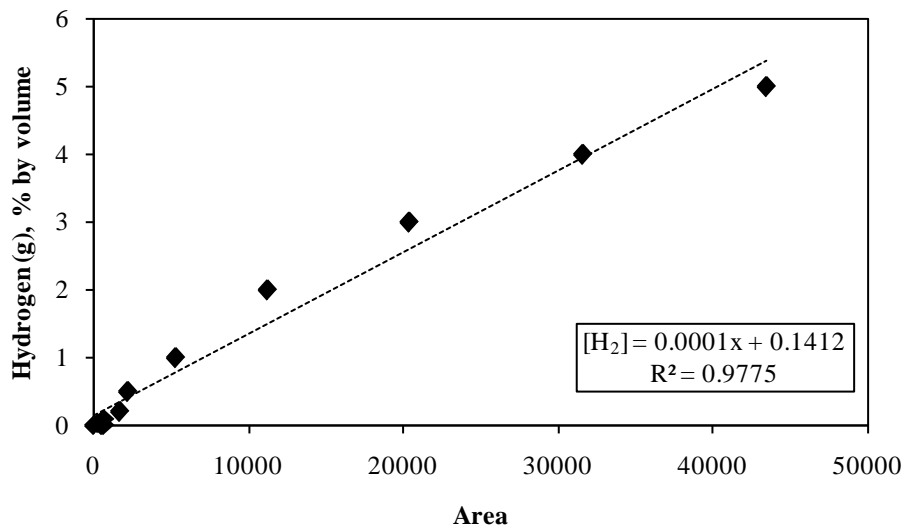
Figure A1 Calibration curve for the measurement of hydrogen gas concentrations

Appendix B: Method for the Detection of Perchlorate Concentration using Ion Chromatography

A Dionex DX-600 ion chromatograph equipped with a conductivity detector suppressor (Dionex AMMS III 2-mm) was used to measure perchlorate. A Dionex AS-16 anion-exchange column (AG-16 guard column) was used to separate the ions in solution. Trace concentrations of perchlorate were measured using a large loop injection (1000 µL, Dionex AS-40 Auto-sampler) using a potassium hydroxide eluent (mobile phase). Samples were filtered using 0.2 µm filter in order to avoid any contamination or clogging in the IC system. The first few milliliters of sample filtrate were discarded in order to avoid any possible contamination from the filters themselves. The sample injection and the mobile phase passed through a guard column and then an AS-16 column where the anions were separated. The separated anions were carried with the mobile phase through a suppressor system that suppresses the mobile phases' high conductivity and detects the increase in conductivity caused by the presence of specific ions. A conductivity detector transmitted the signal to the Chromeleon software, which then performed the integration of the chromatogram and quantified the injected samples.

The IC column was equilibrated for a period of time before samples were run to achieve a total baseline conductivity of less than 3 micro-Siemens in order to minimize interference. The column was regenerated using 50-mN sulfuric acid (H_2SO_4). The regenerant was prepared by adding 5.7-mL of concentrated (18 N) sulfuric acid to 4.0 liters of Millipore water. The IC components can be seen in Table B1 and the basic settings of the instrument can be found in Table B2.

Table B1 Dionex IC components

Component	Description
Autosampler	Model AS40
Chromatography Oven	Model LC25
Eluent Generator	Model EG50 EluGen® Cartridge EGC II KOH Potassium Hydroxide Product No. 058900
Electrochemical Detector	Model ED50
Gradient Pump	Model GS50
Integration Software	Chromeleon Client© Version 6.50 SP3 Build 980
Column	IonPac® AS16 2 x 250 mm
Suppressor	AMMS® III 2-mm PIN 56751
Sample Loop	1000 µL

Table B2 Basic IC Settings

External Settings	
Distilled Water Pressure	$\geq$ 5 psig
Sulfuric Acid Pressure	5 - 15 psig
Operating Conductivity	< 3 µS
Software Settings during Equilibration	
Eluent Concentration	10 mM
Pump Flow Rate	0.35 mL/min
SRS Type	MMS
Oven Temperature	30ºC
Temperature Compensation Factor	1.7%/ ºC

The text below is a copy of two programs used for the analysis and integration of perchlorate peaks using the Dionex Chromeleon software.

Program 1

        Pump_Relay_2.State =   Open
        LoadPosition
        Pressure.LowerLimit =   200
        Pressure.UpperLimit =   3000
        %A.Equate = "%A"
        %B.Equate = "%B"
        %C.Equate = "%C"
        %D.Equate = "%D"
        Pump_InjectValve.LoadPosition
        Data_Collection_Rate =   2.0
        Temperature_Compensation =   1.7
        Oven_Temperature = 30
        Suppressor_Type =   MMS
        Flow = 0.35
        ;%A is the makeup when B,C,D do not = 100%
        %B = 50.0
        %C = 0.0
        %D = 0.0
        Pump.Curve = 5

-2.300 Pump_Relay_2.Closed   Duration=138.00
        Concentration =   2.00
        EluentGenerator.Curve =   5

-0.100 ; this negative step is for command traffic.

 0.000 ECD.Autozero
        ECD_1.AcqOn
        Pump_InjectValve.InjectPosition   Duration=60.00
        Concentration =   2.00
        EluentGenerator.Curve =   5

 4.000 Concentration =   40.00
        EluentGenerator.Curve =   5

15.000 Concentration =   40.00

EluentGenerator.Curve =   5

15.100 Concentration =   80.00
        EluentGenerator.Curve =   5

20.000 Concentration =   80.00
        EluentGenerator.Curve =   5

20.1000   Concentration =   2.00
        EluentGenerator.Curve =   5

23.000 ECD_1.AcqOff

        Wait   Ready
        End

Program 2

Pump_Relay_2.State=   open
    loadposition
        Pressure.LowerLimit =   200
        Pressure.UpperLimit =   3000
        %A.Equate = "%A"
        %B.Equate = "%B"
        %C.Equate = "%C"
        %D.Equate = "%D"
        Pump_InjectValve.LoadPosition
        Data_Collection_Rate =   2.0
        Temperature_Compensation =   1.7
        Oven_Temperature = 30
        Suppressor_Type =   MMS
        Flow = 0.35
        %B =   50.0
        %C =   0.0
        %D =   0.0
        Pump.Curve = 5

-7.000 Concentration =   65.00
        EluentGenerator.Curve =   5

-6.900 Concentration =   6.00
        EluentGenerator.Curve =   5

```
-2.300  Pump_Relay_2.Closed          Duration=138.00

-0.100  ; this negative step is for command traffic.

 0.000  ECD.Autozero
        ECD_1.AcqOn
        Pump_InjectValve.InjectPosition       Duration=120.00

20.000 Concentration =        65.00
        EluentGenerator.Curve =      5

25.000 ECD_1.AcqOff
        Concentration =        65.00
        EluentGenerator.Curve =      5

        Wait    Ready
        End
```

Calibration curves on the IC were prepared such that they covered the expected concentration range and did not extend over more than two orders of magnitude in concentration. A calibration curve was established at the start of each IC run before samples were analyzed. Quality control standards were analyzed among samples to verify the calibration curve as prescribed in EPA Method 314. Typically, after a calibration curve was established, after every tenth sample, and after the last sample, a calibration check at a concentration in the middle of the calibration curve was run. A six point calibration was established by relating the area of the chromatogram peaks to the standards' concentrations. A typical calibration curve can be seen in Figure B1. This calibration curve was prepared within the range of $0 - 100$ μg/L.
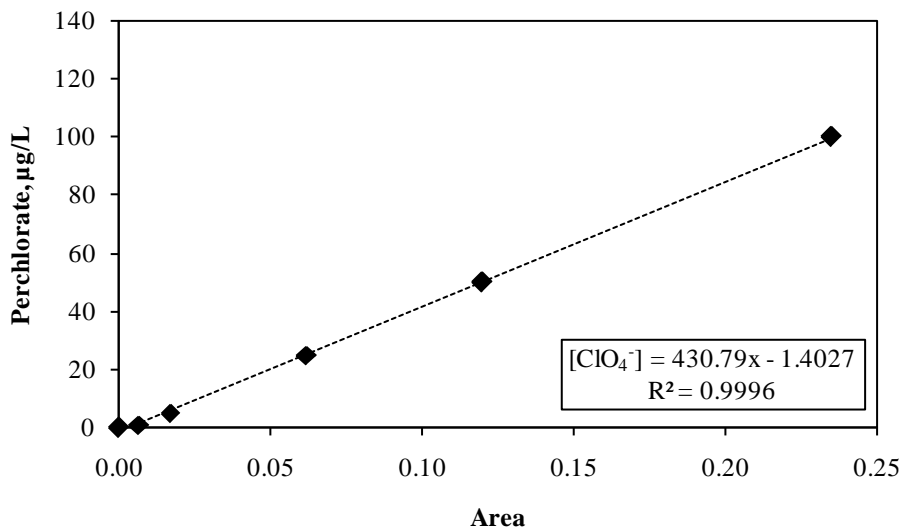
Figure B1 Typical perchlorate IC calibration curve

An initial demonstration of the accuracy and precision of the equipment was performed and the method detection limit was calculated. For the initial demonstration of accuracy, a mean was obtained from running seven duplicate 25 µg/L samples. In order to demonstrate accuracy, the mean should be within the range of 22.5 µg/L and 27.5 µg/L. The value obtained for the mean was 23.6 µg/L. The demonstration of precision is estimated by calculating the percent relative standard deviation (%RSD) from the seven duplicates. The %RSD was found to be 2.88%. The method detection limit (MDL) was calculated by running seven duplicate samples at a concentration thought to be three to five times greater than the MDL over a three-day period. The MDL is the product of the student's t-test value for the 99% confidence level and the standard deviation (S_{n-1}) with n-1 degrees of freedom for the seven duplicates. The student's t-test value for seven replicates is 3.14. An MDL of 0.23 µg/L in Millipore water, an MDL of 1.19 µg/L in the media used for microbial kinetic experiments, and an MDL of 1.41 µg/L in media used

145

during the second period of column operation were obtained using the IC equipment described previously.

Appendix C: Methods for Nitrate Analysis

Nitrate was measured using several different techniques. The choice of the appropriate technique was made at the time of the experiment depending upon the detection limits and ease of use.

Test 'N Tube Reactor/Cuvette Tubes with NitraVer X Reagent (Hach Company)

The procedure for using the Test 'N Tubes is as follows:

Pipette 1-mL of sample into the reactor tube. Cap the tube and invert it one time. Empty the contents of the powder packet into the tube and invert the tube ten times, after the tenth inversion start the timer. After nine minutes measure the absorbance of the liquid in the reactor tube on the spectrophotometer at 410 nm. Millipore water should be used as the blank. A quartz cuvette with a 1.0-cm path length should be used

A calibration curve relating absorbance to nitrate concentration in mg/L as N is shown in Figure C1. A time of nine minutes was used because the absorbance of reagent decreases as time progresses. Nine minutes is not a critical time, but it is important that the samples be measured at the same time that the calibration standards used.
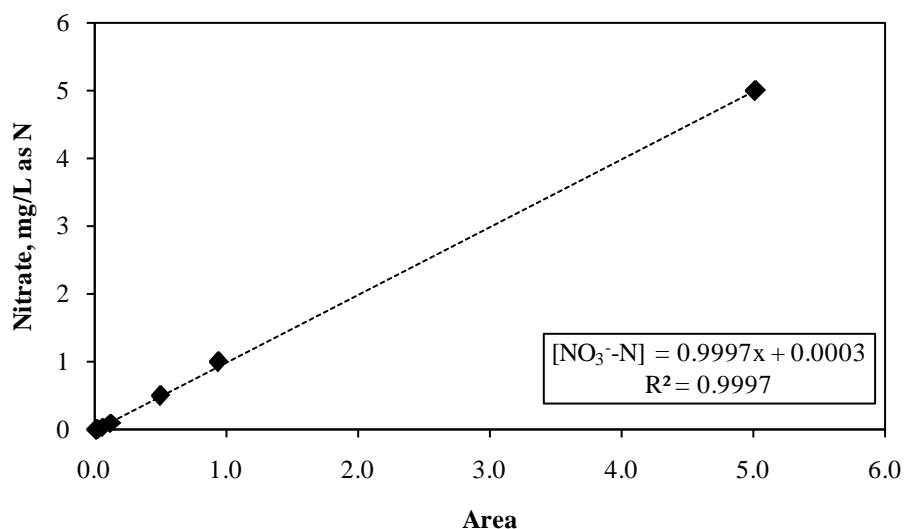
Figure C1 Typical nitrate calibration curve - Hach Test'N Tube technique

Method for the detection of nitrate using ion chromatography

Alternatively, NO_3^--N during the nitrate-limited experiments was measured using a 500-µL loop injection on a Dionex DX-600 IC, equipped with a Dionex ASRS Ultra II 4-mm conductivity detector suppressor, Dionex AS-11 4 x 250 mm column, Dionex AG-11 2 x 50 mm guard column, Dionex EGC II KOH eluent cartridge, and Dionex AS-40 auto-sampler. In order to avoid nitrate peak interference from phosphate, iron (III) chloride was used to precipitate out the phosphate. OnGuard II H cartridges (Dionex, IL) were used to remove soluble iron from solution prior to IC analysis. The basic settings and specifications of the ion chromatography system for nitrate analysis are the same as for perchlorate analysis discussed previously in Appendix B. The %RSD in the microbial kinetic experiment media was found to be 5.5% and the MDL for nitrate was found to be 0.0065 mg/L as N. Typical calibration curves can be seen in Figures C2 and C3. A copy

148

of the IC program used to detect nitrate be seen below. This program was used for analysis and integration of nitrate peaks using Dionex Chromeleon software.
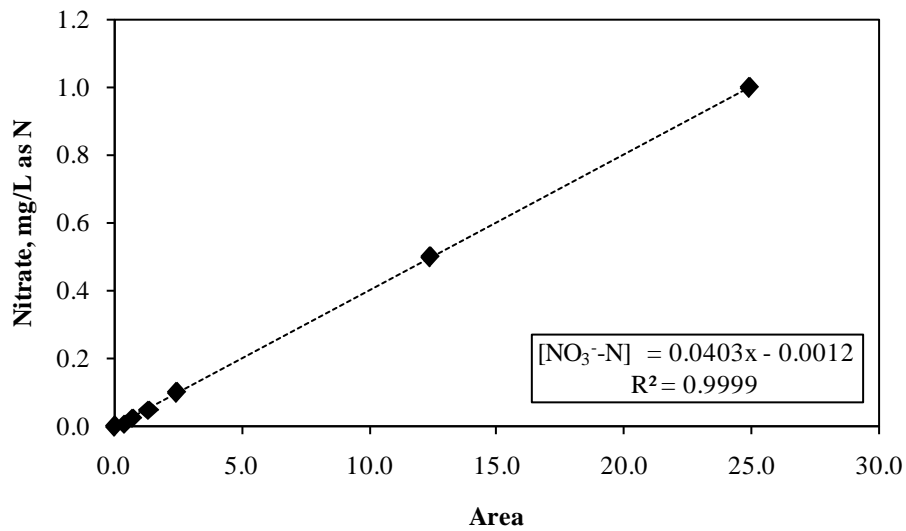
Figure C2 Typical nitrate IC calibration curve (0 – 6 mg/L as N)
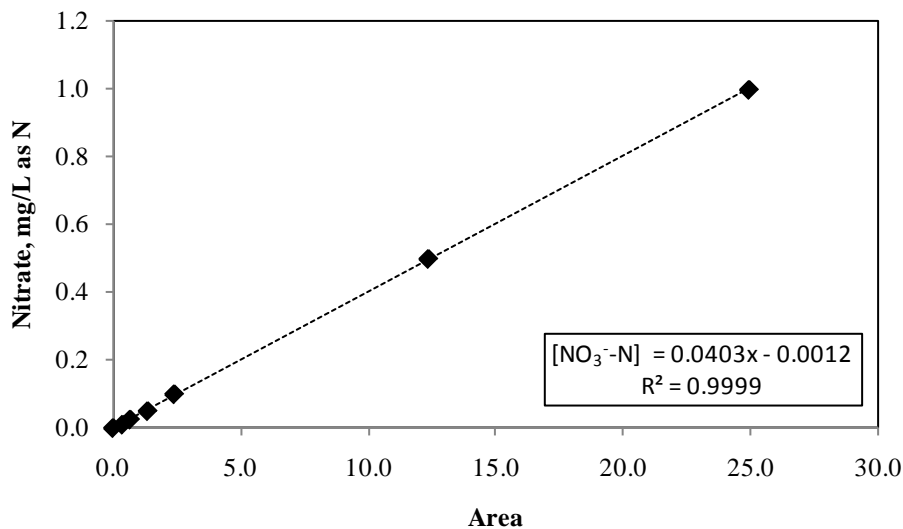
Figure C3 Typical nitrate IC calibration curve (0 – 1.2 mg/L as N)

The equation shown on the chart: $[NO_3^--N] = 0.0403x - 0.0012$, $R^2 = 0.9999$

Pump_Relay_2.State=   open
     loadposition
          Pressure.LowerLimit =   200
          Pressure.UpperLimit =   3000
          %A.Equate = "%A"
          %B.Equate = "%B"
          %C.Equate = "%C"
          %D.Equate = "%D"
          Pump_InjectValve.LoadPosition
          Data_Collection_Rate =   2.0
          Temperature_Compensation =   1.7
          Oven_Temperature = 30
          Suppressor_Type =   ASRS_4mm
          ; Carbonate = 0.0
          ; Bicarbonate =   0.0
          ; Hydroxide = 0.0
          ; Tetraborate =   0.0
          ; Other eluent =   0.0
          ; Recommended Current =   0
          Suppressor_Current =   90

     Flow = 0.9

150

```
            %B =  50.0
            %C =  0.0
            %D =  0.0
            Pump.Curve = 5


-2.300  Pump_Relay_2.Closed         Duration=138.00
            concentration   =1
            EluentGenerator.Curve =      5


-0.100 ;this negative step is for command traffic



0.0   ECD_1.AcqOn
            Pump_InjectValve.InjectPosition      Duration=60.00
        concentration   = 1
            EluentGenerator.Curve =      5

4.0     concentration =        30
            eluentgenerator.curve=5

30.000 ECD_1.AcqOff

            Wait    Ready
            End
```

Appendix D: Optical Density Technique for the Estimation of Microbial Biomass

The biomass concentration was estimated using an optical density technique. Using a spectrophotometer, absorbance measurements were taken from cell suspensions at a wavelength of 600 nm for different cell mass concentrations as measured using TSS (Total Suspended Solids) analysis (Standard Method 2540D). A typical calibration curve for the optical density technique can be seen in Figure D1.
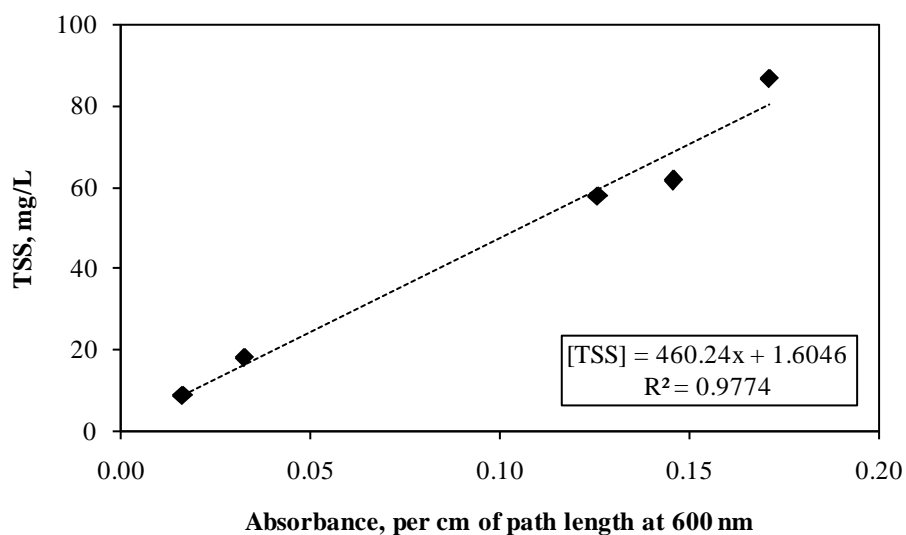
Figure D1 Typical calibration curve for the estimation of biomass

Appendix E: Method for the Operation of the pH-stat

The algorithm used for the pH-stat (Titralab 90 Radiometer) to regulate the speed of the titration was AAA. This is because the buffer intensity of the media used in the experiments was higher than 10^{-5}. The pH value programmed for the pH-stat to maintain was 6.98, which was the typical starting pH of the high phosphate mineral media. The pH-stat was programmed to lower the pH by the addition of either 0.1 M or 0.5 M HCl. The position of the burette AUB901 was selected as 1. The maximum volume of titrant to add is set to 10 - 100 mL. The horizon was set to 14 as calculated by the following formula:

Horizon = - 30 log β

where β is the buffer intensity of the high phosphate mineral media

The time of response to adapt the regulation algorithm (time constant) was set at 10.0 seconds. Every 10 seconds the algorithm checks the pH and the burette adds titrant if necessary. If the experiment lasted longer than 99 hours and 59 minutes, the pH stat-was re-started. The controller displays time, temperature, pH, and volume of titrant. To initiate the pH-stat the following method was used:

1. On the controller, press the Mode key
2. Using the down arrow, select Method pH-stat AAA Method D
3. Using the down arrow, the name of the experiment is typed in
4. Press the sample key

Appendix F: Tracer Test

A step-up and step-down tracer test were performed on the laboratory column prior to column termination in order to model column hydraulics. Lithium was chosen as the non-reactive tracer material. For the step-up tracer test Lithium at a concentration of 1 mg/L was added to one of the column influent tanks and the effluent concentration measured through time (5-mL samples). At the completion of the step-up tracer test the influent source was switched to the second influent tank that did not contain any lithium, in order to perform the step-down tracer test. Prior to the tracer test, the time required for media to reach the column from each of the influent tanks was measured and tracer time measurements adjusted accordingly.

Lithium was measured in duplicate on a Perkin-Elmer AA Analyst 600 Atomic Absorption Spectrometer at a wavelength of 670.8 nm. Samples were acidified with concentrated nitric acid to an acid concentration of 0.2 N. Samples were then filtered using 0.2 µm syringe filters, wasting the first 3-mL of filtrate and subsequently diluted 1:10 and re-acidified. Lithium standards were made in 1:10 diluted column media, acidified with concentrated nitric acid, and spiked with $FeCl_3$ to obtain an iron concentration of 1.1 mg/L to mimic 1:10 diluted column effluent. A standard curve can be seen in Figure F1.

Tracer results can be seen in Figure F2. Figure F2 displays the Cumulative Age Distribution (F(t)), used to describe the flow characteristics under steady-flow conditions. Equation F1 (Lawler and Benjamin, 2007) was used to model the plug flow conditions present in the column as a series of N equi-sized continuous flow stirred tank reactors (CFSTRs) with a hydraulic retention time of the complete tank, τ.

154

$$F(t)=1-\exp\left(-\frac{Nt}{\tau}\right)\sum_{i=1}^{N}\frac{1}{(i-1)!}\left(\frac{Nt}{\tau}\right)^{i-1}$$ Equation F1

Best-fit model results for the step-up tracer test indicated the column is best represented by 10 equi-sized CFSTRs in series with a porosity of 0.53 (Column volume: 589 cm³, flow rate: 3 mL/min). Best-fit results were determined using the Solver routine in Excel by minimizing the normalized sum of squares between the predicted and measured concentrations. Normalization was achieved by dividing the residual sum of squares by the measured concentration squared at that time. Using a value of 10 CFSTRs, Equation F1 was then used to predict the measured results of the step-down tracer test.
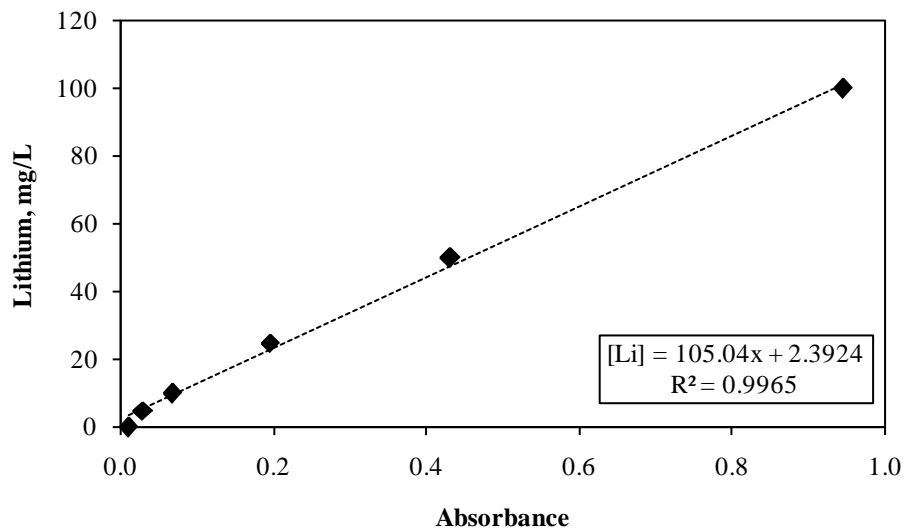
Figure F1 Typical atomic absorption lithium calibration curve
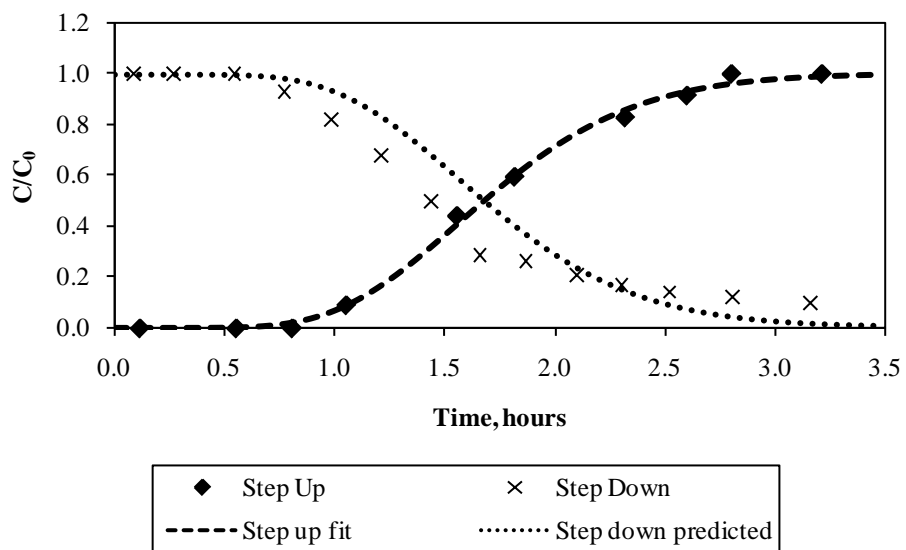
Figure F2 Results of column step-up and step-down lithium tracer test

Appendix G: Typical AQUASIM Model Implementation

Variables

Area_Biofilm
Description: Biofilm area in a reactor (AQUASIM user manual, page 50)
Type: Formula Variable
Unit: m^2
Expression: 4*pi*n_p*(r_p+Z)^2

b
Description: Endogenous decay (Sanchez, 2003)
Type: Formula Variable
Unit: 1/d
Expression: 0.008

Biofilm_Water_Fraction
Description: Water fraction of the biofilm matrix (this is porosity if pore volume does not contain solids)
Type: Program Variable
Reference to: Water Fraction

Column_Area
Description: Cross-section column area per lab set-up
Type: Formula Variable
Unit: m^2
Expression: pi/4*(Column_Diameter)^2

Column_Diameter
Description: Column diameter per lab set-up
Type: Formula Variable
Unit: m
Expression: 5/100

Column_Length
Description: Column length per lab set-up
Type: Formula Variable
Unit: m
Expression: 30/100

Column_Volume
Description: Column volume per lab set-up
Type: Formula Variable
Unit: m^3
Expression: Column_Area*Column_Length

D_P
Description: Diffusivity of perchlorate in water at 25°C (Lide, 1994, p. 427)
Type: Formula Variable
Unit: m^2/d
Expression: 1.55E-04

D_H2
Description: Diffusivity of hydrogen in water at 25°C (Perry and Green, 2008, p. 2-457)
Type: Formula Variable
Unit: m^2/d
Expression: 4.4E-04 (average)

D_O2
Description: Diffusivity of oxygen in water at 25°C (Perry and Green, 2008, p. 427)
Type: Formula Variable
Unit: m^2/d
Expression: 2.16E-04

D_N
Description: Diffusivity of nitrate in water at 25°C (Lide, 1994, p. 427)
Type: Formula Variable
Unit: m^2/d
Expression: 1.64E-04

Gamma_N
Description: Stoichiometric coefficient relating hydrogen and nitrate (Appendix I)
Type: Formula Variable
Unit: g H_2/g NO_3^--N
Expression: 0.481

Gamma_O2
Description: Stoichiometric coefficient relating hydrogen and oxygen (Appendix I)
Type: Formula Variable
Unit: g H_2/g O_2
Expression: 0.164

Gamma_P
Description: Stoichiometric coefficient relating hydrogen and perchlorate ((Appendix I))
Type: Formula Variable
Unit: g H_2/g P
Expression: 0.134

H2
Description: Zero order hydrogen production rate constant (Appendix I)
Type: Constant Variable
Unit: g H_2/g Fe/d
Expression: 1.6E-6

k_d
Description: Endogenous decay coefficient + specific biofim-detachment loss coefficient
(per Rittmann & McCarty, 2001, Equations 4.31, 4.32, & 4.35)
Type: Formula Variable
Unit: 1/d
Expression: if LF<3e-005 then (b+0.0842*Sigma^0.58) else
(b+0.0842*(Sigma/(1+433.2*((LF*100)-0.003))))^0.58) endif

K_O2
Description: Oxygen inhibition coefficient (Grady et al., 1999)
Type: Formula Variable
Unit: g/m^3
Expression: 0.75

Ks_H2
Description: Half-saturation coefficient for hydrogen
Type: Constant Variable
Unit: g H_2/m^3
Expression: 4.52E-03

Ks_P
Description: Half-saturation coefficient for perchlorate
Type: Constant Variable
Unit: g ClO_4^-/m^3
Expression: 2.84E-02

Ks_N
Description: Half-saturation coefficient for nitrate
Type: Constant Variable
Unit: g NO_3^--N/m^3
Expression: 1.53E-01

Ks_O2
Description: Half-saturation coefficient for oxygen
Type: Constant Variable
Unit: g O_2/m^3
Expression: 1.53E-01

k_N
Description: Maximum substrate utilization rate for nitrate
Type: Constant Variable
Unit: g NO_3^--N / g VS/d
Expression: 4.17E-01

k_O2
Description: Maximum substrate utilization rate for oxygen
Type: Constant Variable
Unit: g NO_3^--N / g VS/d
Expression: 4.80E-01

k_P
Description: Maximum substrate utilization rate for perchlorate
Type: Constant Variable
Unit: g ClO_4^-/g VS/d
Expression: 5.43E-02

k_obsN
Description: Abiotic Peerless nitrate degradation at pH 7.2 (Alowitz and Scherer, 2002)
Type: Constant Variable
Unit: 1/d
Expression: 5.3

LF
Description: Biofilm thickness (calculated by AQUASIM)
Type: Program Variable
Unit: m

LF_Initial
Description: Initial biofilm thickness
Type: Formula Variable
Unit: m
Expression: 1E-7

LL_H2
Description: Liquid boundary layer thickness for hydrogen (Wilson and Geankoplis, 1966)
Type: Formula Variable
Unit: m
Expression: (r_p*2)/(1.09*(1/Porosity_Column_Actual)^2/3)*Re^1/3*Sc_H2^1/3

LL_N
Description: Liquid boundary layer thickness for nitrate (Wilson and Geankoplis, 1966)
Type: Formula Variable
Unit: m
Expression: (r_p*2)/(1.09*(1/Porosity_Column_Actual)^2/3)*Re^1/3*Sc_N^1/3

LL_O2
Description: Liquid boundary layer thickness for oxygen (Wilson and Geankoplis, 1966)
Type: Formula Variable
Unit: m
Expression: (r_p*2)/(1.09*(1/Porosity_Column_Actual)^2/3)*Re^1/3*Sc_O2^1/3

LL_P
Description: Liquid boundary layer thickness for perchlorate (Wilson and Geankoplis, 1966)
Type: Formula Variable
Unit: m
Expression: (r_p*2)/(1.09*(1/Porosity_Column_Actual)^2/3)*Re^1/3*Sc_P^1/3

mu
Description: Absolute viscosity of water at 25°C (Tchobanoglous et al., 2003, table C-2)
Type: Formula Variable
Unit: g/cm-d
Expression: 769

M_ZVI
Description: Mass of ZVI in each reactor
Type: Formula Variable
Unit: g ZVI
Expression: 1190/Number_Reactor

Number_Reactor
Description: Number of CFSTRs in series used to model plug-flow in column
Type: Formula Variable
Expression: 10

n_p
Description: Number of particles in each reactor (calculated based on 30 x 40 mesh particles)
Type: Formula Variable
Expression:
(Column_Volume*(1Porosity_Column_Initial))/Number_Reactor*4/3*pi*r_p^3)

Porosity_Column_Actual
Description: Actual porosity of column during a simulation
Type: Formula Variable
Expression: Porosity_Column_Initial*Vol_BulkWater/Vol_Reactor

Porosity_Column_Initial
Description: Assumed initial porosity
Type: Formula Variable
Expression: 0.6

q_H2
Description: Exchange coefficient for hydrogen diffusive link
Type: Formula Variable
Unit: m^3/d
Expression: 1.00E+11

Q_In
Description: Average influent flow to reactors
Type: Constant Variable
Unit: m^3/d
Expression: 4.032E-03

Ratio_FilmD_WaterD
Description: Ratio of film diffusion coefficient ro water diffusion coefficient (Rittmann and McCarty, 2001)
Type: Formula Variable
Expression: 0.8

Re
Description: Reynolds number
Type: Formula Variable
Expression: (rho_water*Vel_Water_Actual*r_p*2*100)/mu

rho_water
Description: Density of water at
Type: Formula Variable
Unit: g/cm^3
Expression: 1

rho_X
Description: Maximum bacterial density in biofilm (per Rittmann and McCarty, p. 220)
Type: Formula Variable
Unit: $g\ VS/m^3$
Expression: 50000

r_p
Description: Radius of iron particles calculated by geometric mean (based on 30 x 40 mesh size)
Type: Formula Variable
Unit: m
Expression: (sqrt(600*425)/2)*1E-6

Sc_H2
Description: Schmidt number for hydrogen
Type: Formula Variable
Expression: mu/(rho_water*D_H2*100^2)

Sc_N
Description: Schmidt number for nitrate
Type: Formula Variable
Expression: mu/(rho_water*D_N*100^2)

Sc_O2
Description: Schmidt number for oxygen
Type: Formula Variable
Expression: mu/(rho_water*D_O2*100^2)

Sc_P
Description: Schmidt number for perchlorate
Type: Formula Variable
Expression: mu/(rho_water*D_P*100^2)

Sigma
Description: Shear stress for use in detachment rate (k_d) (Appendix H)
Type: Formula Variable
Unit: g/cm-s^2
Expression:
(50*mu*Vel_Water_Superficial*SSA_Reactor)/(9*Porosity_Column_Initial^2*7.46E9)

Sin_N
Description: Influent nitrate concentration
Type: Real List Variable
Unit: g NO_3^--N/m^3
Expression: ~ 0-8
Argument: time

Sin_O2
Description: Influent oxygen concentration
Type: Real List Variable
Unit: g/m^3
Expression: ~ 0-4
Argument: time

Sin_P
Description: Influent perchlorate concentration
Type: Real List Variable
Unit: g/m^3
Expression: ~ 0.1
Argument: time

SSA_Particle
Description: Specific surface area of iron particle
Type: Formula Variable
Unit: 1/m
Expression: 3/r_p

SSA_Reactor
Description: Specific surface area based on volume of reactor
Type: Formula Variable
Unit: 1/m
Expression: SSA_Particle*(1-Porosity_Column_Actual)

S_N_Measured
Description: Measured effluent nitrate concentration
Type: Real List Variable
Unit: g NO_3^--N/m^3
Argument: time

S_O2_Measured
Description: Measured effluent oxygen concentration
Type: Real List Variable
Unit: g O_2/m^3
Argument: time

S_P_Measured
Description: Measured effluent perchlorate concentration
Type: Real List Variable
Unit: g P/m^3
Argument: time

S_H2_Measured
Description: Measured effluent hydrogen concentration
Type: Real List Variable
Unit: g P/m^3
Argument: time

Time
Description: Time
Type: Program Variable
Unit: d
Reference to: Time

Vel_Water_Actual
Description: Actual water velocity in the column
Type: Formula Variable
Unit: m/d
Expression: Vel_Water_Superficial/Porosity_Column_Actual

Vel_Water_Superficial
Description: Superficial water velocity in the column
Type: Formula Variable
Unit: m/d
Expression: Q_In/Column_Area

Vol_BulkWater
Description: Bulk water volume
Type: Program Variable
Unit: m^3
Reference to: Bulk volume

Vol_Reactor
Description: Volume of the Reactor (empty reactor volume – volume packing), depends on # of reactors
Type: Program Variable
Unit: m^3
Reference to: Reactor volume
Expression: total volume → 4.34E-04 (10 reactors each with a volume 4.34E-05)

X
Description: Biofilm biomass concentration
Type: Dynamic Volume State Variable
Unit: g VS/m^3

X_Fraction
Description: Biomass fraction of biofilm
Type: Formula Variable
Expression: 0.2

Y_N
Description: Yield for growth with respect to nitrate
Type: Formula Variable
Unit: g VS/g NO_3^--N
Expression: 0.7

Y_O2
Description: Yield for growth with respect to oxygen
Type: Formula Variable
Unit: g VS/g O_2
Expression: 0.22

Y_P
Description: Yield for growth with respect to perchlorate (Sanchez, 2003)
Type: Formula Variable
Unit: g VS/g ClO_4^-
Expression: 0.30

Z
Description: Biofilm distance from substratum
Type: Program Variable
Unit: m
Reference to: Space coordinate z

Processes

Decay

Description:	Endogenous decay and shear
Type:	Dynamic Process
Rate	k_d*X
Stoichiometry:	Variable:Stoichiometric Coefficient
	X:-1

Hydrogen_Production

Description:	Hydrogen production by ZVI
Type:	Dynamic Process
Rate	(H2*M_ZVI)/Vol_Reactor
Stoichiometry:	Variable:Stoichiometric Coefficient
	S_H2:1

Nitrate

Description:	Nitrate biodegradation and microorganism growth
Type:	Dynamic
Rate:	
Stoichiometry:	Variable:Stoichiometric Coefficient
	X:Y_N
	S_N:-1
	S_H2:-Gamma_N

Nitrate Abiotic

Description:	Abiotic nitrate reduction
Type:	Dynamic
Rate:	k_obsN*S_N
Stoichiometry:	Variable:Stoichiometric Coefficient
	S_N:-1

Oxygen
Description: Oxygen biodegradation and microorganism growth
Type: Dynamic
Rate:
Stoichiometry: Variable:Stoichiometric Coefficient
                    X:Y_O2
                    S_O2:-1
                    S_H2:-Gamma_O2

Perchlorate_Nitrate
Description: Perchlorate biodegradation and microorganism growth
Type: Dynamic
Rate:
Stoichiometry: Variable:Stoichiometric Coefficient
                    X:Y_P
                    S_P:-1
                    S_H2:-Gamma_P

Compartments

Reactor_1
Description: Biofilm reactor compartment (1st in Series)
Type: Biofilm reactor compartment
Compartment Index: 0
Active Variables: S_P, X, S_H2, S_O2, S_N
Active Processes: Decay, Oxygen, Perchlorate_Nitrate, Nitrate, Nitrate_Abiotic
Initial Conditions: LF(Biofilm Matrix): LF_Initial
                       X(Biofilm Matrix): rho_X*X_Fraction
Water Inflow: Q_In
Loadings: S_O2: Q_In*Sin_O2
                       S_N: Q_In*Sin_N
                       S_P: Qin*Sin_P
Particulate Variables: X
                       Density: rho_x
                       Surf. Att. Coeff.:   0
                       Surf. Det. Coeff.:   0
                       Vol. Att. Coeff.:   0
                       Vol. Det. Coeff: 0
                       Bound L. Coeff.:   0
                       Pore Diff.:   0
                       Matrix Diff.:   0
Dissolved Variables: S_P:

169

Bound. L. Res.: LL_P/D_P
Pore Diff.: D_N*Ratio_FilmD_WaterD
S_H2:
Bound. L. Res.: LL_H2/D_H2
Pore Diff.: D_N*Ratio_FilmD_WaterD
S_O2:
Bound. L. Res.: LL_O2/D_O2
Pore Diff.: D_N*Ratio_FilmD_WaterD
S_N:
Bound. L. Res.: LL_N/D_N
Pore Diff.: D_N*Ratio_FilmD_WaterD

Reactor Type: Confined
Reactor Volume: 4.35E-4
Pore Volume: Liquid phase only
Biofilm Matrix: Rigid
Surface Detachment: Global velocity → 0
Biofilm Area: Area_Biofilm
Rate Porosity: 0
Num. Grid Points: 22 (active for calculation)
Resolution: low
Accuracy:

Discharge	Rel Acc.: 0.001	Abs. Acc.: 0.001
Volume	Rel Acc.: 0.001	Abs. Acc.: 1E-10
Biofilm Thck.	Rel Acc.: 0.001	Abs. Acc.: 1E-10
Water Frac.	Rel Acc.: 0.001	Abs. Acc.: 0.001

Reactor_2 through Reactor_10 same as above except:

Water Inflow: 0
Loadings: none

Hydrogen_1 through Hydrogen_10
Description: CFSTR for hydrogen production from ZVI
Type: Mixed Reactor Compartment
Compartment: 0
Variables: S_H2
Processes: Hydrogen_Production
Init. Cond.: S_H2(Bulk Volume):0
Input:
     Water Inflow: 0
Volume: 4.34E-5

Reactor Type: Constant volume

Acc:

      Discharge:

            Rel. Accuracy: 0.001

            Abs. Accuracy: 0.001

      Volume:

            Rel. Accuracy: 0.001

            Abs. Accuracy: 0.001

Appendix H: Biofilm Loss in Model

Shear Stress [sigma] Derivation

Biofilm loss in the AQUASIM model was not controlled by the functionality associated with the Batch Reactor Compartments (BRC) and instead a biofilm specific loss rate, b' (Rittman, 1982; Wahman et al., 2007), was used. The biofilm specific loss rate uses biofilm thickness, the endogenous decay coefficient, and shear stress to calculate an overall loss rate. The shear stress expression derived for use in the biofilm specific loss rate differs from the derivation of Rittmann (1982) and can be seen below as developed by David G. Wahman, Ph.D.

The basic difference between the Wahman derivation of the shear stress used in the ZVI/biotic model and the assumed derivation of Rittmann (1982) is the application of the pressure force. In the Wahman shear stress expression, based on the work of Leva (1959), the pressure force was assumed to act on the pore volume. The assumed shear stress derivation of Rittmann (1982) assumes the pressure force acts on the total volume. By assuming the pressure force acts on the total volume, the shear stress expression of Rittmann (1982) over predicts the shear stress by a factor of porosity^{-1} and b' by a factor of porosity$^{-0.58}$. The derivations are as follows:

Wahman Derivation of Shear Stress

Equate the shear force (F_{Shear}) resisting the pressure force ($F_{Pressure}$):

$$F_{Pressure} = F_{Shear}$$

$$\Delta p A_R \varepsilon = \sigma S V_R$$

Where Δp = Pressure drop $[F/L^2]$
A_R = Cross-sectional area of the reactor $[L^2]$
ε = Porosity [-]
σ = Shear stress $[F/L^2]$
S = Particle surface area per volume of bed $[1/L]$
V_R = Volume of the reactor $[L^3]$

$$\Delta p = \frac{\sigma S V_R}{A_R \varepsilon} = \frac{\sigma S L}{\varepsilon}$$

$$\varphi_s = \frac{A_p}{A} \qquad \text{Equation 3-17 (Leva, 1959)}$$

Where φ_s = Particle-shape factor [-]
A_p = Surface area of spherical particle $[L^2]$
A = Surface area of arbitrarily shaped particle $[L^2]$

$$S = \frac{N_p A_p}{V_R} = \frac{N_p A \varphi_s}{V_R} \text{ Definition of S}$$

Where N_p = Number of particles in the reactor [-]

$$f_m = \frac{D_p \rho \varphi_s^{3-n} \varepsilon^3 \Delta p}{2G^2 L (1-\varepsilon)^{3-n}} \qquad \text{Equation 6-166 (Perry et al., 1997)}$$

Where f_m = Modified friction factor [-]
D_p = Average particle diameter [L]
ρ = Fluid density $[M/L^3]$
G = Fluid superficial mass velocity $[M/T\text{-}L^2]$
L = Depth of bed [L]
n = Exponent from Figure 6-46 as a function of Reynolds number (Re) (Perry et al., 1997)

$$u_0 = \frac{G}{\rho}$$

Where u_0 = Superficial velocity [L/T]

$$Re = \frac{D_p G}{\mu} = \frac{D_p u_0 \rho}{\mu}$$ Equation 6-167 (Perry et al., 1997)

Where Re = Reynolds number [-]
μ = Fluid viscosity [M/L-T]

For Re<10, n=1 Figure 6-46 (Perry et al., 1997)

Fore Re<10, then $f_m = \dfrac{100}{Re} = \dfrac{100}{\dfrac{D_p u_0 \rho}{\mu}} = \dfrac{100\mu}{D_p u_0 \rho}$ Equation 6-168 (Perry et al., 1997)

$$\frac{100\mu}{D_p u_0 \rho} = \frac{D_p \rho \varphi_s^2 \varepsilon^3 \Delta p}{2G^2 L(1-\varepsilon)^2} = \frac{D_p \rho \varphi_s^2 \varepsilon^3 \Delta p}{2(u_0 \rho)^2 L(1-\varepsilon)^2} = \frac{D_p \varphi_s^2 \varepsilon^3 \Delta p}{2u_0^2 L \rho (1-\varepsilon)^2} = \frac{D_p \varphi_s^2 \varepsilon^3 \dfrac{\sigma SL}{\varepsilon}}{2u_0^2 L \rho (1-\varepsilon)^2} = \frac{D_p \varphi_s^2 \varepsilon^3 \sigma SL}{2u_0^2 L \rho (1-\varepsilon)^2 \varepsilon} = \frac{D_p \varphi_s^2 \varepsilon^2 \sigma S}{2u_0^2 \rho (1-\varepsilon)^2}$$

$$\sigma = \frac{200\mu u_0^2 \rho (1-\varepsilon)^2}{D_p u_0 \rho D_p \varphi_s^2 \varepsilon^2 S} = \frac{200\mu u_0 (1-\varepsilon)^2}{D_p^2 \varphi_s^2 \varepsilon^2 S}$$ Equation H1

The above (Equation H1) shear stress equation is an equivalent form of the shear stress equation of Rittmann (1982) that follows, but it is not mathematically the same.

Further simplification of the Wahman shear stress equation (Equation H1) can be performed, as seen below. This simplification was not done by Rittmann (1982).

$$D_p = \frac{6V_p}{A_p} = \frac{6V_p}{A\varphi_s} = \frac{\dfrac{6(1-\varepsilon)V_R}{N_p}}{A\varphi_s} = \frac{6(1-\varepsilon)V_R}{N_p A\varphi_s} = \frac{6(1-\varepsilon)}{S}$$ Page 47 (Leva, 1959)

Where V_p = Volume of the particle [L^3]

174

$$\sigma = \frac{200\mu u_0 (1-\varepsilon)^2}{D_p^2 \varphi_s^2 \varepsilon^2 S} = \frac{200\mu u_0 (1-\varepsilon)^2}{\dfrac{6^2 (1-\varepsilon)^2}{S^2} \varphi_s^2 \varepsilon^2 S} = \frac{50\mu u_0 S}{9\varphi_s^2 \varepsilon^2}$$

For spherical particles, $\varphi_s = 1$

$$\sigma = \frac{50\mu u_0 S}{9\varepsilon^2}$$

Assumed Derivation of Shear Stress of Rittmann (1982)

Rittmann (1982) appears to use the pressure force as applied to the total volume and assume spherical particles ($\varphi_s = 1$).

Equate the shear force (F_{Shear}) resisting the pressure force ($F_{Pressure}$):

$$F_{Pressure} = F_{Shear}$$

$$\Delta p A_R = \sigma S V_R$$

Where Δp = Pressure drop $[F/L^2]$
A_R = Cross-sectional area of the reactor $[L^2]$
σ = Shear stress $[F/L^2]$
S = Particle surface area per volume of bed $[1/L]$
V_R = Volume of the reactor $[L^3]$

$$\Delta p = \frac{\sigma S V_R}{A_R} = \sigma S L$$

$$\varphi_s = \frac{A_p}{A} = 1 \quad \text{Equation 3-17 (Leva, 1959) assuming spherical particles } (\varphi_s = 1)$$

Where φ_s = Particle-shape factor [-]
A_p = Surface area of spherical particle $[L^2]$
A = Surface area of arbitrarily shaped particle $[L^2]$

$$S = \frac{N_p A_p}{V_R} = \frac{N_p A \varphi_s}{V_R} \quad \text{Definition of S}$$

Where N_p = Number of particles in the reactor [-]

$$f_m = \frac{D_p \rho \varphi_s^{3-n} \varepsilon^3 \Delta p}{2G^2 L(1-\varepsilon)^{3-n}} \quad \text{Equation 6-166 (Perry et al., 1997)}$$

Where f_m = Modified friction factor [-]

$\quad$ D_p = Average particle diameter [L]

$\quad$ ρ = Fluid density [M/L^3]

$\quad$ ε = Porosity [-]

$\quad$ G = Fluid superficial mass velocity [$M/T\text{-}L^2$]

$\quad$ L = Depth of bed [L]

$\quad$ n = Exponent from Figure 6-46 as a function of Reynolds number (Re) (Perry et al., 1997)

$$u_0 = \frac{G}{\rho}$$

$\quad$ Where u_0 = Superficial velocity [L/T]

$$Re = \frac{D_p G}{\mu} = \frac{D_p u_0 \rho}{\mu} \quad \text{Equation 6-167(Perry et al., 1997)}$$

$\quad$ Where Re = Reynolds number [-]

$\quad$ μ = Fluid viscosity [M/L-T]

For Re<10, n=1 Figure 6-46 (Perry et al., 1997)

$$\text{Fore Re<10, then } f_m = \frac{100}{Re} = \frac{100}{\dfrac{D_p u_0 \rho}{\mu}} = \frac{100\mu}{D_p u_0 \rho} \quad \text{Equation 6-168 (Perry et al., 1997)}$$

Assuming spherical particles ($\varphi_s = 1$)

$$\frac{100\mu}{D_p u_0 \rho} = \frac{D_p \rho \varepsilon^3 \Delta p}{2G^2 L(1-\varepsilon)^2} = \frac{D_p \rho \varepsilon^3 \Delta p}{2(u_0 \rho)^2 L(1-\varepsilon)^2} = \frac{D_p \varepsilon^3 \Delta p}{2u_0^2 L \rho (1-\varepsilon)^2} = \frac{D_p \varepsilon^3 \sigma S L}{2u_0^2 L \rho (1-\varepsilon)^2} = \frac{D_p \varepsilon^3 \sigma S L}{2u_0^2 L \rho (1-\varepsilon)^2} = \frac{D_p \varepsilon^3 \sigma S}{2u_0^2 \rho (1-\varepsilon)^2}$$

$$\sigma = \frac{200\mu u_0^2 \rho (1-\varepsilon)^2}{D_p u_0 \rho D_p \varepsilon^3 S} = \frac{200\mu u_0 (1-\varepsilon)^2}{D_p^2 \varepsilon^3 S} \quad \text{Rittmann (1982)} \quad \text{Equation H2}$$

The shear stress equation of Wahman (Equation H1) is an equivalent form of the shear stress equation of Rittmann (1982) that follows, but it is not mathematically the same.

177

Further simplification can be done on the shear stress equation of Rittmann (1982) (Equation H2).

$$D_p = \frac{6V_p}{A_p} = \frac{6V_p}{A\varphi_s} = \frac{\frac{6(1-\varepsilon)V_R}{N_p}}{A\varphi_s} = \frac{6(1-\varepsilon)V_R}{N_pA\varphi_s} = \frac{6(1-\varepsilon)}{S}$$ Page 47 (Leva, 1959)

Where V_p = Volume of the particle [L^3]

$$\sigma = \frac{200\mu u_0(1-\varepsilon)^2}{D_p^2\varepsilon^3S} = \frac{200\mu u_0(1-\varepsilon)^2}{\frac{6^2(1-\varepsilon)^2}{S^2}\varepsilon^3S} = \frac{50\mu u_0S}{9\varepsilon^3}$$

$$\sigma = \frac{50\mu u_0S}{9\varepsilon^3}$$ (Rittmann (1982) derivation)

$$\sigma = \frac{50\mu u_0S}{9\varepsilon^2}$$ (Wahman derivation)

Rittmann (1982) derivation overpredicts shear stress by the factor $\frac{1}{\varepsilon}$, which results in a detachment coefficient (b_{det}) that is overpredicted by the factor $\frac{1}{\varepsilon^{0.58}}$. For a typical $\varepsilon = 0.40$, this results in a shear stress that is 2.5 times as great and b_{det} that is 1.7 times as great.

Appendix I: Raw column data and calculations

I.1. MCCARTY'S ENERGETICS

(McCarty, 1975)

Perchlorate (Sanchez, 2003)

$0.5H_2(g) + 0.075ClO_4^- + 0.1HCO_3^- + 0.08H^+ + 0.02NH_4^+ \rightarrow$

$0.02C_5H_7O_2N + 0.56H_2O + 0.075Cl^-$

Nitrate (Sanchez, 2003)

$0.5H_2(g) + 0.15NO_3^- + 0.065HCO_3^- + 0.2H^+ + 0.013NH_4^+ \rightarrow 0.013C_5H_7O_2N + 0.48H_2O$

$+ 0.074N_2(g)$

Oxygen

$0.5H_2(g) + 0.049CO_2 + 0.012HCO_3^- + 0.012NH_4^+ + 0.19O_2 \rightarrow 0.012C_5H_7O_2N + 0.49H_2O$
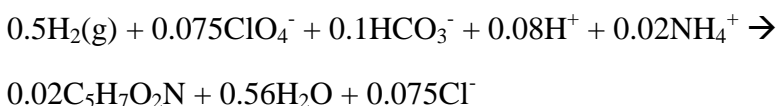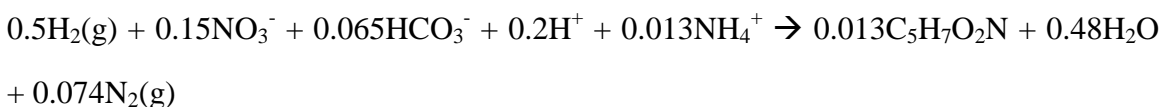
I.2. HYDROGEN PRODUCTION

The hydrogen consumed due to oxygen and perchlorate degradation was calculated by assuming the difference between the influent and effluent concentrations was due to autohydrogenotrophic consumption by the microorganisms. The hydrogen production rate in the column was estimated using the column flow rate, reaction stoichiometry (Section I.1), effluent hydrogen concentration, and mass of iron in the column. The hydrogen production rate was first presented as Equation 4.2 and can be seen below as Equation I.1.

$$r_{H_2} = \frac{-QS_{I,H_2} + QS_{E,H_2} + Q(S_{I,O_2} - S_{E,O_2})\gamma_{O_2} + Q(S_{I,ClO_4} - S_{E,O_2})\gamma_{ClO_4}}{M_{ZVI}}$$ Equation I.1

where:

r_{H_2} = hydrogen production rate in column [$M_{H2}/M_{Fe(0)}$T]

Q = volumetric flow rate of column [L^3/T]

S_{I,O_2} = influent concentration of oxygen [M/T]

S_{I,ClO_4} = influent concentration of perchlorate [M/T]

S_{I,H_2} = influent concentration of hydrogen gas [M/T]

S_{E,O_2} = effluent concentration of oxygen [M/T]

S_{E,ClO_4} = effluent concentration of perchlorate [M/T]

S_{E,H_2} = effluent concentration of hydrogen [M/T]

γ_{O_2} = stoichiometric ratio H_2/O_2 [M_{H2}/M_{O2}]

γ_{ClO_4} = stoichiometric ratio H_2/ClO_4^- [M_{H2}/M_{ClO4}]

M_{ZVI} = mass of ZVI in column [M]

The calculation below demonstrates based on the batch hydrogen production rates (Section 4.3.1) ZVI filings have the potential to provide the necessary hydrogen concentrations needed for biodegradation of perchlorate if the environmental conditions are favorable.

Hydrogen production rate required to biologically reduce 100 µg/L of perchlorate at a ground water flow rate of 1 m/d and a 1-m x 1-m x 2-m PRB

$$1\frac{m^3}{day} \, x \, 100\frac{\mu g \; ClO_4^-}{L} \, x \, \frac{1000 \, L}{m^3} \, x \, \frac{1 \; \mu mol \; ClO_4^-}{99.5 \; \mu g \; ClO_4^-} \, x \, \frac{1 \; mol \; ClO_4^-}{1 \; x \; 10^6 \mu mol \; ClO_4^-} \, x \, \frac{0.5 \; mol \; H_2}{0.075 \; mol \; ClO_4^-}$$

$$= 7x10^{-3}\frac{mol \; H_2}{day}$$

Hydrogen production rate in a 1-m x 1-m x 2-m PRB

volume $= 2 \; m^3$

porosity $= 0.6$

volume Fe^0 $= 0.8 \; m^3$

density Fe^0 $= 7.87 \; x \; 10^6 \; g/m^3$

BET surface area Fe^0 $= 1.112 \; m^2/g$

H_2 rate Millipore $H_2O = 6.43 \; x \; 10\text{-}6 \; mols \; H_2/m^2 \; Fe^0/day$ (Table 4.5)

$$0.8 \; m^3 \; Fe^0 x \; 7.87 \; x \; 10^6 \frac{g \; Fe^0}{m^3} \, x \, \frac{1.112 \; m^2 Fe^0}{g \; Fe^0} \, x \, \frac{6.43 \; x \; 10^{-6} mols \; H_2}{m^2 Fe^0 \; day} = 43 \frac{mols \; H_2}{day} \; \checkmark$$

The calculation below demonstrates that during the initial 220-day operating period of the ZVI/biotic column, the hydrogen production rate in the column was such that excess hydrogen was available to biologically degrade the influent perchlorate and oxygen (Section 4.3.4).

Hydrogen production rate required to biologically reduce influent perchlorate

(~105 µg/L)

$$3x10^{-3}\frac{L}{min} \ x \ 105 \frac{\mu g \ ClO_4^-}{L} \ x \frac{1 \ \mu mol \ ClO_4^-}{99.5 \ \mu g \ ClO_4^-} \ x \frac{1 \ mol \ ClO_4^-}{1 \ x \ 10^6 \mu mol \ ClO_4^-} \ x \frac{0.5 \ mol \ H_2}{0.075 \ mol \ ClO_4^-} =$$

$$2.1x10^{-8}\frac{mol \ H_2}{min}$$

Hydrogen production rate required to biologically reduce influent oxygen (~1.5 mg/L)

$$3x10^{-3}\frac{L}{min} \ x \ 1.5 \frac{mg \ O_2}{L} \ x \frac{1 \ mmol \ O_2}{32 \ mg \ O_2} \ x \frac{1 \ mol \ O_2}{1 mmol \ O_2} \ x \frac{0.5 \ mol \ H_2}{0.19 \ mol \ O_2} = 3.7x10^{-7}\frac{mol \ H_2}{min}$$

Minimum hydrogen production rate in the column

(effluent H_2 concentration 2.3 x 10^{-4} M (aq))

$$3x10^{-3}\frac{L}{min} \ x \ 2.3x10^{-4}\frac{mol \ H_2}{L} = 6.9x10^{-7}\frac{mol \ H_2}{min} \ \checkmark$$

I.3. Column data

Days	Influent DO	Influent pH	Influent ClO_4^-	Influent NO_3^-	Effluent DO	Effluent pH	Effluent ClO_4^-	Effluent NO_3^-	Effluent H_2 (aq)
	mg/L	-	ug/L	mg/L as N	mg/L	-	ug/L	mg/L as N	M
1	1.1	7.1	106		< 1	7.7	107		1.68E-04
4	1.0	7.4	117		< 1	7.9	111		1.58E-04
6	1.0	6.9	125		< 1	7.6	93		2.35E-04
9		6.7	109			7.5	66		3.66E-04
11	1.2	7.0	121		< 1	7.7	32		3.29E-04
13	1.1	7.1	115		< 1	7.8	30		
16	1.2	6.9	115		< 1	7.9	22		2.99E-04
19	1.2	7.1	112		< 1	7.8	21		1.81E-04
23	1.4	6.7			< 1	7.6			2.81E-04
26	1.0	6.8			< 1	7.5			2.39E-04
30	1.1	7.5	114		< 1	7.8	8		3.33E-04
34	1.0	7.2	120		< 1	7.7	19		4.18E-04
37	1.0	7.4	113		< 1	7.8	18		5.70E-04
43	1.2	7.3	91		< 1	7.7	9		
51	1.0	7.5	118		< 1	8.1	3		4.54E-04
55	< 1	7.2			< 1	7.7	4		4.99E-04
60	1.0	7.4	93		< 1	7.7	34		3.66E-04
63	1.2	7.0	108		< 1	7.6	9		5.39E-04
68	1.2	7.0	96		< 1	7.5	7		3.36E-04
75	1.3	7.2	126		< 1	7.7	7		1.70E-04
80	1.0	6.8	107			7.5	19		4.72E-04
86	1.4	7.2	105		< 1	7.6	7		4.73E-04
89	1.4	6.8	106		< 1	7.4	6		7.00E-04
96	1.3	7.1	106		< 1	7.6	27		5.82E-04
100	1.3	6.9	111		< 1	7.4	0		4.11E-04
108	1.4	7.1	102		< 1	7.6	5		5.78E-04
116	1.2	7.1	101		< 1	7.9	4		4.24E-04
121	1.4	7.0	111		< 1	7.5	15		6.07E-04
128	1.2	7.3			< 1	7.7	10		4.38E-04
134	1.1	7.0	119		< 1	7.4	8		5.20E-04
150	1.7	7.1	109		< 1	7.3	5		6.03E-04
156	1.0	7.0	92		< 1	7.3	4		3.36E-04
162	1.3	7.0	93		< 1	7.3	0		4.29E-04
172	1.2	7.2	113		< 1	7.4	4		3.43E-04
178	1.6	6.9	102		< 1	7.2	9		4.13E-04
188	1.5	-	105		< 1	7.1	4		3.67E-04
199	1.4	6.9	104		< 1	7.1	4		3.13E-04
227	< 1	7.0			< 1	7.2	0		3.33E-04
232	1.2	7.0	95		< 1	7.2	0		2.55E-04
241	1.4	7.1	111	2.1	< 1	7.4	0	0.08	3.57E-04
246	1.2	7.7	103	1.9		7.5	0	0.05	2.84E-04
253	1.5	7.2	100	1.9	< 1	7.3	0	0.03	3.54E-04
260	1.5	7.5	93	3.8	< 1	7.6	0	0.05	1.39E-04
267	2.4	7.1	106	4.3	< 1	7.3	0	0.02	2.79E-04
272	5.0	7.0	100	3.4	1.2	7.2	0	0.05	4.30E-04
278	1.4	7.1	110	6.9	< 1	7.4	16	0.12	4.69E-05
289	1.7	6.9	107	7.9	< 1	7.2	63	1.46	0.00E+00
290	1.8	6.9	103	7.8	< 1	7.2	52	0.76	0.00E+00
294	1.5	7.0	107	8.3	< 1	7.3	9	0.04	9.59E-05
310	1.0	7.2	149	8.4	< 1	7.5	73	2.34	0.00E+00
314	1.3	6.9	108	7.8	< 1	7.3	72	1.06	0.00E+00
318	3.0	7.0	95	7.5	1.2	7.3	72	2.28	0.00E+00
321	1.3	7.1	102	7.9	< 1	7.3	81	2.77	0.00E+00
325	2.0	7.1	108	7.9	< 1	7.3	98	3.25	0.00E+00
328	1.2	7.1	98	7.8	< 1	7.3	76	2.65	0.00E+00
332	2.0	7.0	99		< 1	7.2	0		2.78E-04
335	2.0	7.1	99		< 1	7.3	0		2.65E-04
342	2.2	7.1	103		< 1	7.3	0		2.45E-04
346	2.6		98			7.5	0		2.11E-04
348	2.9	7.2	96		1.5	7.4	0		2.69E-04
354	2.0	7.0	104		1.4	7.2	0		2.94E-04
362	1.6	7.0	90		< 1	7.2	0		3.70E-04
368	1.5	7.2	100		< 1	7.4	0		
378	2.0	7.4	94			7.6	0		2.70E-04
391	1.6	7.0	104		< 1	7.2	0		3.23E-04
436	2.9	7.0	100		< 1	7.3	3		4.30E-04
473	1.5	7.2	101		< 1	7.3	0		
495	2.0	7.4	41		< 1	7.3	0		2.20E-04
510	1.8	7.1	95		< 1	7.2	0		2.07E-04
524	2.2	7.2			< 1	7.3	0		3.91E-04

Figure I1 Raw continuous-flow ZVI/biotic column data

I.4. EDS

Table I1 EDS elemental ratio analysis virgin ZVI

	Ratio of	Average	Standard Deviation
Sample 1	Fe/O	0.96	0.38
	Fe/C	5.42	2.54
Sample 2	Fe/O	0.42	0.03
	Fe/C	1.95	0.45
Sample 3	Fe/O	0.74	0.25
	Fe/C	3.15	2.16

Table I2 EDS elemental ratio analysis column inlet

	Ratio of	Average	Standard Deviation
Sample 1	Fe/P	9.24	2.26
	Fe/C	4.21	-
	Fe/O	1.23	0.88
Sample 2	Fe/O	0.53	0.01
Sample 3	Fe/O	0.83	0.16
	Fe/C	0.25	0.03

Table I3 EDS elemental ratio analysis column outlet

	Ratio of	Average	Standard Deviation
Sample 1	Fe/O	1.12	0.51
	Fe/C	5.47	3.48
Sample 2	Fe/O	0.29	0.02
	Fe/P	1.85	0.48
Sample 3	Fe/O	0.62	0.15
	Fe/P	15.6	5.45

Appendix J: T-RFLP
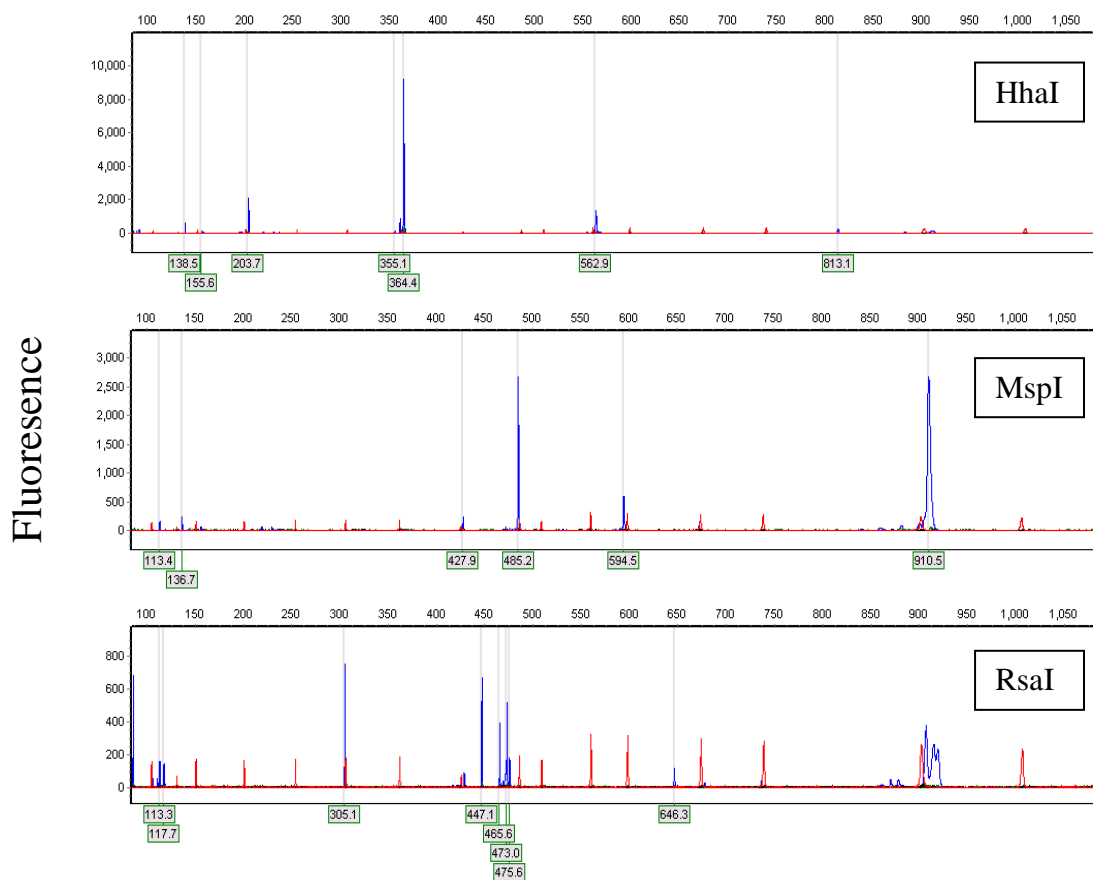
Length of terminal restriction fragment (base pairs)

Figure J1. Microbial profiling by T-RFLP

(Representative electropherograms for three restriction enzymes (HhaI, MspI, RsaI) are shown. Sizes indicated for the restriction fragments correspond to putative identifications of: Dechlormonas *spp. (203.7, 427.9, 117.7) and* Ideonella dechloratans *(364.4, 136.7))*

References

Agrawal, A.; Ferguson, W. J.; Gardner, B. O.; Christ, J. A.; Bandstra, J. Z.; Tratnyek, P. G., Effects of carbonate species on the kinetics of dechlorination of 1,1,1-trichloroethane by zero-valent iron. Environmental Science & Technology 2002, 36, (20), 4326-4333.

Alowitz, M. J.; Scherer, M. M., Kinetics of nitrate, nitrite, and Cr(VI) reduction by iron metal. Environmental Science & Technology 2002, 36, (3), 299-306.

Aziz, C. E.; Georgiou, G.; Speitel, G. E., Cometabolism of chlorinated solvents and binary chlorinated solvent mixtures using M-trichosporium OB3b PP358. Biotechnology and Bioengineering 1999, 65, (1), 100-107.

Belay, N.; Daniels, L., Elemental metals as electron sources for biological methane formation from CO_2. Antonie van Leeuwenhoek 1990, 57, (1), 1-7.

Berthouex, P.M.; Brown, L.C.; Statistics for Environmental Engineers. 2nd ed.; CRC Press: Florida, 2002.

Bokermann, C.; Dahmke, A.; Steiof, M., Hydrogen evolution from zero-valent iron in batch systems. In The Second International Conference on Remediation of Chlorinated and Recalcitrant Compounds, Wickramanayake, G. B.; Gavaskar, A. R.; Chen, A. S. C., Eds. Battelle Press: Monterey, California, 2000; Vol. 6, pp 433-439.

Bruce, R. A.; Achenbach, L. A.; Coates, J. D., Reduction of (per)chlorate by a novel organism isolated from paper mill waste. Environmental Microbiology 1999, 1, (4), 319-329.

California Department of Public Health, Perchlorate in drinking water. http://www.cdph.ca.gov/CERTLIC/DRINKINGWATER/Pages/Perchlorate.aspx (January 19, 2009) 2008.

Cao, J.; Elliott, D.; Zhang, W.-x., Perchlorate reduction by nanoscale iron particles. Journal of Nanoparticle Research 2005, 7, (4), 499-506.

Charlot, G., Selected constants: oxidation-reduction potentials of inorganic substances in aqueous solution. Cement and Concrete Association of Australia, Butterworths: Sydney, 1971.

Chaudhuri, S. K.; O'Connor, S. M.; Gustavson, R. L.; Achenbach, L. A.; Coates, J. D., Environmental factors that control microbial perchlorate reduction. Applied and Environmental Microbiology 2002, 68, (9), 4425-4430.

Chen, G.; Ozaki, H.; Terashima, Y., Modelling of the simultaneous removal of organic substances and nitrogen in a biofilm. Water Science and Technology 1989, 21, (8), 791-804.

Cheng, I. F.; Muftikian, R.; Fernando, Q.; Korte, N., Reduction of nitrate to ammonia by zero-valent iron. Chemosphere 1997, 35, (11), 2689-2695.

Choe, S.; Liljestrand, H. M.; Khim, J., Nitrate reduction by zero-valent iron under different pH regimes. Applied Geochemistry 2004, 19, (3), 335-342.

Clesceri, L. S.; Greenberg, A. E.; Eaton, A. D., Standard methods for the examination of water and wastewater. 20th ed.; American Public Health Association: Washington, D.C., 1998.

Coates, J. D.; Achenbach, L. A., Microbial perchlorate reduction: Rocket-fuelled metabolism. Nature Reviews Microbiology 2004, 2, (7), 569-580.

Coates, J. D.; Michaelidou, U.; Bruce, R. A.; O'Connor, S. M.; Crespi, J. N.; Achenbach, L. A., Ubiquity and diversity of dissimilatory (per)chlorate-reducing bacteria. Applied Environmental Microbiology 1999, 65, (12), 5234-5241.

Coates, J. D.; Michaelidou, U.; O'Connor, S. M.; Bruce, R. A.; Achenbach, L. A., The Diverse Microbiology of (Per)Chlorate Reduction. Kluwer Academic/Plenum Publishers: New York, 2000.

188

Da Silva, M. L. B.; Johnson, R. L.; Alvarez, P. J. J., Microbial characterization of groundwater undergoing treatment with a permeable reactive iron barrier. Environmental Engineering Science 2007, 24, (8), 1122-1127.

Dasgupta, P. K.; Martinelango, P. K.; Jackson, W. A.; Anderson, T. A.; Tian, K.; Tock, R. W.; Rajagopalan, S., The origin of naturally occurring perchlorate: The role of atmospheric processes. Environmental Science & Technology 2005, 39, (6), 1569-1575.

De Groef, B.; Decallonne, B.; Van der Geyten, S.; Darras, V.; Bouillon, R., Perchlorate versus other environmental sodium/iodide symporter inhibitors: potential thyroid-related health effects. European Journal of Endocrinology 2006, 155, (1), 17-25.

De Groot, G.; Stouthamer, A., Regulation of reductase formation in Proteus mirabilis. I. Formation of reductases and enzymes of the formic hydrogenlyase complex in the wild type and in chlorate-resistant mutants. Archiv für Mikrobiologie 1969, 66, (3), 220.

Dean, J. A.; Lange, N. A.; Knovel, A., Lange's handbook of chemistry. McGraw-Hill: New York, 1999.

Dejournett, T. D.; Alvarez, P. J. J., Combined microbial-Fe(0) treatment system to remove nitrate from contaminated groundwater. Bioremediation Journal 2000, 4, (2), 149 - 154.

Egert, M.; Friedrich, M. W., Post-amplification Klenow fragment treatment alleviates PCR bias caused by partially single-stranded amplicons. Journal of Microbiological Methods 2005, 61, (1), 69-75.

Ericksen, G. E., The Chilean nitrate deposits. American Scientist 1983, 71, (4), 366-374.

Gandhi, S.; Oh, B.-T.; Schnoor, J. L.; Alvarez, P. J. J., Degradation of TCE, Cr(VI), sulfate, and nitrate mixtures by granular iron in flow-through columns under different microbial conditions. Water Research 2002, 36, (8), 1973-1982.

Gerlach, R.; Cunningham, A. B.; Caccavo, F., Dissimilatory iron-reducing bacteria can influence the reduction of carbon tetrachloride by iron metal. Environmental Science & Technology 2000, 34, (12), 2461-2464.

Giblin, T. L.; Herman, D. C.; Frankenberger, W. T., Removal of perchlorate from ground water by hydrogen-utilizing bacteria. Journal of Environmental Quality 2000, 29, (4), 1057-1062.

Gillham, R. W.; O'Hannesin, S. F., Enhanced degradation of halogenated aliphatics by zero-valent iron. Ground Water 1994, 32, (6), 958-969.

Ginner, J. L.; Alvarez, P. J. J.; Smith, S. L.; Scherer, M. M., Nitrate and nitrate reduction by Fe0: Influence of mass transport, temperature, and denitrifying micrboes. Environmental Engineering Science 2004, 21, (2), 219-229.

Ginsberg, G. L.; Haitis, D. B.; Zoeller, R. T.; Rice, D. C., Evaluation of the U.S. EPA/OSWER preliminary remediation goal for perchlorate in groundwater: Focus on exposure tonursing infants. Environmental Health Perspectives 2007, 115, (3), 361-369.

Good, N.; Winget, G.; Winter, W.; Connolly, T.; Izawa, S.; Singh, R., Hydrogen Ion Buffers for Biological Research. Biochemistry 1966, 5, (2), 467-477.

Gotpagar, J.; Lyuksyutov, S.; Cohn, R.; Grulke, E.; Bhattacharyya, D., Reductive dehalogenation of trichloroethylene with zero-valent iron: Surface profiling microscopy and rate enhancement studies. Langmuir 1999, 15, (24), 8412-8420.

Gould, J., The kinetics of hexavalent chromium reduction by metallic iron. Water Research 1982, 16, 871-877.

Grady, C. P. L.; Daigger, G. T.; Lim, H. C.; NetLibrary Inc., Biological wastewater treatment. 2nd ed.; Marcel Dekker: New York, 1999.

Greenwood, N. N.; Earnshaw, A., Chemistry of the elements. Butterworth-Heinemann: Oxford; Boston, 1997.

Greiner, P.; McLellan, C.; Bennett, D.; Ewing, A., Occurrence of perchlorate in sodium hypochlorite. Journal - American Water Works Association 2008, 100, (11).

Gu, B.; Ku, Y.; Brown, G. M., Treatment of perchlorate-contaminated groundwater using highly selective, regenerable ion-exchange technology: A pilot-scale demonstration Remediation Journal 2002a, 12, (2), 51-68.

Gu, B.; Phelps, T. J.; Liang, L.; Dickey, M. J.; Roh, Y.; Kinsall, B. L.; Palumbo, A. V.; Jacobs, G. K., Biogeochemical dynamics in zero-valent iron columns: Implications for permeable reactive barriers. Environmental Science & Technology 1999, 33, (13), 2170-2177.

Gu, B.; Watson, D. B.; Wu, L.; Phillips, D. H.; White, D. C.; Zhou, J., Microbiological characteristics in a zero-valent iron reactive barrier. Environmental Monitoring and Assessment 2002b, 77, (3), 293-309.

Gujer, W.; Henze, M., Activated sludge modelling and simulation. Water Science & Technology 1991, 23, (4), 1011-1023.

Gullick, R. Q.; Lechvallier, M. W.; Barhorst, T. A. S., Occurrence of perchlorate in drinking water sources. Journal American Water Works Association 2001, 93, (1), 66-77.

Hatzinger, P. B., Perchlorate biodegradation for water treatment. Environmental Science & Technology 2005, 39, (11), 239a-247a.

Henderson, A. D.; Demond, A. H., Long-term performance of zero-valent iron permeable reactive barriers: A critical review. Environmental Engineering Science 2007, 24, (4), 401.

Huang, H.; Sorial, G. A., Perchlorate remediation in aquatic systems by zero valent iron. Environmental Engineering Science 2007, 24, (7), 917-926.

Huang, Y. H.; Zhang, T. C., Kinetics of nitrate reduction at near-neutral pH. Journal of Environmental Engineering 2002a, 128, (7), 604-611.

Huang, Y. H.; Zhang, T. C., Kinetics of nitrate reduction by iron at near neutral pH. Journal of Environmental Engineering 2002b, 128, (7), 604-611.

Johnson, T. L.; Scherer, M. M.; Tratnyek, P. G., Kinetics of halogenated organic compound degradation by iron metal. Environmental Science & Technology 1996, 30, (8), 2634-2640.

Kengen, S. W. M.; Rikken, G. B.; Hagen, W. R.; van Ginkel, C. G.; Stams, A. J. M., Purification and characterization of (per)chlorate reductase from the chlorate-respiring strain GR-1. Journal of Bacteriology 1999, 181, (21), 6706-6711.

Kimbrough, D.; Parekh, P., Occurrence and co-occurrence of perchlorate and nitrate in California drinking water sources. Journal American Water Works Association 2007, 99, (9), 126-132.

Kirk, A. B.; Martinelango, P. K.; Tian, K.; Dutta, A.; Smith, E. E.; Dasgupta, P. K., Perchlorate and iodide in dairy and breast Milk. Environmental Science & Technology 2005, 39, (7), 2011-2017.

Klausen, J.; Vikesland, P. J.; Kohn, T.; Burris, D. R.; Ball, W. P.; Roberts, A. L., Longevity of granular iron in groundwater treatment processes: solution composition effects on reduction of organohalides and nitroaromatic compounds. Environmental Science & Technology 2003, 37, (6), 1208-18.

Kurt, M.; Dunn, I. J.; Bourne, J. R., Biological denitrification of drinking water using autotrophic organisms in a fluidized-bed biofilm reactor. Biotechnology and Bioengineering 1987, 29, (4), 493-501.

Lawler, D. F.; Benjamin, M., Physical / Chemical treatment processes for water and wastewater McGraw-Hill Companies: 2007; Vol. 2 (forthcoming).

Leva, M., Fluidization. McGraw-Hill Book Company: New York, 1959.

Liang, L.; Korte, N.; Gu, B.; Puls, R.; Reeter, C., Geochemical and microbial reactions affecting the long-term performance of in situ iron barriers. Advances in Environmental Research 2000, 4, (4), 273-286.

Lide, D. R., CRC handbook of chemistry and physics. CRC Press: Boca Raton; London, 1994.

Lide, D. R., CRC handbook of chemistry and physics : a ready-reference book of chemical and physical data. 86th ed.; CRC Press: Boca Raton, Fla., 2005.

Liessens, J.; Vanbrabant, J.; Vos, P.; Kersters, K.; Verstraete, W., Mixed culture hydrogenotrophic nitrate reduction in drinking water. Microbial Ecology 1992, 24, (3), 271-290.

Logan, B., Assessing the outlook for perchlorate remediation. Environmental Science & Technology 2001, 35, (23), 482 A-487 A.

Logan, B. E.; LaPoint, D., Treatment of perchlorate- and nitrate-contaminated groundwater in an autotrophic, gas phase, packed-bed bioreactor. Water Research 2002, 36, (14), 3647-3653.

Marsh, T. L., Terminal restriction fragment length polymorphism (T-RFLP): An emerging method for characterizing diversity among homologous populations of amplification products. Current Opinion in Microbiology 1999, 2, (3), 323-327.

Marsh, T. L.; Saxman, P.; Cole, J.; Tiedje, J., Terminal restriction rragment length polymorphism analysis program, a web-based research tool for microbial community analysis. Applied Environmental Microbiology 2000, 66, (8), 3616-3620.

Massachusetts Department of Public Health, Addressing perchlorate and other emerging contaminants in massachusetts. http://www.mass.gov/dep/water/drinking/percfs77.htm (January 19, 2009) 2009.

McCarty, P. L., Stoichiometry of biological reactions. Progress in Water Technology 1975, 7, 157-172.

Miller, J. P.; Logan, B. E., Sustained perchlorate degradation in an autotrophic, gas-phase, packed-bed bioreactor. Environmental Science & Technology 2000, 34, (14), 3018-3022.

Mishra, D.; Farrell, J., Understanding nitrate reactions with zerovalent iron using Tafel analysis and electrochemical impedance spetcroscopy Environmental Science & Technology 2005, 39, (2), 645-650.

Moore, A. M.; De Leon, C. H.; Young, T. M., Rate and extent of aqueous perchlorate removal by iron surfaces. Environmental Science & Technology 2003, 37, (14), 3189-98.

Murray, C.; Egan, S.; Kim, H.; Beru, N.; Bolger, P., US Food and Drug Administration's Total Diet Study: Dietary intake of perchlorate and iodine. Journal of Exposure Science and Environmental Epidemiology 2008, 18, (6), 571-580.

National Research Council (U.S.). Division of Earth Sciences., Health implications of perchlorate ingestion. National Academies Press: Washington, D.C., 2005; p xvi, 260 p.

Nerenberg, R.; Kawagoshi, Y.; Rittmann, B. E., Kinetics of a hydrogen-oxidizing, perchlorate-reducing bacterium. Water Research 2006, 40, (17), 3290-3296.

Nerenberg, R.; Rittmann, B. E.; Najm, I., Perchlorate reduction in a hydrogen-based membrane-biofilm reactor. Journal - American Water Works Association 2002, 94, (11), 103-114.

Nolan, B. T.; Ruddy, B. C.; Hitt, K. J.; Helsel, D. R., Risk of Nitrate in Groundwaters of the United States A National Perspective. Environmental Science & Technology 1997, 31, (8), 2229-2236.

O'Connor, S. M.; Coates, J. D., Universal immunoprobe for (per)chlorate-reducing bacteria. Applied Environmental Microbiology 2002, 68, (6), 3108-3113.

Oh, Y. J.; Song, H.; Shin, W. S.; Choi, S. J.; Kim, Y.-H., Effect of amorphous silica and silica sand on removal of chromium(VI) by zero-valent iron. Chemosphere 2007, 66, (5), 858-865.

Ortiz de Montellano, D. Simulation of perchlorate removal in the presence of zero-valent iron. Departmental Report, The University of Texas at Austin, 2006.

Perry, R. H.; Green, D. W., Perry's chemical engineers' handbook. 8th ed.; McGraw-Hill: New York, 2008.

Perry, R. H.; Green, D. W.; Maloney, J. O., Perry's Chemical Engineers' Handbook. 7th ed.; McGraw-Hill Companies, Inc.: New York, 1997.

Powell, R. M.; Puls, R. W., Proton generation by dissolution of intrinsic or augmented aluminosilicate minerals for in situ contaminant remediation by zero-valence-state iron. Environmental Science & Technology 1997, 31, (8), 2244-2251.

Powell, R. M.; Puls, R. W.; Hightower, S. K.; Sabatini, D. A., Coupled iron corrosion and chromate reduction: mechanisms for substrate remediation. Environmental Science & Technology 1995, 29, (8), 1913-1922.

Rajagopalan, S.; Anderson, T. A.; Fahlquist, L.; Rainwater, K. A.; Ridley, M.; Jackson, W. A., Widespread presence of naturally occurring perchlorate in high plains of Texas and New Mexico. Environmental Science & Technology 2006, 40, (10), 3156-3162.

Ralston, M. L.; Jennrich, R. I., Dud, A derivative-free algorithm for nonlinear least squares. Technometrics 1978, 20, (1), 7-14.

Rao, B.; Anderson, T. A.; Orris, G. J.; Rainwater, K. A.; Rajagopalan, S.; Sandvig, R. M.; Scanlon, B. R.; Stonestrom, D. A.; Walvoord, M. A.; Jackson, W. A., Widespread natural perchlorate in unsaturated zones of the southwest United States. Environmental Science & Technology 2007, 41, (13), 4522-4528.

Reardon, E. J., Anaerobic corrosion of granular iron: measurement and interpretation of hydrogen evolution rates. Environmental Science & Technology 1995, 29, (12), 2936-2945.

Reichert, P., AQUASIM - A tool for simulation and data analysis of aquatic systems. Water Science & Technology 1994, 30, (2), 21-30.

Reichert, P., Design techniques of a computer program for identification of processes and simulation of water quality in aquatic systems. Environmental Software 1995, 10, (3), 199-210.

Reichert, P., AQUASIM 2.0 - User Manual, Tutorial. Swiss Federal Institute for Environmental Science and Technology (EAWAG): Dubendorf, Switzerland, 1998.

Renner, R., EPA perchlorate decision flawed, say advisers. Environmental Science & Technology 2009, 43, (3), 553-554.

Rikken, G. B.; Kroon, A. G. M.; van Ginkel, C. G., Transformation of (per)chlorate into chloride by a newly isolated bacterium: Reduction and dismutation. Applied Microbiology and Biotechnology 1996, 45, (3), 420-426.

Rittman, B., The effect of shear stress on biofilm loss rate. Biotechnology and Bioengineering 1982, 24, (2).

Rittmann, B. E.; McCarty, P. L., Environmental biotechnology: principles and applications. McGraw-Hill: Boston, 2001.

Robinson, J. A. In Determining microbial kinetic parameters using nonlinear regression analysis, Advances in Microbial Ecology, 1985; 1985; pp 61-114.

Rodríguez-Maroto, J.; García-Herruzo, F.; García-Rubio, A.; Gómez-Lahoz, C.; Vereda-Alonso, C., Kinetics of the chemical reduction of nitrate by zero-valent iron. Chemosphere 2009, 74, (6), 804-809.

Ruangchainikom, C.; Liao, C. H.; Anotai, J.; Lee, M. T., Characteristics of nitrate reduction by zero-valent iron powder in the recirculated and CO(2)-bubbled system. Water Res 2006, 40, (2), 195-204.

Sanchez, A. F. J. Zero-valent iron-enhanced bioremediation for the treatment of perchlorate in groundwater. Ph. D. Dissertation, The University of Texas at Austin, Austin, Texas, 2003.

Schaefer, C. E.; Fuller, M. E.; Condee, C. W.; Lowey, J. M.; Hatzinger, P. B., Comparison of biotic and abiotic treatment approaches for co-mingled perchlorate, nitrate, and nitramine explosives in groundwater. Journal of Contaminant Hydrology 2007, 89, (3-4), 231-250.

Scherer, M. M.; Balko, B. A.; Gallagher, D. A.; Tratnyek, P. G., Correlation analysis of rate constants for dechlorination by zero-valent iron. Environmental Science & Technology 1998, 32, (19), 3026-3033.

Schier, J.; Wolkin, A.; Valentin-Blasini, L.; Belson, M.; Kieszak, S.; Rubin, C.; Blount, B., Perchlorate exposure from infant formula and comparisons with the perchlorate reference dose. Journal of Exposure Science and Environmental Epidemiology 2009.

Schlicker, O.; Ebert, M.; Fruth, M.; Weidner, M.; Wüst, W.; Dahmke, A., Degradation of TCE with iron: The role of competing chromate and nitrate reduction. Ground Water 2000, 38, (3), 403-409.

Shrout, J. D.; Scheetz, T. E.; Casavant, T. L.; Parkin, G. F., Isolation and characterization of autotrophic, hydrogen-utilizing, perchlorate-reducing bacteria. Applied Microbiology and Biotechnology 2005a, 67, (2), 261-268.

Shrout, J. D.; Williams, A. G. B.; Scherer, M. M.; Parkin, G. F., Inhibition of bacterial perchlorate reduction by zero-valent iron. Biodegradation 2005b, 16, (1), 23-32.

Siantar, D. P.; Schreier, C. G.; Chou, C.-S.; Reinhard, M., Treatment of 1,2-dibromo-3-chloropropane and nitrate-contaminated water with zero-valent iron or hydrogen/palladium catalysts. Water Research 1996, 30, (10), 2315-2322.

Siddiqui, M.; LeChevallier, M.; Ban, J.; Phillips, T.; Pivinski, J., Occurence of perchlorate and methyl tertiary butyl ether (MTBE) in groudwater of the American water system; American Water Works Service Company, Inc.: Vorhees, NJ, 1998.

Smith, L. H.; Kitanidis, P. K.; McCarty, P. L., Numerical modeling and uncertainties in rate coefficients for methane utilization and TCE cometabolism by a methane-

oxidizing mixed culture. Biotechnology and Bioengineering 1997, 53, (3), 320-331.

Smith, L. H.; McCarty, P. L.; Kitanidis, P. K., Spreadsheet method for evaluation of bichemical reaction rate coefficients and their uncertainties by weighted nonlinear least-squares analysis of the integrated monod equation Applied Environmental Microbiology 1998, 64, (6), 2044-2050.

Son, A.; Lee, J.; Chiu, P. C.; Kim, B. J.; Cha, D. K., Microbial reduction of perchlorate with zero-valent iron. Water Research 2006, 40, (10), 2027-2032.

Steinberg, L. M.; Trimble, J. J.; Logan, B. E., Enzymes responsible for chlorate reduction by Pseudomonas sp. are different from those used for perchlorate reduction by Azospira sp. FEMS Microbiology Letters 2005, 247, (2), 153-159.

Su, C.; Puls, R. W., Removal of added nitrate in the single, binary, and ternary systems of cotton burr compost, zerovalent iron, and sediment: Implications for groundwater nitrate remediation using permeable reactive barriers. Chemosphere 2007, 67, (8), 1653-1662.

Tchobanoglous, G.; Burton, F. L.; Stensel, H. D.; Metcalf; Eddy, Wastewater engineering: treatment and reuse. McGraw-Hill: Boston, 2003.

Till, B. A.; Weathers, L. J.; Alvarez, P. J. J., Fe(0)-Supported autotrophic denitrification. Environmental Science & Technology 1998, 32, (5), 634-639.

Tri-Agency Permeable Reactive Barrier Initiative, Evaluation of permeable reactive barrier performance. http://clu-in.org/download/rtdf/2-PRBperformance_web.pdf (January 19, 2009) 2002.

United States Environmental Protection Agency. National Primary Drinking Water Regulations: Maximum Contaminant Levels and Maximum Residual Disinfectant Levels. Federal Register, 141.62, 1992.

United States Environmental Protection Agency, Known perchlorate releases in the U.S. as of 3/25/2005. (11/13/2008) 2005a.

United States Environmental Protection Agency, Perchlorate monitoring results: Henderson, Nevada to the Lower Colorado River. http://ndep.nv.gov/bca/file/perchlorateeighthmonrpt123105.pdf (January 19, 2009) 2005b.

United States Environmental Protection Agency, Unregulated contaminated monitoring rule. http://www.epa.gov/safewater/ucmr.html (January 19, 2009) 2005c.

United States Environmental Protection Agency, Interim drinking water health advisory for perchlorate (EPA 822-R-08-025)

United States Food and Drug Administration, Perchlorate questions and answers. http://www.cfsan.fda.gov/~dms/clo4qa.html (Januart 19, 2009) 2004.

Urbansky, E. T., Perchlorate chemistry: Implications for analysis and remediation. Bioremediation Journal 1998, 2, (2), 81-95.

Urbansky, E. T., Perchlorate as an environmental contaminant. Environmental Science and Pollution Research International 2002, 9, (3), 187-92.

Urbansky, E. T.; Brown, S. K., Perchlorate retention and mobility in soils. Journal of Environmental Monitoring 2003, 5, (3), 455-462.

van Ginkel, C. G.; Rikken, G. B.; Kroon, A. G. M.; Kengen, S. W. M., Purification and characterization of chlorite dismutase: a novel oxygen-generating enzyme. Archives of Microbiology 1996, 166, (5), 321-326.

van Ginkel, S. W.; Ahn, C. H.; Badruzzaman, M.; Roberts, D. J.; Lehman, S. G.; Adham, S. S.; Rittmann, B. E., Kinetics of nitrate and perchlorate reduction in ion-exchange brine using the membrane biofilm reactor (MBfR). Water Research 2008, 42, (15), 4197-4205.

van Nooten, T.; Springael, D.; Bastiaens, L., Positive impact of microorganisms on the performance of laboratory-scale permeable reactive iron barriers. Environmental Science & Technology 2008, 42, (5), 1680-1686.

Wahman, D. G.; Katz, L. E.; Speitel, G. E., Jr., Cometabolism of trihalomethanes by nitrosomonas europaea. Applied Environmental Microbiology 2005, 71, (12), 7980-7986.

Wahman, D. G.; Katz, L. E.; Speitel, G. E., Jr., Modeling of trihalomethane cometabolism in nitrifying biofilters. Water Research 2007, 41, (2), 449-57.

Waller, A. S.; Cox, E. E.; Edwards, E. A., Perchlorate-reducing microorganisms isolated from contaminated sites. Environmental Microbiology 2004, 6, (5), 517-527.

Wang, C.; Lippincott, L.; Meng, X., Kinetics of biological perchlorate reduction and pH effect. Journal of Hazardous Materials 2008, 153, (1-2), 663-669.

Wang, H.-C.; Eaton, A. D.; Narloch, B., National assessment of perchlorate contamination occurrence. AWWA Research Foundation and American Water Works Association: Denver, CO, 2002.

Wanner, O.; Morgenroth, E., Biofilm modeling with AQUASIM. Water Science and Technology 2004, 49, (11-12), 137-144.

Whitman, G. W.; Russell, R. P.; Altieri, V. J., Effect of hydrogen-ion concentration on the submerged corrosion of steel. Industrial & Engineering Chemistry 1924, 16, (7), 665-670.

Wilson, E. J.; Geankoplis, C. J., Liquid mass transfer at very low reynolds numbers in packed beds. Industrial & Engineering Chemistry Fundamentals 1966, 5, (1), 9-14.

Xu, J. L.; Song, Y. U.; Min, B. K.; Steinberg, L.; Logan, B. E., Microbial degradation of perchlorate: Principles and applications. Environmental Engineering Science 2003, 20, (5), 405-422.

Xu, J. L.; Trimble, J. J.; Steinberg, L.; Logan, B. E., Chlorate and nitrate reduction pathways are separately induced in the perchlorate-respiring bacterium Dechlorosoma sp KJ and the chlorate-respiring bacterium Pseudomonas sp PDA. Water Research 2004, 38, (3), 673-680.

Yu, X. Y.; Amrhein, C.; Deshusses, M. A.; Matsumoto, M. R., Perchlorate reduction by autotrophic bacteria in the presence of zero-valent iron. Environmental Science & Technology 2006, 40, (4), 1328-1334.

Yu, X. Y.; Amrhein, C.; Deshusses, M. A.; Matsumoto, M. R., Perchlorate reduction by autotrophic bacteria attached to zerovalent iron in a flow-through reactor. Environmental Science & Technology 2007, 41, (3), 990-997.

Zawaideh, L. L.; Zhang, T. C., The effects of pH and addition of an organic buffer (HEPES) on nitrate transformation in Fe0-water systems. Water Science and Technology 1998, 38, 107-115.

Vita

Mara Rachel London was born in Bryan, Texas on August 10, 1977, daughter of Karen and Steven D. London. She attended Texas A&M University where she obtained a B.S. in Civil Engineering, graduating *cum laude*. Upon graduation, she worked for three years as an engineer-in-training for Kimley-Horn and Associates. In 2003, she decided to return to school to specialize in Environmental Engineering and joined the Environmental and Water Resources Engineering Graduate Program at The University of Texas at Austin. She was awarded a M.S. in Environmental and Water Resources Engineering and continued on to pursue a doctoral degree. During her time at The University of Texas she taught General Chemistry I and II for the General Engineering Program. She has accepted a faculty position at Gonzaga University in Spokane, Washington following the completion of her Ph.D.

Permanent address: 6127 Wigton, Houston, Texas, 77096

This dissertation was typed by the author.